12-2021

Mechanisms and Applications of Improved Protein Analysis by Desorption Electrospray Ionization Mass Spectrometry (DESI-MS)

Roshan Javanshad
Western Michigan University, rjavanshad@gmail.com

MECHANISMS AND APPLICATIONS OF IMPROVED PROTEIN ANALYSIS BY DESORPTION ELECTROSPRAY IONIZATION MASS SPECTROMETRY (DESI-MS)

by

Roshan Javanshad

A dissertation submitted to the Graduate College
in partial fulfillment of the requirements
for the degree of Doctor of Philosophy
Chemistry
Western Michigan University
December 2021

Doctoral Committee:

Andre R. Venter, Ph.D., Chair
Todd J. Barkman, Ph.D.
David L. Huffman, Ph.D.
Kelly A. Teske, Ph.D.

MECHANISMS AND APPLICATIONS OF IMPROVED PROTEIN ANALYSIS BY DESORPTION ELECTROSPRAY IONIZATION MASS SPECTROMETRY (DESI-MS)

Roshan Javanshad, Ph.D.

Western Michigan University, 2021

Electrospray ionization mass spectrometry (ESI-MS) is a soft ionization technique that allows detection of macromolecules, such as intact proteins, by the formation of multiply charged ions from solutions. Desorption electrospray ionization mass spectrometry (DESI-MS) is an ambient ionization technique that directly samples analyte from a surface during ESI-MS analysis. Although DESI-MS is highly accomplished at the analyses of metabolites, lipids, and other small molecules, it is far more limited when it comes to protein analysis. While most of the field in ambient ionization MS has moved towards primarily applications, our approach has been to explore the use of DESI-MS and direct ESI-MS to answer fundamental scientific questions. Understanding the mechanisms by which proteins are analyzed with these techniques provides essential insight into protein behavior and enables improving these techniques even further.

The presented work focuses on improving DESI-based protein analysis via solution-phase and gas-phase additives and understanding the underlying mechanisms by which these additives improve protein signal. DESI-MS and complementary direct ESI-MS experiments were used to (1) investigate the effect of amino acid additives on protein signal, (2) understand the mechanism by which amino acid additives improve protein signal during DESI-MS, (3) investigate the effect of organic solvent vapors on protein signal, and (4) incorporate these

techniques and findings into developing a novel method for rapid analysis of immobilized His-tagged proteins.

As a result, we were able to successfully improve protein analysis by DESI-MS through the addition of L-serine to the desorption solvent. Serine was shown to act as a solubility enhancing additive through improving dissolution of unfolding proteins during the extraction/desorption step of DESI-MS, potentially by inhibiting aggregation. Exposing the DESI-MS sampling region to ethyl acetate vapors also improved the signal intensity of proteins similar to previously reported ESI-MS observations. Finally, the potential application of direct ESI-MS and DESI-MS for rapid analysis of immobilized recombinant His-tagged proteins from Ni-NTA and Cu-NTA coated surfaces was evaluated. We successfully demonstrated the capture and release of recombinant His-tagged human ubiquitin from Ni-NTA and Cu-NTA surfaces by DESI-MS. Furthermore, we show the detection of His-tagged recombinant protein directly out of complex solutions containing the total protein fraction of the *E. coli* expression system and the lysis buffer, after purifying on Ni- and Cu-NTA plates. This work demonstrated the potential of direct ESI-MS and DESI-MS for rapid analysis of recombinant His-tagged proteins from crude bacterial cell lysate.

ACKNOWLEDGMENTS

First, I would like to thank Professor Andre Venter, for generously allowing me to forge my own path under his guidance and mentorship. I am forever grateful for your support and kindness. Thank you for everything you have taught me over the past five years, your patience, and your advice.

To my committee members, thank you for your time and support. I would like to especially thank Dr. Todd Barkman for his generous support and guidance. Thank you for the delightful science conversations and brainstorming sessions. Dr. David Huffman and Dr. Kelly Teske, thank you for your kind support and thoughtful discussions on my projects. Many thanks to The Department of Chemistry faculty and staff. Pam McCartney, Michelle Barnes, Lisah Crall, Courtney Buchmaster, Sean Bashaw and Dr. Kevin Blair, thank you for helping me with various technical issues.

My dear friend and senior lab mate, Elahe Honarvar, you have truly been an older sister to me. I owe so much of my personal and professional development to you. Thank you for being such a wonderful human being. My friend and comrade, Tara Maser, it was great going through this Ph.D. journey with you. Thank you for your friendship, compassion and for making difficult moments endurable. Other group member, past and present, it was great having you in lab and sharing this experience with you.

Baharnaz Gord, my dearest and oldest friend, we have gone through so much together over the past 14 years, and I couldn't have had a better best friend. Thank you for always being there for me in the best of times and worst of times. I couldn't have done this without you.

Finally, I want to thank my wonderful family, whose love and support allowed me to accomplish what I have this far. Above all, I want to thank my amazing parents who have unconditionally loved and supported me in life. Thank you for setting such good examples of resiliency and hard work.

Roshan Javanshad

TABLE OF CONTENTS

Table of Contents—Continued

CHAPTER

Table of Contents—Continued

CHAPTER

Table of Contents—Continued

CHAPTER

LIST OF TABLES

LIST OF FIGURES

List of Figures—Continued

List of Figures—Continued

List of Figures—Continued

LIST OF ABBREVIATIONS

ABC .....ammonium bicarbonate

ACN .....acetonitrile

APCI ..... atmospheric pressure chemical ionization

API .....atmospheric pressure ionization

BSA.....bovine serum albumin

CAII .....carbonic anhydrase isozyme II

CEM..... charge ejection model

CRM..... charge residue model

CS.....charge state

CSD..... charge state distribution

Cyt *c*..... cytochrome *c*

DESI..... desorption electrospray ionization

EESI ..... extractive electrospray ionization

ESI..... electrospray ionization

ESSI .....electrosonic spray ionization

FA ..... formic acid

HICS ..... highest intensity charge state

HOCS.....highest observed charge state

IEM .....ion evaporation model

List of Abbreviations—Continued

LESA.....liquid extraction surface analysis

LMJ-SSP..... liquid microjunction-surface sampling probe

LOCS .....lowest observed charge state

Myo ..... myoglobin

MeOH .....methanol

MS.....mass spectrometry

MW .....molecular weight

m/z.....mass-to-charge ratio

n-ESI .....nano ESI

PA ..... proton affinity

PE.....polyethylene

PTFE ..... polytetrafluoroethylene

RSD..... relative standard deviation

Ser ..... serine

SDC..... spray desorption collection

PREFACE

The present work describes my efforts to engage in research on the interface of chemistry and biology through one of the most valuable areas with such interdisciplinary nature, the study of proteins using mass spectrometry. This dissertation presents my research dedicated to expanding our understanding of protein dissolution and ionization by desorption electrospray ionization (DESI) along with direct electrospray ionization (ESI) mass spectrometry (MS) and exploring the application of DESI and direct ESI in developing recombinant protein assays. The results I presented here were collected during the last five years as a Ph.D. student in Dr. Andre Venter's research laboratory, under his direct supervision, and with the generous support of my dissertation committee members, especially Dr. Todd Barkman from The Biological Sciences Department at Western Michigan University. I have been greatly fortunate to work on research projects entirely supported by the National Science Foundation (NSF) under grant numbers CHE 2003379 and CHE 1508626. Most of the original research presented in this dissertation has already been published in reputable peer-reviewed journals such as Analyst (RCS), The Journal of the American Society for Mass Spectrometry (ACS), and Analytical Methods (RCS).

CHAPTER 1

1. INTRODUCTION

1.1 On desorption and direct electrospray ionization mass spectrometry for analysis of proteins

Mass spectrometry (MS) is an analytical technique that detects and identifies molecules primarily based on their mass and electric charge. The detected ions are typically presented in a mass spectrum, which is a plot of ion signal intensity as a function of mass-to-charge ratio (m/z). A mass spectrometry analysis can be carried out on intact molecules without any type of fragmentation via soft ionization techniques, and it can also yield fragments of the molecule by in-source fragmentation or tandem mass spectrometry (also known as MS/MS or MS^n). Both purified compounds and molecules from highly complex mixtures can be detected and analyzed by mass spectrometry. This capability, alongside speed, sensitivity, and selectivity, makes mass spectrometry an indispensable analytical technique and one of the most dominant analytical instruments.

Since its invention in the early 20^{th} century, mass spectrometry has found numerous applications in a wide variety of fields. This exponential growth is in part thanks to the discovery of soft ionization methods. Soft ionization refers to any process that can ionize a molecule with little to no fragmentation. Electrospray ionization (ESI) is an important soft ionization technique that can produce gas-phase ions from solutes in a solution. ESI stands out from the crowd because, in addition to producing singly charged ions, it can produce multiply charged ions as well. This ability is especially useful for analyzing large macromolecules because it can ionize

macromolecules without fragmentation while also effectively enabling mass analyzers to detect these intact large molecules by increasing the number of charges and consequently lowering the m/z values. ESI is useful for analyzing different classes of compounds, but perhaps the most remarkable application of ESI is the analysis of biological macromolecules such as proteins. In fact, John B. Fenn was awarded a share of the 2002 Nobel Prize in Chemistry for "the development of ESI for analysis of biological macromolecules, or as famously remembered, "electrospray wings for molecular elephants".[1]

ESI-MS is a product of steady contributions for more than 400 years. The reports regarding the physics of charged droplets go back to 1600. Abbé Jean-Antoine Nollet performed the first ESI experiment in the 18th century.[2] The disintegration of charged droplets such as those produced in ESI was described in 1882,[3] and the first account of the ESI phenomenon was published in 1917.[4] ESI-MS for chemical analysis was an idea developed by Malcolm Dole in the late 1960s in the pursuit of observing synthetic polymers and measuring their mass.[5] Subsequent work by Fenn and co-workers finally demonstrated the ground-breaking ability of ESI-MS for analysis of proteins with molecular weights far beyond a mass analyzer's upper mass limit in the late 1980s.[6] Ever since then, ESI-MS has become one of the most popular techniques for mass spectrometry methods to study proteins and has exponentially grown into a large and diverse field, encompassing quantitative,[7-8] structural,[9-10] and proteomics studies,[11-13] just to mention a few.

In 2004, desorption electrospray ionization mass spectrometry (DESI-MS) was developed for the analysis of compounds under ambient conditions.[14] During DESI, a desorption solvent extracts the analytes from a solid or even liquid sample (sampling step), followed by ESI for ionization (ionization step) and subsequent MS detection of the extracted analytes. While highly

accomplished in analyzing small molecules, DESI struggles with a hallmark capability of ESI, namely protein analysis, even though the two techniques are closely related and share the same ionization mechanisms.[15-16] Although it is generally said that lower sensitivity in DESI-MS of proteins is mainly due to inefficient protein desorption, deconstruction of DESI into independent desorption and ionization steps demonstrated that proteins, large and small, desorb equally well. It is, in fact, inefficient protein dissolution during the DESI-MS extraction that is mostly responsible for the poor performance of DESI-MS in protein analysis.[16-17] This dissertation is primarily focused on improving protein analysis by DESI-MS through the help of additives, and understanding the biochemical basis of how these additives can help protein analysis in DESI-MS. The close similarity in ionization yet different timeframes of sampling methods between DESI and ESI provides a unique opportunity to investigate protein behavior during dissolution and ionization. This type of study can be used to further understand how additives can improve protein solubility and/or ionization, in general, but more specifically for DESI-MS analysis. Finally, this knowledge will allow us to expand the applications of DESI-MS for protein analysis beyond what is currently possible.

1.2 The structure of the dissertation

A detailed background of ESI and DESI mechanisms, particularly for protein analysis, is provided in Chapter 2. This chapter also explains the challenges of protein analysis by DESI and the previous investigations into the reason behind the struggle, which lay the foundation of my research on additives that enhance protein analysis in DESI-MS and their mechanism of action. My work on improving protein analysis by DESI through different additives is described in Chapters 3 and 4. Chapter 3 examines the effect of solution-phase additives, in particular the amino acid L-serine, on protein analysis by DESI and shows that in addition to removing salt

adducts from proteins as it does in ESI,[18] serine can increase protein signal intensity in DESI under denaturing conditions. In Chapter 4, a systematic study was carefully designed to investigate the mechanism of the protein signal improvement observed in Chapter 3. This fundamental study investigated the effect of additives on protein solubility and dissolution by interpreting results from complementary DESI and direct ESI experiments, using L-serine as a model additive. Overall, this study demonstrated the capability of DESI and complementary ESI experiments as a novel tool for understanding the mechanism of action for solubility-enhancing additives, which is a novel application of DESI-MS for protein studies. In Chapter 5, the effect of gas-phase additives on improving protein analysis by DESI through the exposure of the sampling area to organic vapors with the help of a custom-built enclosure is discussed, and the effect on protein charge state distribution and signal intensity is compared to the previously published literature on the effects of organic vapors on ESI-MS of proteins. Chapter 6 details my efforts to expand the application of DESI in protein analysis by investigating detection and purification of His-tagged recombinant proteins from the bacterial cell lysate through immobilization on Ni-NTA and Cu-NTA coated surfaces by DESI and direct ESI. Lastly, in Chapter 7, I conclude the dissertation with final remarks and prospects for future research.

1.3 References

1. Fenn, J. B., Electrospray Wings for Molecular Elephants (Nobel lecture). *Angewandte Chemie International Edition* **2003,** *42* (33), 3871-3894.
2. Dumont, Q.; Cole, R. B., Jean-Antoine Nollet: The Father of Experimental Electrospray. *Mass Spectrometry Reviews* **2014,** *33* (6), 418-423.
3. Rayleigh, L., XX. On the Equilibrium of Liquid Conducting Masses Charged with Electricity. *The London, Edinburgh, and Dublin Philosophical Magazine and Journal of Science* **1882,** *14* (87), 184-186.
4. Zeleny, J., Instability of Electrified Liquid Surfaces. *Physical Review* **1917,** *10* (1), 1-6.
5. Dole, M.; Mack, L. L.; Hines, R. L.; Mobley, R. C.; Ferguson, L. D.; Alice, M. B., Molecular Beams of Macroions. *The Journal of Chemical Physics* **1968,** *49* (5), 2240-2249.
6. Meng, C.; Mann, M.; Fenn, J., Of Protons or Proteins. *Zeitschrift für Physik D Atoms, Molecules and Clusters* **1988,** *10* (2), 361-368.

7. Bantscheff, M.; Schirle, M.; Sweetman, G.; Rick, J.; Kuster, B., Quantitative Mass Spectrometry in Proteomics: a Critical Review. *Analytical and Bioanalytical Chemistry* **2007,** *389* (4), 1017-1031.
8. Cupp-Sutton, K. A.; Wu, S., High-throughput Quantitative Top-down Proteomics. *Molecular omics* **2020,** *16* (2), 91-99.
9. Heck, A. J., Native Mass spectrometry: a Bridge Between Interactomics and Structural Biology. *Nature Methods* **2008,** *5* (11), 927-933.
10. Leney, A. C.; Heck, A. J., Native Mass Spectrometry: What Is in the Name? *Journal of the American Society for Mass Spectrometry* **2016,** *28* (1), 5-13.
11. Gygi, S. P.; Aebersold, R., Mass Spectrometry and Proteomics. *Current Opinion in Chemical Biology* **2000,** *4* (5), 489-494.
12. Aebersold, R.; Mann, M., Mass Spectrometry-based Proteomics. *Nature* **2003,** *422* (6928), 198-207.
13. Donnelly, D. P.; Rawlins, C. M.; DeHart, C. J.; Fornelli, L.; Schachner, L. F.; Lin, Z.; Lippens, J. L.; Aluri, K. C.; Sarin, R.; Chen, B., Best Practices and Benchmarks for Intact Protein Analysis for Top-down Mass Spectrometry. *Nature Methods* **2019,** *16* (7), 587-594.
14. Takats, Z.; Wiseman, J. M.; Gologan, B.; Cooks, R. G., Mass Spectrometry Sampling Under Ambient Conditions with Desorption Electrospray Ionization. *Science* **2004,** *306* (5695), 471-473.
15. Shin, Y.-S.; Drolet, B.; Mayer, R.; Dolence, K.; Basile, F., Desorption Electrospray Ionization-Mass Spectrometry of Proteins. *Analytical Chemistry* **2007,** *79* (9), 3514-3518.
16. Douglass, K. A.; Venter, A. R., Protein Analysis by Desorption Electrospray Ionization Mass Spectrometry and Related Methods. *Journal of Mass Spectrometry* **2013,** *48* (5), 553-560.
17. Douglass, K. A.; Jain, S.; Brandt, W. R.; Venter, A. R., Deconstructing Desorption Electrospray Ionization: Independent Optimization of Desorption and Ionization by Spray Desorption Collection. *Journal of The American Society for Mass Spectrometry* **2012,** *23* (11), 1896-1902.
18. Campbell, D. I.; Ferreira, C. R.; Eberlin, L. S.; Cooks, R. G., Improved Spatial Resolution in the Imaging of Biological Tissue Using Desorption Electrospray Ionization. *Analytical and Bioanalytical Chemistry* **2012,** *404* (2), 389-398.

CHAPTER 2

2. ANALYSIS OF PROTEINS BY ELECTROSPRAY AND DESORPTION ELECTROSPRAY IONIZATION MASS SPECTROMETRY

Sections of this chapter are adapted with permission from

R. Javanshad, and A. R. Venter

Anal. Methods, 2017, **9**, 4896

2.1 Introduction to electrospray ionization

The electrospray process has a long history of use as a mechanism to electrostatically disperse liquids and for generating aerosols predating its application for ionization with mass spectrometric analysis [1]. The physical mechanisms of charged droplet formation by electrospray has been widely studied and is well-accepted. Unfortunately, not all the processes that happen during ESI are well-understood. The processes by which ionization occurs in ESI, for example, are still controversial and actively under investigation. Electrospray leads to the formation of small, highly charged droplets which subsequently produce gas-phase ions. Production of gas-phase ions from solution in ESI usually takes place under atmospheric pressure and can be described in three major steps: (1) production of charged droplets at the tip of the electrospray; (b) droplet shrinkage due to solvent evaporation and repeated droplet fission leading to very small, highly charged droplets capable of producing gas-phase ions; and (3) the various mechanisms by which gas-phase ions are believed to be released from these droplets. Below is a

brief account of what is currently known about the processes that lead to ionization, with focus on positive mode ESI.[2-3]

2.1.1 Formation of charged droplets in ESI

Upon application of a high voltage (typically around 1-4 kV) to a conducting solution in a capillary close to a counter electrode (for example a "plate" in the mass spectrometer sampling system), the charged solution is ejected from the tip of the capillary by formation of a Taylor cone.[4] A Taylor cone is formed because the electric field at the tip of the capillary is very strong and results in ion separation in the solution and accumulation of the electrolytes with opposite polarity to the counter-electrode at the solvent meniscus. Solvation and surface tension hinders the ions from traveling towards the counter electrode, and the meniscus deforms into a cone. If the applied electric field is high enough to overcome surface tension, a fine jet emerges from the cone, resulting in formation of small, highly charge micro droplets. The droplets are positively charged due to an excess of positively charged electrolytes such as H^+, Na^+, NH_4^+ and K^+ (also called charge carriers) at the surface and tip of the Taylor cone. The opposing ions (negative in the case of positive mode ESI) are oxidized at the capillary wall completing the electrical circuit. This type of charging that depends on separation of positive and negative ions into opposite directions is known as the electrophoretic mechanism.

The charged droplets produced from the Taylor cone move in the air (atmospheric pressure) towards the mass spectrometer (technically the counter electrode in the mass spectrometer), while undergoing solvent evaporation. As the charge density builds up in the shrinking droplet, there comes a point where charge repulsion approaches the surface tension of the shrinking droplet, known as the Rayleigh limit.[5] At the Rayleigh limit, a Coulomb fission of the droplet

takes place, forming smaller progeny droplets. This fission process repeats until very small, charged droplets with radii of few nanometers are formed that are ultimately capable of producing gas-phase ions.[2-3] The described process is illustrated in Figure 2.1.

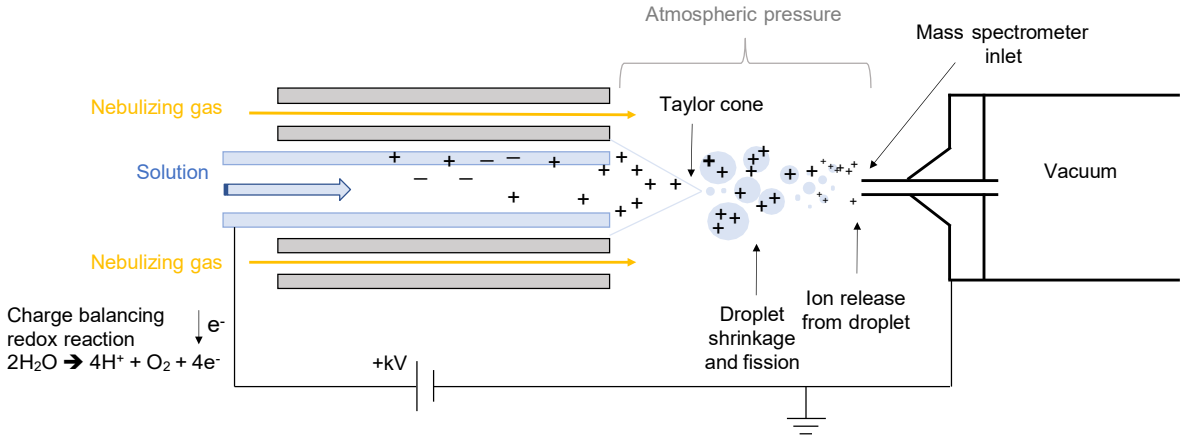

Figure 2.1. Schematic of the major steps in formation of ions from solution by electrospray ionization operated in positive mode.

2.1.2 Protein ionization in ESI

The intricacies in the final events of ESI that lead to formation of gaseous ions remain controversial, especially for complex systems such as intact proteins. It is accepted that gaseous ions that are ultimately detected by the mass spectrometer are produced from the last progeny droplets that have nanometer radii.[3] During ionization, the molecule can acquire a certain number of charges, depending on molecules characteristics and the experimental conditions. The ions are detected as peaks based on their mass-to-charge ratio (m/z). Unlike most small molecules that usually form a single peak in ESI, large molecules such as proteins typically form a distribution of peaks at different m/z values. Each peak corresponds to the mass of the protein divided by a certain number of charges, also known as a *charge state*. The molecular mass of a

protein can be calculated by knowing the m/z value of at least two adjacent charge states in the mass spectrum using equation (1), or by using deconvolution algorithms.[6-7]

$$P_{z} (m/z) = (M + z_{z})/z_{z}$$

$$P_{z+1} (m/z) = (M + (z_{z} + 1))/(z_{z} + 1) \quad (1)$$

For proteins, the distribution of peaks in the mass spectrum is called the protein charge state distribution (CSD). For a given set of experimental conditions, the protein CSD often appears approximately normally distributed.[8] The CSD of a protein is sometimes referred to as the protein "envelope", encompassing all the charge states in the distribution. As illustrated in Figure 2.2 the lowest observed charge state (LOCS), the highest observed charge state (HOCS) and the highest intensity charge state (HICS) are the descriptors of a protein envelope. Folded proteins typically yield a narrow CSD with a small number of charges on the protein peaks. In contrast, unfolded proteins yield broad CSD consisting of highly charged protein peaks. Figure 2.2 demonstrates differences of CSD of the same protein in folded and unfolded states.

Without a doubt, protein CSD has a significant dependence on protein conformation.[9-11] Numerous studies with a variety of biophysical techniques coupled to mass spectrometry, such as hydrogen/deuterium exchange,[12-13] and ion mobility,[14-15] support the relationship between charges on the protein and protein conformation, although the nuances of the relationship between protein CSD and conformation in solution are still under debate.[16-17] Nevertheless, it is generally accepted that ESI-MS can indeed capture some aspects, if not all, of protein solution conformations in the gas-phase by "freezing-out" structures that are in equilibrium in solution as

gas-phase ions.[18-21] This freezing process occurs due to evaporative-cooling, caused by rapid droplet desolvation.[22-23] Within the cooled droplet, energy barriers between protein conformations on the free-energy landscape become more difficult to overcome, resulting in kinetically "freezing out" the protein structures in the absence of a lubricating solvent and rapid proton transfer. As a result, the trapped solution-conformations emerge into the gas-phase as desolvated ions with a specific number of protons (or other charge carriers) depending on the exposed acidic and basic residues, contributing to the observation of the charge state distribution. In this way, dehydration and kinetic trapping enables retention of the protein solution-like conformations, which makes ESI extremely sensitive to protein structure and a valuable tool for structural analysis.[21, 24]

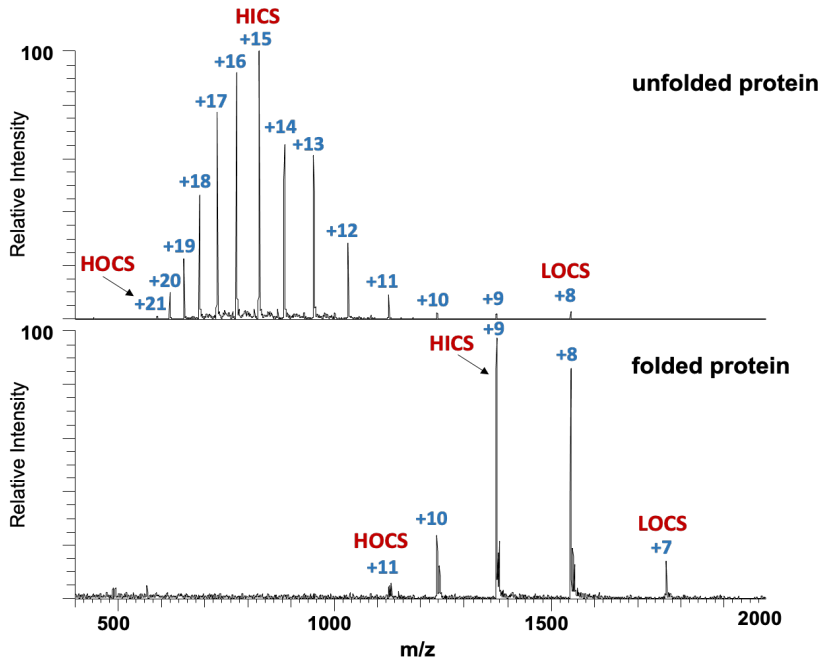

Figure 2.2. Mass spectra of a multiply charged protein, cytochrome *c* with molecular mass of 12.3 kDa, in unfolded and folded conformation.

Currently, there are three mechanisms that explain formation/release of the gas-phase ions from electrospray droplets, as illustrated in Figure 2.3: the ion evaporation model (IEM),[25] the charge residue model (CRM) and the more recently proposed chain ejection model (CEM)[26]. It is commonly accepted that small molecules with low molecular weight ionize by IEM while large molecules such as globular proteins and polymers ionize through CRM. CEM was proposed for ionization of disorderly polymers and unfolded proteins. The IEM typically yields the singly protonated ion of the analyte. The IEM is based on the fact that the electric field in the charged nanodroplet is sufficiently high to cause the ejection of small solvated ions from the droplet surface due to charge repulsion, overcoming surface tension and solvation forces.[25]

Generally, it is well accepted that folded, globular proteins ionize primarily by CRM.[27] In the CRM model, proteins ionize when the repetitious solvent evaporation and droplet fission result in the formation of droplets approaching the size of a single analyte that eventually evaporate to dryness. As this solvent shell is evaporating, the analyte becomes charged through a charge transfer process between the charge carriers on the surface of the droplet and the analyte molecule.[28] It has been shown that CRM droplets remain close to the Rayleigh limit throughout the entire evaporation process, implying that the droplet loses charges as it shrinks, possibly through IEM ejection of charge carriers or small molecules.[29] This is particularly interesting for globular, folded protein ionization, as experimental results showing charges on folded proteins are very close to the calculated Rayleigh charge of protein-sized water droplet.[30-31]

As CRM fell short on explaining the very broad CSD centered at high number of charges on unfolded proteins, the CEM model was proposed. Molecular dynamics (MD) simulations predict that in the last step of the ESI process, the unfolded proteins leave the shrinking droplet in a manner similar to IEM. According to the CEM model, unfolded proteins are driven to the

surface of electrospray droplet by hydrophobic and electrostatic forces, and gradually the unfolded protein is ejected from the droplet via a protruding "tail" that undergoes a charge equilibrium with the droplet due to H^+ migration. The H^+ transfer process results in the ejection of the polypeptide chain with a high number of charges. The MD studies on CEM accurately predicted the experimental data of unfolded protein charge states, highlighting the important role of protein conformation on observed charge state distribution.[26, 32]

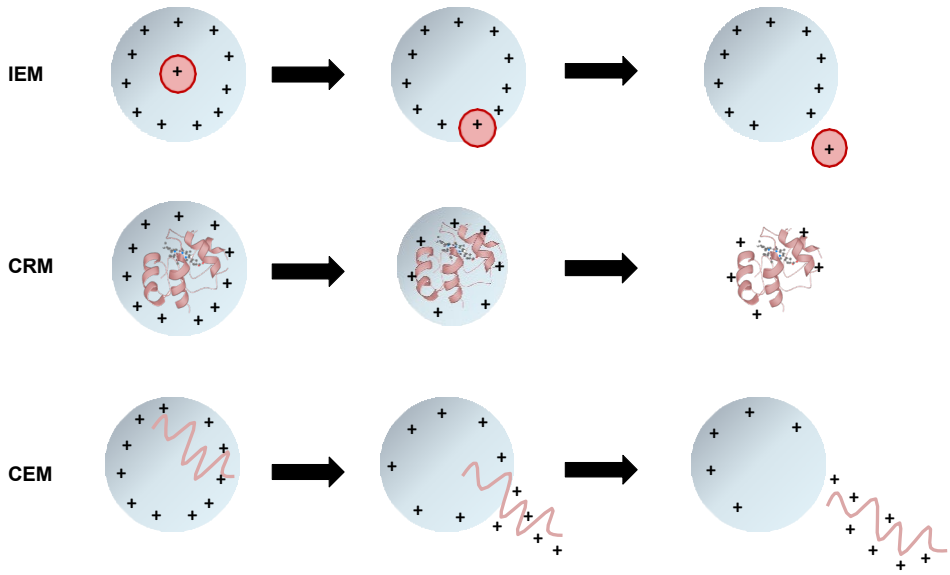

Figure 2.3. Schematic of ESI ionization models. IEM: ion evaporation model for small molecules, CRM: charge residue model for large, globular proteins, CEM: chain ejection model for large, unfolded proteins.[3]

CEM shares some resemblance to IEM. Although it was initially believed protein ionization by IEM is kinetically unfavorable,[3] recent MD simulations and ion mobility experiments have shown that small proteins in larger droplets (5.5 nm radius) can ionize via IEM, provided that the protein carries a sufficiently large positive charge in solution.[33] Overall, the three proposed models IEM/CRM/CEM, demonstrated in Figure 2.3, can now account for

most of the scenarios in ESI, and active research is still unraveling the final steps of the ESI process for different types of analytes.

2.2 Introduction to direct and ambient methods

Development of ambient ionization mass spectrometry in the mid 2000s revolutionized sample analysis by mass spectrometry.[34] Ambient ionization is the term used for any method in which ions are formed in an ion source outside the vacuum system of the mass spectrometer, under "ambient conditions". Ambient conditions refer to the intention that the sample is analyzed in its natural environment, although this is seldom achieved in practice. While it is often said that ambient ionization methods do not require sample preparation,[34-37] it is more accurate to say these methods frequently require no sample preparation, other than the sample processing that takes place during the analysis. In other words, *ambient ionization is a form of ionization where sample preparation takes place in real-time and proximal to the ionization, during the analysis of analytes*.[38]

It is important to distinguish between ambient and direct analysis. A purely ambient analysis is one where the sample is available for mass spectrometry analysis without any prior sample preparation or, in the ultimate case, the mass spectrometer is taken to the sample for analysis without disturbing the sample from its native environment. Ambient methods typically do the bulk of sample processing during the analysis step and rely on the mass spectrometer for separation and detection. A direct analysis usually requires some, but often minimal sample preparation, prior to the analysis. Direct methods rely on offline sample preparation (such as extraction, dissolving, desalting, etc.), while the analysis relies on the mass spectrometer alone for separation, similar to ambient methods. The immediacy and degree of sample preparation differentiates ambient analysis methods from direct mass spectrometry analysis. Direct analysis

is also frequently performed using the so-called ambient ionization sources, where some prior sample preparation precedes the real time-proximal sample processes inherent in the technique. Figure 2.4 illustrates the difference between ambient, direct, and hyphenated techniques coupled to mass spectrometry.

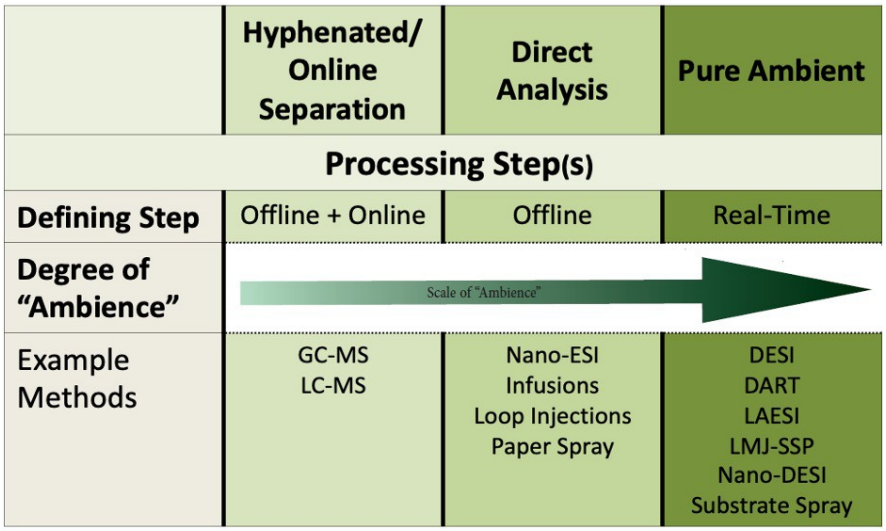

Figure 2.4. Differences between ambient, direct, and hyphenated techniques coupled to mass spectrometry.[38] *Anal. Methods*, 2017, **9**, 4896-4907. Copyright © 2017 The Royal Society of Chemistry.

In all the mentioned ambient and direct methods, ions are usually produced by well-known atmospheric pressure ionization (API) methods such as ion−molecule reactions, photochemical ionization, or from charged droplets by ESI mechanisms as discussed in Section 2.2.[36-37, 39-46]

Since the introduction of ambient ionization through the development of desorption electrospray ionization (DESI)[34] and direct analysis in real time (DART),[47] more than 80 ambient ionization methods have been developed.[38, 48-49] These methods have been reviewed extensively and categorized through various approaches in the past two decades.[50-51] An obvious approach is

for methods to be arranged primarily by either the sampling method or the ionization method, although it is common to first separate the methods by one aspect and then a second.[52] When primarily differentiated by sample processing, the techniques are often arranged based on the desorption mechanisms of (1) liquid extraction, (2) spallation/laser ablation and (3) thermal desorption.[51] Another "technique-centric" organization system based on both the extraction/desorption technique and ionization mechanism was used by Harris *et al.*[36] There are also subcategory reviews that are focused on the chemical aspects of liquid extraction-based methods[39] or the accompanying chemical processes.[53] A more detailed description of all ambient techniques and different categorization approaches can be found in our review article on this topic, provided in Appendix A. Below is a description of the liquid extraction-based methods, in particular desorption electrospray ionization (DESI), which is the main focus of this dissertation.

2.2.1 Liquid extraction methods

Sampling in extraction-based techniques generally involve liquid-solid extraction such as in DESI,[34] nano-DESI,[54] Liquid microjunction (LMJ),[55-56] liquid extraction surface analysis (LESA)[57] as shown in Figure 2.5. Liquid-liquid extraction is also possible with techniques such as liquid-DESI[58] and extractive electrospray ionization (EESI).[59] There are three major extraction-based methods for sample processing in ambient ionization: (1) spray desorption, (2) liquid microjunction and (3) substrate spray. These methods are organized based on the process by which the analyte is directed towards the ionization step. In spray desorption techniques (e.g., DESI), a spray of solvent generates charged droplets that form a thin layer on the sample, where the analyte is rapidly extracted from the surface followed by transfer of the ions or charged droplets to the atmospheric pressure ion inlet of the mass spectrometer. In liquid microjunction techniques (such as nano-DESI and LESA), a continuous-flow liquid stream forms a

microjunction on the surface and extraction occurs in-line. The analyte is then transported to an ionization source, usually ESI.

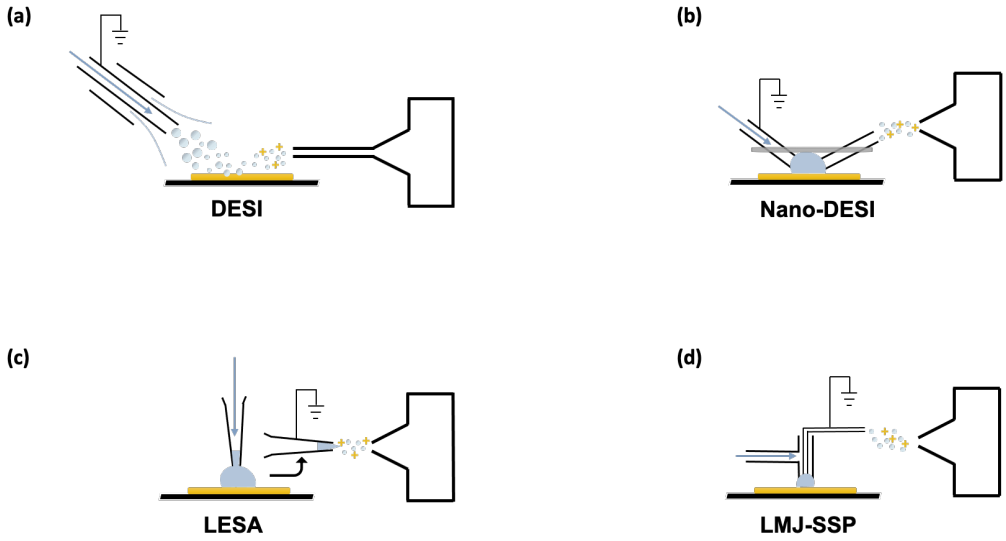

Figure 2.5. Schematic of liquid-extraction based ambient methods. (a) desorption electrospray ionization (DESI), (b) nano-DESI, (c), liquid extraction surface analysis (LESA), and (d) liquid microjunction-surface sampling probe (LMJ-SSP).

Extraction is greatly affected by solubility. In general, increasing solubility improves the response. It is important to note that in spray desorption methods where analysis of sample on a solid surface is desired (e.g., DESI), the desorption spray forms a liquid layer on the surface and extracts the dried sample through dissolution processes. In methods where the sample is already in liquid state (such as Liquid-DESI), dissolution is not part of the mechanism. Instead, mixing of the two liquid phases occur. For some types of analyte which do not readily dissolve on the time scale of the solid surface methods, such as proteins,[46] liquid-sampling methods and liquid-junction methods have been found to be much more sensitive than the spray desorption methods.[60-61]

2.2.2 Desorption electrospray ionization (DESI)

Among the different ambient methods developed, DESI is still one of the most readily adopted and widely used techniques.[34, 62-63] The success of DESI can partly be attributed to the fact that building a DESI source is relatively easy and low cost[64] and the solvent can be optimized for analyzing different compounds by changing its composition. The typical DESI setup is made of two co-axial capillaries that form a sprayer similar to a pneumatically assisted electrospray. The outer capillary delivers N_2 as nebulizing gas, and the inner capillary delivers a continuous flow of solvent. Upon applying voltage to the sprayer, pneumatically accelerated solvent droplets produced by electrospray process are directed at the surface with velocities around 100 to 120 m/s which extract the sample and guide it towards the mass spectrometer for detection by ESI.[65]

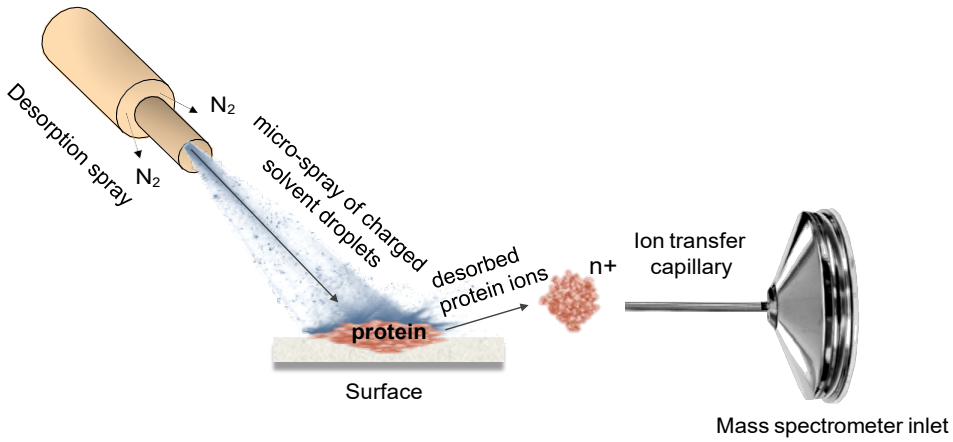

Figure 2.6. A simple schematic of DESI-MS analysis.

The sample analysis in DESI occurs through five steps, known as the "droplet pickup" process:[65-66] (1) formation of a spray plume (primary droplets) directed at the sample;[67-68] (2) formation of a micro-localized liquid layer on the sample surface;[69-71] (3) dissolution/extraction of the analyte into the liquid layer;[66-67] (4) release of analyte containing droplets (secondary droplets or also known as progeny droplets) from the liquid layer by pneumatically accelerated

primary droplets;[68, 70-71] and finally, (5) analyte ion generation from charged secondary droplets through ESI mechanisms.

In addition to parameters that can affect the electrospray process, many other parameters affect the signal obtained by DESI-MS,[72] including but not limited to, solvent composition,[67, 73] sprayer construction and geometry,[74] surface type,[75-76] relative humidity[77] and of course, the analyte's characteristics. Despite the complexity of the DESI process, over the last 18 years, DESI-MS has found widespread applications in many fields, including clinical studies[78-80], forensics[81-84], and pharmaceutical studies.[85-88] The rapid growth of DESI-MS is mainly thanks to its capabilities in performing high-throughput analysis[89-92] and imaging.[93-96] DESI-MS is still mostly considered for analysis of smaller molecules such as metabolites and lipids, while reports of protein analysis by DESI-MS are few and far between. Despite recent advances in *in situ* surface sampling of intact proteins from tissues by other ambient techniques such as LESA[97-98], and Nano-DESI,[99-101] the non-contact nature of DESI signifies an important advantage and motivates further development and improvements of DESI-MS for protein analysis.[102-103]

2.2.3. Methods used to improve protein analysis by DESI-MS

While it has often been stated that lower sensitivity in DESI of proteins is largely due to inefficient protein desorption, previous investigations of desorption during DESI-MS by spray desorption collection (SDC), which separates desorption from the ionization process, have shown that proteins, large and small, desorb equally well.[104-105] Moreover, a comparison between DESI and other liquid extraction-based techniques provide a different explanation for the impeded detection of proteins by DESI-MS. The timeframe for dissolution of proteins during DESI is much shorter than other liquid extraction-based techniques such as liquid-DESI, nano-

DESI, liquid extraction surface analysis (LESA) and liquid microjunction surface sampling probe.[104-105] Therefore, the slow and inefficient protein dissolution during the DESI extraction step is likely the major contributor to the poor performance of DESI for proteins.[105] DESI is commonly believed to follow the same electrospray ionization mechanisms of IEM, CRM and CEM, depending on analyte properties, as discussed in Section 2.2. Hence, the mass spectra acquired by DESI is very similar to ESI,[106-107] but not necessarily always identical.[108]

Several approaches to improve protein detection by DESI have focused on instrumentation, such as integration of a high field asymmetric waveform ion mobility (FAIMS) ion mobility to DESI-MS,[102] using a heated ion transfer inlet combined with traveling wave ion mobility separation,[103] removing the ion transfer inlet for direct ionization[109] and utilizing a two-step configuration for pre-wetting and delayed desorption of proteins.[110] However, additives offer an economical and more convenient and versatile alternative for enhancing protein signal in DESI-MS without significant modifications or additions to the standard setup. Optimizing the solvent composition[103] as well as using solution-phase additives such as formic acid and ammonium bicarbonate[111] are beneficial in proteins analysis by DESI-MS. For instance, simply adding ammonium bicarbonate to the DESI solvent system increased signal to noise ratio (S/N) of proteins 2- to 3-fold compared to a formic acid solvent system, and up to 7-fold compared to aqueous methanol solvent systems. A powerful additive for enhancing protein detection with the addition of serine is shown in Chapter 3, while Chapter 5 demonstrates benefits to using vapor phase additives. Finally, incorporation of an optimized geometry-independent DESI source can mitigate some of the intrinsic irreproducibility of DESI[74, 112] due to many variables in the source geometry and maximize the efficiency of the analysis in general.[113]

2.3 Conclusions

The aim of this chapter was to provide background information about ESI and DESI mechanisms as they relate to protein analysis by DESI-MS. Additional background information that pertains to each sub-project is provided in the appropriate chapters. We take advantage of the similarities between DESI and ESI in terms of ionization, together with the fact that the droplet pickup process is highly dependent on the analyte's solubility and dissolution, to investigate methods for improving protein analysis during DESI-MS, and to develop a mechanistic understanding of the observed improvements.

2.4 References

1. Fenn, J. B.; Mann, M.; Meng, C. K.; Wong, S. F.; Whitehouse, C. M., Electrospray Ionization–Principles and Practice. *Mass Spectrometry Reviews* **1990,** *9* (1), 37-70.
2. Kebarle, P.; Verkerk, U. H., Electrospray: From Ions in Solution to Ions in the Gas Phase, What We Know Now. *Mass Spectrometry Reviews* **2009,** *28* (6), 898-917.
3. Konermann, L.; Ahadi, E.; Rodriguez, A. D.; Vahidi, S., Unraveling the Mechanism of Electrospray Ionization. *Analytical Chemistry* **2013**, *85* (1), 2-9.
4. Taylor, G. I., Disintegration of Water Drops in an Electric Field. *Proceedings of the Royal Society of London Series A Mathematical and Physical Sciences* **1964,** *280* (1382), 383-397.
5. Rayleigh, L., Xx. On the Equilibrium of Liquid Conducting Masses Charged with Electricity. *The London, Edinburgh, and Dublin Philosophical Magazine and Journal of Science* **1882,** *14* (87), 184-186.
6. Marty, M. T.; Baldwin, A. J.; Marklund, E. G.; Hochberg, G. K.; Benesch, J. L.; Robinson, C. V., Bayesian Deconvolution of Mass and Ion Mobility Spectra: From Binary Interactions to Polydisperse Ensembles. *Analytical Chemistry* **2015,** *87* (8), 4370-4376.
7. Zhang, Z.; Marshall, A. G., A Universal Algorithm for Fast and Automated Charge State Deconvolution of Electrospray Mass-to-Charge Ratio Spectra. *Journal of The American Society for Mass Spectrometry* **1998,** *9* (3), 225-233.
8. Dobo, A.; Kaltashov, I. A., Detection of Multiple Protein Conformational Ensembles in Solution Via Deconvolution of Charge-State Distributions in Esi Ms. *Analytical Chemistry* **2001,** *73* (20), 4763-4773.
9. Chowdhury, S. K.; Katta, V.; Chait, B. T., Probing Conformational Changes in Proteins by Mass Spectrometry. *Journal of the American Chemical Society* **1990,** *112* (24), 9012-9013.
10. Loo, J. A.; Loo, R. R. O.; Udseth, H. R.; Edmonds, C. G.; Smith, R. D., Solvent-Induced Conformational Changes of Polypeptides Probed by Electrospray-Ionization Mass Spectrometry. *Rapid Communications in Mass Spectrometry* **1991,** *5* (3), 101-105.
11. Grandori, R., Origin of the Conformation Dependence of Protein Charge-State Distributions in Electrospray Ionization Mass Spectrometry. *Journal of Mass Spectrometry* **2003,** *38* (1), 11-15.
12. Yan, X.; Watson, J.; Ho, P. S.; Deinzer, M. L., Mass Spectrometric Approaches Using Electrospray Ionization Charge States and Hydrogen-Deuterium Exchange for Determining Protein Structures and Their Conformational Changes. *Molecular & Cellular Proteomics* **2004,** *3* (1), 10-23.

13. Konermann, L.; Tong, X.; Pan, Y., Protein Structure and Dynamics Studied by Mass Spectrometry: H/D Exchange, Hydroxyl Radical Labeling, and Related Approaches. *Journal of Mass Spectrometry* **2008,** *43* (8), 1021-1036.
14. Scarff, C. A.; Thalassinos, K.; Hilton, G. R.; Scrivens, J. H., Travelling Wave Ion Mobility Mass Spectrometry Studies of Protein Structure: Biological Significance and Comparison with X-Ray Crystallography and Nuclear Magnetic Resonance Spectroscopy Measurements. *Rapid Communications in Mass Spectrometry: An International Journal Devoted to the Rapid Dissemination of Up-to-the-Minute Research in Mass Spectrometry* **2008,** *22* (20), 3297-3304.
15. Canzani, D.; Laszlo, K. J.; Bush, M. F., Ion Mobility of Proteins in Nitrogen Gas: Effects of Charge State, Charge Distribution, and Structure. *The Journal of Physical Chemistry A* **2018,** *122* (25), 5625-5634.
16. Li, J.; Santambrogio, C.; Brocca, S.; Rossetti, G.; Carloni, P.; Grandori, R., Conformational Effects in Protein Electrospray-Ionization Mass Spectrometry. *Mass Spectrometry Reviews* **2016,** *35* (1), 111-122.
17. Khristenko, N.; Amato, J.; Livet, S.; Pagano, B.; Randazzo, A.; Gabelica, V., Native Ion Mobility Mass Spectrometry: When Gas-Phase Ion Structures Depend on the Electrospray Charging Process. *Journal of The American Society for Mass Spectrometry* **2019,** *30* (6), 1069-1081.
18. El-Baba, T. J.; Woodall, D. W.; Raab, S. A.; Fuller, D. R.; Laganowsky, A.; Russell, D. H.; Clemmer, D. E., Melting Proteins: Evidence for Multiple Stable Structures Upon Thermal Denaturation of Native Ubiquitin from Ion Mobility Spectrometry-Mass Spectrometry Measurements. *Journal of the American Chemical Society* **2017,** *139* (18), 6306-6309.
19. Ruotolo, B. T.; Robinson, C. V., Aspects of Native Proteins Are Retained in Vacuum. *Current Opinion in Chemical Biology* **2006,** *10* (5), 402-408.
20. McAllister, R. G.; Metwally, H.; Sun, Y.; Konermann, L., Release of Native-Like Gaseous Proteins from Electrospray Droplets Via the Charged Residue Mechanism: Insights from Molecular Dynamics Simulations. *Journal of the American Chemical Society* **2015,** *137* (39), 12667-12676.
21. Silveira, J. A.; Fort, K. L.; Kim, D.; Servage, K. A.; Pierson, N. A.; Clemmer, D. E.; Russell, D. H., From Solution to the Gas Phase: Stepwise Dehydration and Kinetic Trapping of Substance P Reveals the Origin of Peptide Conformations. *Journal of the American Chemical Society* **2013,** *135* (51), 19147-19153.
22. Lee, S.-W.; Freivogel, P.; Schindler, T.; Beauchamp, J., Freeze-Dried Biomolecules: Ft-Icr Studies of the Specific Solvation of Functional Groups and Clathrate Formation Observed by the Slow Evaporation of Water from Hydrated Peptides and Model Compounds in the Gas Phase. *Journal of the American Chemical Society* **1998,** *120* (45), 11758-11765.
23. Breuker, K.; McLafferty, F. W., Stepwise Evolution of Protein Native Structure with Electrospray into the Gas Phase, 10− 12 to 102 S. *Proceedings of the National Academy of Sciences* **2008,** *105* (47), 18145-18152.
24. Raab, S. A.; El-Baba, T. J.; Laganowsky, A.; Russell, D. H.; Valentine, S. J.; Clemmer, D. E., Protons Are Fast and Smart; Proteins Are Slow and Dumb: On the Relationship of Electrospray Ionization Charge States and Conformations. *Journal of The American Society for Mass Spectrometry* **2021,** *32* (7), 1553-1561.
25. Iribarne, J.; Thomson, B., On the Evaporation of Small Ions from Charged Droplets. *The Journal of Chemical Physics* **1976,** *64* (6), 2287-2294.
26. Konermann, L.; Rodriguez, A. D.; Liu, J., On the Formation of Highly Charged Gaseous Ions from Unfolded Proteins by Electrospray Ionization. *Analytical Chemistry* **2012,** *84* (15), 6798-6804.
27. De La Mora, J. F., Electrospray Ionization of Large Multiply Charged Species Proceeds Via Dole's Charged Residue Mechanism. *Analytica Chimica Acta* **2000,** *406* (1), 93-104.
28. Dole, M.; Mack, L. L.; Hines, R. L.; Mobley, R. C.; Ferguson, L. D.; Alice, M. B., Molecular Beams of Macroions. *The Journal of Chemical Physics* **1968,** *49* (5), 2240-2249.

29. Hogan Jr, C. J.; Carroll, J. A.; Rohrs, H. W.; Biswas, P.; Gross, M. L., Combined Charged Residue-Field Emission Model of Macromolecular Electrospray Ionization. *Analytical Chemistry* **2009,** *81* (1), 369-377.
30. Heck, A. J.; Van Den Heuvel, R. H., Investigation of Intact Protein Complexes by Mass Spectrometry. *Mass Spectrometry Reviews* **2004,** *23* (5), 368-389.
31. Kaltashov, I. A.; Mohimen, A., Estimates of Protein Surface Areas in Solution by Electrospray Ionization Mass Spectrometry. *Analytical Chemistry* **2005,** *77* (16), 5370-5379.
32. Metwally, H.; Duez, Q.; Konermann, L., Chain Ejection Model for Electrospray Ionization of Unfolded Proteins: Evidence from Atomistic Simulations and Ion Mobility Spectrometry. *Analytical Chemistry* **2018,** *90* (16), 10069-10077.
33. Aliyari, E.; Konermann, L., Formation of Gaseous Proteins Via the Ion Evaporation Model (Iem) in Electrospray Mass Spectrometry. *Analytical Chemistry* **2020,** *92* (15), 10807-10814.
34. Takats, Z.; Wiseman, J. M.; Gologan, B.; Cooks, R. G., Mass Spectrometry Sampling under Ambient Conditions with Desorption Electrospray Ionization. *Science* **2004,** *306* (5695), 471-473.
35. Venter, A.; Nefliu, M.; Graham Cooks, R., Ambient Desorption Ionization Mass Spectrometry. *TrAC Trends in Analytical Chemistry* **2008,** *27* (4), 284-290.
36. Harris, G. A.; Galhena, A. S.; Fernandez, F. M., Ambient Sampling/Ionization Mass Spectrometry: Applications and Current Trends. *Analytical Chemistry* **2011,** *83* (12), 4508-4538.
37. Huang, M.-Z.; Cheng, S.-C.; Cho, Y.-T.; Shiea, J., Ambient Ionization Mass Spectrometry: A Tutorial. *Analytica Chimica Acta* **2011,** *702* (1), 1-15.
38. Javanshad, R.; Venter, A., Ambient Ionization Mass Spectrometry: Real-Time, Proximal Sample Processing and Ionization. *Analytical Methods* **2017,** *9* (34), 4896-4907.
39. Badu-Tawiah, A. K.; Eberlin, L. S.; Ouyang, Z.; Cooks, R. G., Chemical Aspects of the Extractive Methods of Ambient Ionization Mass Spectrometry. *Annual Review of Physical Chemistry* **2013,** *64*, 481-505.
40. Cole, R. B., *Electrospray and Maldi Mass Spectrometry: Fundamentals, Instrumentation, Practicalities, and Biological Applications*. John Wiley & Sons: 2011.
41. Trimpin, S.; Wang, B.; Lietz, C. B.; Marshall, D. D.; Richards, A. L.; Inutan, E. D., New Ionization Processes and Applications for Use in Mass Spectrometry. *Critical Reviews in Biochemistry and Molecular Biology* **2013,** *48* (5), 409-429.
42. Konermann, L.; Ahadi, E.; Rodriguez, A. D.; Vahidi, S., Unraveling the Mechanism of Electrospray Ionization. *Analytical Chemistry* **2013**, *85* (1), 2-9.
43. Hogan Jr, C. J.; Carroll, J. A.; Rohrs, H. W.; Biswas, P.; Gross, M. L., A Combined Charged Residue-Field Emission Model of Macromolecular Electrospray Ionization. *Analytical Chemistry* **2009,** *81* (1), 369-377.
44. Daub, C. D.; Cann, N. M., How Are Completely Desolvated Ions Produced in Electrospray Ionization: Insights from Molecular Dynamics Simulations. *Analytical Chemistry* **2011,** *83* (22), 8372-8376.
45. Chung, J. K.; Consta, S., Release Mechanisms of Poly (Ethylene Glycol) Macroions from Aqueous Charged Nanodroplets. *The Journal of Physical Chemistry B* **2012,** *116* (19), 5777-5785.
46. Douglass, K. A.; Venter, A. R., Predicting the Highest Intensity Ion in Multiple Charging Envelopes Observed for Denatured Proteins During Electrospray Ionization Mass Spectrometry by Inspection of the Amino Acid Sequence. *Analytical Chemistry* **2013,** *85* (17), 8212-8218.
47. Cody, R. B.; Laramée, J. A.; Durst, H. D., Versatile New Ion Source for the Analysis of Materials in Open Air under Ambient Conditions. *Analytical chemistry* **2005,** *77* (8), 2297-2302.
48. Monge, M. E.; Harris, G. A.; Dwivedi, P.; Fernández, F. M., Mass Spectrometry: Recent Advances in Direct Open Air Surface Sampling/Ionization. *Chemical Reviews* **2013,** *113* (4), 2269-2308.
49. Venter, A. R.; Douglass, K. A.; Shelley, J. T.; Hasman Jr, G.; Honarvar, E., Mechanisms of Real-Time, Proximal Sample Processing During Ambient Ionization Mass Spectrometry. *Analytical Chemistry* **2014,** *86* (1), 233-249.

50. Lebedev, A. b. T., Ambient Ionization Mass Spectrometry. *Russian Chemical Reviews* **2015,** *84* (7), 665-692.
51. Venter, A. R.; Douglass, K. A.; Shelley, J. T.; Hasman, G.; Honarvar, E., Mechanisms of Real-Time, Proximal Sample Processing During Ambient Ionization Mass Spectrometry. *Analytical Chemistry* **2014,** *86* (1), 233-249.
52. Huang, M.-Z.; Yuan, C.-H.; Cheng, S.-C.; Cho, Y.-T.; Shiea, J., Ambient Ionization Mass Spectrometry. *Annual Review of Analytical Chemistry* **2010,** *3*, 43-65.
53. Ifa, D. R.; Wu, C.; Ouyang, Z.; Cooks, R. G., Desorption Electrospray Ionization and Other Ambient Ionization Methods: Current Progress and Preview. *Analyst* **2010,** *135* (4), 669-681.
54. Roach, P. J.; Laskin, J.; Laskin, A., Nanospray Desorption Electrospray Ionization: An Ambient Method for Liquid-Extraction Surface Sampling in Mass Spectrometry. *Analyst* **2010,** *135* (9), 2233-2236.
55. Van Berkel, G. J.; Sanchez, A. D.; Quirke, J. M. E., Thin-Layer Chromatography and Electrospray Mass Spectrometry Coupled Using a Surface Sampling Probe. *Analytical Chemistry* **2002,** *74* (24), 6216-6223.
56. Wachs, T.; Henion, J., Electrospray Device for Coupling Microscale Separations and Other Miniaturized Devices with Electrospray Mass Spectrometry. *Analytical Chemistry* **2001,** *73* (3), 632-638.
57. Kertesz, V.; Van Berkel, G. J., Liquid Microjunction Surface Sampling Coupled with High-Pressure Liquid Chromatography− Electrospray Ionization-Mass Spectrometry for Analysis of Drugs and Metabolites in Whole-Body Thin Tissue Sections. *Analytical Chemistry* **2010,** *82* (14), 5917-5921.
58. Miao, Z.; Chen, H., Direct Analysis of Liquid Samples by Desorption Electrospray Ionization-Mass Spectrometry (Desi-Ms). *Journal of the American Society for Mass Spectrometry* **2009,** *20* (1), 10-19.
59. Chen, H.; Venter, A.; Cooks, R. G., Extractive Electrospray Ionization for Direct Analysis of Undiluted Urine, Milk and Other Complex Mixtures without Sample Preparation. *Chemical Communications* **2006,** (19), 2042-2044.
60. Ferguson, C. N.; Benchaar, S. A.; Miao, Z.; Loo, J. A.; Chen, H., Direct Ionization of Large Proteins and Protein Complexes by Desorption Electrospray Ionization-Mass Spectrometry. *Analytical Chemistry* **2011,** *83* (17), 6468-6473.
61. Kocurek, K. I.; Griffiths, R. L.; Cooper, H. J., Ambient Ionisation Mass Spectrometry for in Situ Analysis of Intact Proteins. *Journal of Mass Spectrometry* **2018,** *53* (7), 565-578.
62. Ferreira, C.; Alfaro, C. M.; Pirro, V.; Cooks, R. G., Desorption Electrospray Ionization Mass Spectrometry Imaging: Recent Developments and Perspectives. *Journal of Biomolecular Techniques: JBT* **2019,** *30* (Suppl), S46-.
63. Beneito-Cambra, M.; Gilbert-López, B.; Moreno-González, D.; Bouza, M.; Franzke, J.; García-Reyes, J. F.; Molina-Díaz, A., Ambient (Desorption/Ionization) Mass Spectrometry Methods for Pesticide Testing in Food: A Review. *Analytical Methods* **2020,** *12* (40), 4831-4852.
64. Zemaitis, K. J.; Wood, T. D., Integration of 3d-Printing for a Desorption Electrospray Ionization Source for Mass Spectrometry. *Review of Scientific Instruments* **2020,** *91* (10), 104102.
65. Venter, A.; Sojka, P. E.; Cooks, R. G., Droplet Dynamics and Ionization Mechanisms in Desorption Electrospray Ionization Mass Spectrometry. *Analytical Chemistry* **2006,** *78* (24), 8549-8555.
66. Badu-Tawiah, A.; Bland, C.; Campbell, D. I.; Cooks, R. G., Non-Aqueous Spray Solvents and Solubility Effects in Desorption Electrospray Ionization. *Journal of The American Society for Mass Spectrometry* **2010,** *21* (4), 572-579.
67. Green, F.; Salter, T.; Gilmore, I.; Stokes, P.; O'connor, G., The Effect of Electrospray Solvent Composition on Desorption Electrospray Ionisation (Desi) Efficiency and Spatial Resolution. *Analyst* **2010,** *135* (4), 731-737.
68. Olumee, Z.; Callahan, J. H.; Vertes, A., Droplet Dynamics Changes in Electrostatic Sprays of Methanol− Water Mixtures. *The Journal of Physical Chemistry A* **1998,** *102* (46), 9154-9160.

69. Zivolic, F.; Zancanaro, F.; Favretto, D.; Ferrara, S. D.; Seraglia, R.; Traldi, P., Pneumatically Assisted Desorption/Ionization: 1. Some Thoughts on the Possible Ionization Mechanism (S). *Journal of mass spectrometry* **2010,** *45* (4), 411-420.
70. Costa, A. B.; Cooks, R. G., Simulation of Atmospheric Transport and Droplet–Thin Film Collisions in Desorption Electrospray Ionization. *Chemical Communications* **2007,** (38), 3915-3917.
71. Costa, A. B.; Cooks, R. G., Simulated Splashes: Elucidating the Mechanism of Desorption Electrospray Ionization Mass Spectrometry. *Chemical Physics Letters* **2008,** *464* (1-3), 1-8.
72. Campbell, D. I.; Ferreira, C. R.; Eberlin, L. S.; Cooks, R. G., Improved Spatial Resolution in the Imaging of Biological Tissue Using Desorption Electrospray Ionization. *Analytical and Bioanalytical Chemistry* **2012,** *404* (2), 389-398.
73. Eberlin, L. S.; Ferreira, C. R.; Dill, A. L.; Ifa, D. R.; Cheng, L.; Cooks, R. G., Non-Destructive, Histologically Compatible Tissue Imaging by Desorption Electrospray Ionization Mass Spectrometry. *Chembiochem: a European Journal of Chemical Biology* **2011,** *12* (14), 2129-2132.
74. Tillner, J.; Wu, V.; Jones, E. A.; Pringle, S. D.; Karancsi, T.; Dannhorn, A.; Veselkov, K.; McKenzie, J. S.; Takats, Z., Faster, More Reproducible Desi-Ms for Biological Tissue Imaging. *Journal of The American Society for Mass Spectrometry* **2017,** *28* (10), 2090-2098.
75. Volný, M.; Venter, A.; Smith, S. A.; Pazzi, M.; Cooks, R. G., Surface Effects and Electrochemical Cell Capacitance in Desorption Electrospray Ionization. *Analyst* **2008,** *133* (4), 525-531.
76. Kertesz, V.; Van Berkel, G. J., Improved Imaging Resolution in Desorption Electrospray Ionization Mass Spectrometry. *Rapid Communications in Mass Spectrometry: An International Journal Devoted to the Rapid Dissemination of Up-to-the-Minute Research in Mass Spectrometry* **2008,** *22* (17), 2639-2644.
77. Feider, C. L.; DeHoog, R. J.; Sans, M.; Zhang, J.; Krieger, A.; Eberlin, L. S., Desi Spray Stability in the Negative Ion Mode Is Dependent on Relative Humidity. *Journal of The American Society for Mass Spectrometry* **2018,** *30* (2), 376-380.
78. Wiseman, J. M.; Evans, C. A.; Bowen, C. L.; Kennedy, J. H., Direct Analysis of Dried Blood Spots Utilizing Desorption Electrospray Ionization (Desi) Mass Spectrometry. *Analyst* **2010,** *135* (4), 720-725.
79. Woolman, M.; Tata, A.; Bluemke, E.; Dara, D.; Ginsberg, H. J.; Zarrine-Afsar, A., An Assessment of the Utility of Tissue Smears in Rapid Cancer Profiling with Desorption Electrospray Ionization Mass Spectrometry (Desi-Ms). *Journal of The American Society for Mass Spectrometry* **2016,** *28* (1), 145-153.
80. Wiseman, J. M.; Kennedy, J. H., Analysis of Dried Blood Spots Using Desi Mass Spectrometry. In *Mass Spectrometry in Metabolomics*, Springer: **2014**, 291-297.
81. Wójtowicz, A.; Wietecha-Posłuszny, R., Desi-Ms Analysis of Human Fluids and Tissues for Forensic Applications. *Applied Physics A* **2019,** *125* (5), 1-9.
82. Sugiura, Y.; Sugiyama, E.; Suematsu, M., Desi-Based Imaging Mass Spectrometry in Forensic Science and Clinical Diagnosis. In *Ambient Ionization Mass Spectrometry in Life Sciences*, Elsevier: **2020**, 107-118.
83. Fresnais, M.; Haefeli, W. E.; Burhenne, J.; Longuespée, R., Rapid Drug Detection in Whole Blood Droplets Using a Desorption Electrospray Ionization Static Profiling Approach–a Proof-of-Concept. *Rapid Communications in Mass Spectrometry* **2020,** *34* (6), e8614.
84. Morelato, M.; Beavis, A.; Kirkbride, P.; Roux, C., Forensic Applications of Desorption Electrospray Ionisation Mass Spectrometry (Desi-Ms). *Forensic Science International* **2013,** *226* (1-3), 10-21.
85. Fresnais, M.; Haefeli, W. E.; Burhenne, J.; Longuespée, R., Advances in Clinical Pharmacology: Rapid Detection of Small Molecules in Solid Samples at Atmospheric Pressure Using Desorption Electrospray Ionization. *Omics: a journal of integrative biology* **2020,** *24* (1), 53-54.
86. Lubin, A.; Cabooter, D.; Augustijns, P.; Cuyckens, F., One Drop Chemical Derivatization–Desi-Ms Analysis for Metabolite Structure Identification. *Journal of Mass Spectrometry* **2015,** *50* (7), 871-878.

87. Roscioli, K. M.; Tufariello, J. A.; Zhang, X.; Li, S. X.; Goetz, G. H.; Cheng, G.; Siems, W. F.; Hill, H. H., Desorption Electrospray Ionization (Desi) with Atmospheric Pressure Ion Mobility Spectrometry for Drug Detection. *Analyst* **2014,** *139* (7), 1740-1750.
88. Weston, D. J.; Bateman, R.; Wilson, I. D.; Wood, T. R.; Creaser, C. S., Direct Analysis of Pharmaceutical Drug Formulations Using Ion Mobility Spectrometry/Quadrupole-Time-of-Flight Mass Spectrometry Combined with Desorption Electrospray Ionization. *Analytical chemistry* **2005,** *77* (23), 7572-7580.
89. Sobreira, T. J. P.; Avramova, L.; Szilagyi, B.; Logsdon, D. L.; Loren, B. P.; Jaman, Z.; Hilger, R. T.; Hosler, R. S.; Ferreira, C. R.; Koswara, A., High-Throughput Screening of Organic Reactions in Microdroplets Using Desorption Electrospray Ionization Mass Spectrometry (Desi-Ms): Hardware and Software Implementation. *Analytical Methods* **2020,** *12* (28), 3654-3669.
90. Wleklinski, M.; Loren, B. P.; Ferreira, C. R.; Jaman, Z.; Avramova, L.; Sobreira, T. J.; Thompson, D. H.; Cooks, R. G., High Throughput Reaction Screening Using Desorption Electrospray Ionization Mass Spectrometry. *Chemical science* **2018,** *9* (6), 1647-1653.
91. Morato, N. M.; Holden, D. T.; Cooks, R. G., High-Throughput Label-Free Enzymatic Assays Using Desorption Electrospray-Ionization Mass Spectrometry. *Angewandte Chemie International Edition* **2020,** *59* (46), 20459-20464.
92. Logsdon, D. L.; Li, Y.; Paschoal Sobreira, T. J.; Ferreira, C. R.; Thompson, D. H.; Cooks, R. G., High-Throughput Screening of Reductive Amination Reactions Using Desorption Electrospray Ionization Mass Spectrometry. *Organic Process Research & Development* **2020,** *24* (9), 1647-1657.
93. Wiseman, J. M.; Ifa, D. R.; Song, Q.; Cooks, R. G., Tissue Imaging at Atmospheric Pressure Using Desorption Electrospray Ionization (Desi) Mass Spectrometry. *Angewandte Chemie International Edition* **2006,** *45* (43), 7188-7192.
94. Wiseman, J. M.; Ifa, D. R.; Zhu, Y.; Kissinger, C. B.; Manicke, N. E.; Kissinger, P. T.; Cooks, R. G., Desorption Electrospray Ionization Mass Spectrometry: Imaging Drugs and Metabolites in Tissues. *Proceedings of the National Academy of Sciences* **2008,** *105* (47), 18120-18125.
95. Cordeiro, F. B.; Jarmusch, A. K.; León, M.; Ferreira, C. R.; Pirro, V.; Eberlin, L. S.; Hallett, J.; Miglino, M. A.; Cooks, R. G., Mammalian Ovarian Lipid Distributions by Desorption Electrospray Ionization–Mass Spectrometry (Desi-Ms) Imaging. *Analytical and Bioanalytical Chemistry* **2020,** *412* (6), 1251-1262.
96. Quartier, J.; Rao, W.; Slade, S.; Métral, F.; Lapteva, M.; Kalia, Y. N., Desi-Ms Imaging to Visualize Spatial Distribution of Xenobiotics and Endogenous Lipids in the Skin. *International Journal of Pharmaceutics* **2021**, 120967.
97. Griffiths, R. L.; Cooper, H. J., Direct Tissue Profiling of Protein Complexes: Toward Native Mass Spectrometry Imaging. *Analytical Chemistry* **2016,** *88* (1), 606-609.
98. Griffiths, R. L.; Sisley, E. K.; Lopez-Clavijo, A. F.; Simmonds, A. L.; Styles, I. B.; Cooper, H. J., Native Mass Spectrometry Imaging of Intact Proteins and Protein Complexes in Thin Tissue Sections. *International Journal of Mass Spectrometry* **2019,** *437*, 23-29.
99. Hale, O. J.; Cooper, H. J., Native Mass Spectrometry Imaging of Proteins and Protein Complexes by Nano-Desi. *Analytical Chemistry* **2021,** *93* (10), 4619-4627.
100. Hsu, C.-C.; Chou, P.-T.; Zare, R. N., Imaging of Proteins in Tissue Samples Using Nanospray Desorption Electrospray Ionization Mass Spectrometry. *Analytical Chemistry* **2015,** *87* (22), 11171-11175.
101. Hale, O. J.; Hughes, J. W.; Cooper, H. J., Simultaneous Spatial, Conformational, and Mass Analysis of Intact Proteins and Protein Assemblies by Nano-Desi Travelling Wave Ion Mobility Mass Spectrometry Imaging. *International Journal of Mass Spectrometry* **2021**, 468, 116656.
102. Garza, K. Y.; Feider, C. L.; Klein, D. R.; Rosenberg, J. A.; Brodbelt, J. S.; Eberlin, L. S., Desorption Electrospray Ionization Mass Spectrometry Imaging of Proteins Directly from Biological Tissue Sections. *Analytical Chemistry* **2018,** *90* (13), 7785-7789.
103. Towers, M. W.; Karancsi, T.; Jones, E. A.; Pringle, S. D.; Claude, E., Optimised Desorption Electrospray Ionisation Mass Spectrometry Imaging (Desi-Msi) for the Analysis of Proteins/Peptides

Directly from Tissue Sections on a Travelling Wave Ion Mobility Q-Tof. *Journal of The American Society for Mass Spectrometry* **2018,** *29* (12), 2456-2466.
104. Douglass, K. A.; Jain, S.; Brandt, W. R.; Venter, A. R., Deconstructing Desorption Electrospray Ionization: Independent Optimization of Desorption and Ionization by Spray Desorption Collection. *Journal of The American Society for Mass Spectrometry* **2012,** *23* (11), 1896-1902.
105. Douglass, K. A.; Venter, A. R., Protein Analysis by Desorption Electrospray Ionization Mass Spectrometry and Related Methods. *Journal of Mass Spectrometry* **2013,** *48* (5), 553-560.
106. Shin, Y.-S.; Drolet, B.; Mayer, R.; Dolence, K.; Basile, F., Desorption Electrospray Ionization-Mass Spectrometry of Proteins. *Analytical Chemistry* **2007,** *79* (9), 3514-3518.
107. Takats, Z.; Wiseman, J. M.; Cooks, R. G., Ambient Mass Spectrometry Using Desorption Electrospray Ionization (Desi): Instrumentation, Mechanisms and Applications in Forensics, Chemistry, and Biology. *Journal of Mass Spectrometry* **2005,** *40* (10), 1261-1275.
108. Honarvar, E.; Venter, A. R., Comparing the Effects of Additives on Protein Analysis between Desorption Electrospray (Desi) and Electrospray Ionization (Esi). *Journal of The American Society for Mass Spectrometry* **2018,** *29* (12), 2443-2455.
109. Ambrose, S.; Housden, N. G.; Gupta, K.; Fan, J.; White, P.; Yen, H. Y.; Marcoux, J.; Kleanthous, C.; Hopper, J. T.; Robinson, C. V., Native Desorption Electrospray Ionization Liberates Soluble and Membrane Protein Complexes from Surfaces. *Angewandte Chemie* **2017,** *129* (46), 14655-14660.
110. Maser, T. L.; Honarvar, E.; Venter, A. R., Delayed Desorption Improves Protein Analysis by Desorption Electrospray Ionization Mass Spectrometry. *Journal of The American Society for Mass Spectrometry* **2020,** *31* (4), 803-811.
111. Honarvar, E.; Venter, A. R., Ammonium Bicarbonate Addition Improves the Detection of Proteins by Desorption Electrospray Ionization Mass Spectrometry. *Journal of The American Society for Mass Spectrometry* **2017,** *28* (6), 1109-1117.
112. Abbassi-Ghadi, N.; Jones, E. A.; Veselkov, K. A.; Huang, J.; Kumar, S.; Strittmatter, N.; Golf, O.; Kudo, H.; Goldin, R. D.; Hanna, G. B., Repeatability and Reproducibility of Desorption Electrospray Ionization-Mass Spectrometry (Desi-Ms) for the Imaging Analysis of Human Cancer Tissue: A Gateway for Clinical Applications. *Analytical Methods* **2015,** *7* (1), 71-80.
113. Venter, A.; Cooks, R. G., Desorption Electrospray Ionization in a Small Pressure-Tight Enclosure. *Analytical Chemistry* **2007,** *79* (16), 6398-6403.

CHAPTER 3

3. ADDITION OF SERINE IMPROVES PROTEIN ANALYSIS BY DESI-MS

Reprinted (adapted) with permission from
R. Javanshad, E. Honarvar and A. R. Venter
J. Am. Soc. Mass Spectrom. **2019**, 30, 4, 694–703

3.1 Introduction

The resemblance of DESI spectra to typical ESI spectra alongside little to no sample preparation prior to analysis gives DESI an advantage over many other ionization techniques.[125] Indeed, since its development just over a decade ago, DESI has shown great versatility for investigating an assortment of analytes[68] such as intact bacteria in vitro and in vivo,[126-128] secondary metabolites,[129-130] diverse compounds in the pharmaceutical industry,[131-135] thin-layer chromatography,[136-139] and imaging a wide variety of analytes from biological tissues,[107-108, 140-141] recently including imaging of low molecular weight proteins.[142-143] However, DESI suffers a significant mass-dependent loss in sensitivity. As the mass of the protein increases, the limit of detection increases exponentially.[75,144] Although it is commonly believed ESI and DESI are similar in ionization mechanism, however, there is evidence that suggests differences between the two.[145] Ionization in DESI is commonly believed to involve the "droplet pick-up" mechanism, i.e., extraction of the analyte into the solvent surface layer, followed by liberation of secondary solvent droplets, and finally electrospray ionization mechanisms.[80] Our group has

previously developed methods that enable investigating desorption and ionization steps of DESI independently.[17, 146] Those results suggested that the loss in protein signal intensity was not due to problems with physical desorption or ionization, but rather due to incomplete protein dissolution during the desorption step, which results in distribution of protein signal across nonspecific protein-adducts.

A simple method for improving protein solubility and long-term stability, especially in a concentrated solution of proteins, is the addition of amino acids.[147-148] Such amino acid stabilizers are routinely added to protein solutions during biochemical processes and are favorable additives due to their low cost and safety. Arginine (Arg) and proline (Pro) stabilizers have been shown to suppress protein aggregation during refolding,[149-153] presumably by increasing the solubility of aggregated proteins.[154-155] Histidine (His)[156] and Alanine (Ala)[157] have demonstrated stabilizing capabilities by suppressing heat-induced denaturation. The stabilizing effect of amino acids against thermal denaturation of proteins and non-covalent protein complexes has been confirmed in ESI-MS.[158]

Adducts caused by non-volatile salts such as alkali metal ions Na^+ and K^+ can cause salt-induced "signal suppression"[159-163] and deteriorate signal to noise ratio (S/N)[164-165] even at micromolar concentrations.[166] Several methods have been developed to address this problem in ESI-MS, such as buffer loading,[159, 165, 167-169] supercharging reagents,[170] organic vapors,[171] and additives such as volatile buffers[172-175] or salts such as ammonium acetate,[167] ammonium bicarbonate, and formic acid.[159] A recent addition to the list of additives is free amino acids which at low millimolar concentration showed removal of sodium adducts during native nESI-MS of large proteins, increased S/N ~4 fold, and caused peak narrowing by 10 fold.[176] In this

study by Clarke *et al.* serine was the most successful amino acid in reducing sodium adduction to native state proteins during ESI-MS, and removal of up to 1 mM NaCl was demonstrated.

DESI, much like ESI, also suffers from well-known interferences caused by non-volatile salts.[177] Similar approaches regarding additives have been carried out for DESI-MS spray solvent composition, and some of these additives were successful at improving DESI-MS sensitivity, selectivity, and limit of detection for smaller analytes.[82, 178-180] Data have shown that the addition of ammonium bicarbonate to the DESI solvent system can improve S/N for some proteins between two to three fold relative to the same solvent system containing 0.1% (v/v) formic acid, and more than seven times relative to 50% MeOH:H_2O.[181]

In this study, we explored the effect of serine as an additive on the analysis of proteins by DESI-MS with different solvent systems. Different proteins with high and low isoelectric point (pI) and molecular weights ranging from 12 kDa to 66 kDa were studied to assess the efficacy of serine in adduct removal and enhancing protein signal. Data show that sodium adducts could be significantly reduced from spiked protein, and signal intensity improvement with co-additives was observed, which can be attributed to improvement in dissolution and desorption during the droplet pickup process in DESI.

3.2 Experimental

3.2.1 Samples and reagents

Equine cytochrome *c* (Cyt *c*, 12.3 kDa, pI=10.5), bovine hemoglobin alpha subunit (Hb, 15.1 kD, pI= 8.0), bovine myoglobin (Myo, 16.7 kDa, pI=6.8), bovine erythrocyte carbonic anhydrase isozyme II (CAII, 30.0 kDa, pI=4.7) and bovine serum albumin (BSA, 66 kDa, pI= 5.8) were purchased from Sigma-Aldrich (St. Louis, MO). Proteins were used without further

purification unless stated otherwise. Ammonium bicarbonate and L-serine were obtained from Sigma-Aldrich (St. Louis, MO). HPLC-MS grade methanol and LC-MS grade formic acid were purchased from Fluka Analytical (Morris Plains, NJ). Ultrapure water was supplied from Thermo-Barnstead Water Polisher. Porous-polyethylene surfaces (PE) with an average pore size of 15-45 μm (POREX-4900) were purchased from Interstate Specialty Products (Sutton, MA).

3.2.2 Protein solutions and solvent systems

Stock solutions of each individual protein were made by dissolving lyophilized protein powder in ultrapure water to a final concentration of 400 μM. Serial dilution from 100 mM NaCl solution was used to spike Na^+ ions into protein solutions prior to spraying the sample on PE surface. To create homogenous lines of protein, a pneumatically assisted nebulizer made of two coaxial fused silica capillaries[182] was used to spray 80 μM cyt *c*, 80 μM Myo, 160 μM CAII and 160 μM Hb and 80 μM BSA separately on the PE surfaces. The height of the sample sprayer from the surface was ~2 mm. Nebulizing gas pressure and flow rate were optimized around 100 psi and 3 μl/min. The result was protein bands with an average bandwidth of 1 mm, which gave an approximate surface concentration of 25 pmol/mm^2 for cytochrome *c*, myoglobin, and BSA and about 50 pmol/mm^2 for Hb and CAII.

All solvent systems were prepared in 50% MeOH:H_2O. Aqueous stock solutions of 2.0 M ammonium bicarbonate and 2.0 M ammonium acetate were used to prepare 200 mM dilutions in 50%MeOH. LC-MS grade formic acid was used to prepare 0.1% (v/v) formic acid in 50% MeOH. Serial dilutions from aqueous 1.0 M serine stock solution were used to make different concentrations of L-serine. All the solvent systems and the stock solutions were prepared daily before the analysis.

3.2.3 DESI source and mass spectrometry

A linear ion trap mass spectrometer, LTQ (Thermo Scientific, Waltham, MA, USA) was combined with a 3-dimensional translational stage (Purdue University, West Lafayette, IN, USA) for DESI analysis. An electrospray emitter was prepared from a Swagelok T-piece and two coaxial fused silica capillary tubing.[182] The outer capillary (for sheath gas) was approximately 20 mm in length with an outer diameter of 430 μm and an inner diameter of 320 μm. The internal capillary (for solvent) had an outer diameter of 220 μm and inner diameter of 50 μm. The solvent capillary extended through the T-piece and was connected to a syringe pump which delivered the solvent and extended 0.5 mm beyond the outer gas capillary. A spray potential of +4.0 kV was applied to the liquid junction of a stainless-steel syringe needle which delivered solvent at flow rate 5 μL/min with N_2 as nebulizing gas at 100 psi. The distances between sprayer tip and LTQ heated extended capillary were approximately 4 mm, and 1 mm from the sprayer to the surface, while the incident spray angle was 55°. The capillary temperature was set at 250°C. Transfer capillary voltage and tube lens voltages were 30 V and 130 V. For native state conserving conditions, DESI solvents were 50% MeOH:H_2O or 200 mM ammonium acetate in 50% MeOH:H_2O. For denaturing conditions, the solvent was 200 mM ammonium bicarbonate in 50% MeOH:H_2O or 0.1% v/v formic acid in 50% MeOH:H_2O. ESI experiments were performed with similar conditions, except instead of desorption of proteins from the PE surface, 10 μM protein in each solvent system was directly sprayed into the mass spectrometer inlet.

3.2.4 Data analysis

Mass spectra were collected by Xcalibur software (2.0.7) and viewed in Qual Browser (Thermo Scientific). Four independent trials were conducted for each solvent system. In each independent trial, 4 lines were perpendicularly scanned and averaged. Signal intensity and S/N

for each trial were calculated based on the averaged spectra of scanned lines. MagTran software (1.03) was used for charge state deconvolution to give the "zero-charge" spectra and integrated protein signal intensity as described by Zhang and Marshall using the ZScore algorithm.[24] Error bars represent ± mean standard deviation.

3.3 Results and discussion

3.3.1 Effect of serine on sodium removal in DESI

Cytochrome *c* without added sodium chloride. The effect of serine was first studied on mass spectrometry grade cytochrome *c* without the addition of salt. Multiple studies on sodium adduction have concluded that lower charge states are more susceptible to sodium adduction,[166-167, 183-184] and as expected, cytochrome *c* charge states 7+ and 8+ were heavily adducted peaks in the spectra even without doping sodium chloride in the depositing solution. Sodium adduction of cytochrome *c* charge states 7+ and 8+ when sprayed with 50% MeOH:H_2O and 200 mM ammonium bicarbonate (ABC) in 50% MeOH:H_2O with and without 1 mM serine are compared in Figure 3.1.

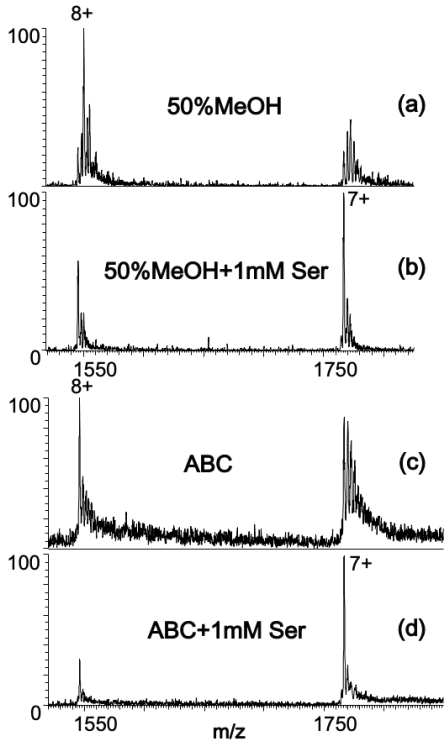

Figure 3.1. Representative DESI-MS spectra of cytochrome *c* charge state 8+ and 7+ with different desorption sprays. Sprayed with (a) 50% MeOH:H_2O and (b) 1 mM serine added to 50% MeOH:H_2O, (c) denaturing solvent additive 200 mM ammonium bicarbonate (ABC) in 50% MeOH:H_2O and (d) 1 mM serine added to 200 mM ammonium bicarbonate (ABC) in 50% MeOH:H_2O. The base peak in panel (a) was $[M+5H^+ +3Na^+]^{8+}$ and in other panels $[M+7H^+]^{7+}$ or $[M+8H^+]^{8+}$ as indicated.

In Figure 3.1 (a), aqueous cytochrome *c* without any addition of sodium chloride was analyzed from PE surface with 50% MeOH:H_2O, a standard solvent which has been shown to often produce "native-like" charge states of proteins in DESI,[185] and was compared to spray containing no other additive but 1 mM serine added to 50% MeOH:H_2O in Figure 3.1 (b). The result was a considerable sharpening of both charge states by removing adducts that spread the signal over multiple peaks and a significant increase in protonated peak intensity, especially for charge state 7+. Sodium removal from the same two charge states was also evaluated when the denaturing additive ammonium bicarbonate (ABC) was added into the desorbing spray. This additive was previously shown to increase signal to noise ratio of cytochrome *c* drastically in

DESI.[181] The addition of ABC leads to an increase in the proportion of the protonated form to both charge states 8+ and 7+, compared to 50% MeOH:H_2O, but still had multiple adduct peaks (Figure 3.1 (c)). These adducts were significantly further removed with the addition of 1 mM serine (Figure 3.1 (d)) together with ABC. The addition of 10 mM serine, however, did not yield better signal, and in fact, suppressed protein signals in both solvent systems, presumably due to high abundances of stable serine clusters, especially protonated serine octamer at m/z 840 and protonated serine dimer at m/z 211 (as discussed later). Formation and characteristics of serine,[186] and other amino acid clusters, have been reported and extensively studied by electrospray mass spectrometry.[187] Mass spectra of complete charge state distributions can be found in Figure 3.2.

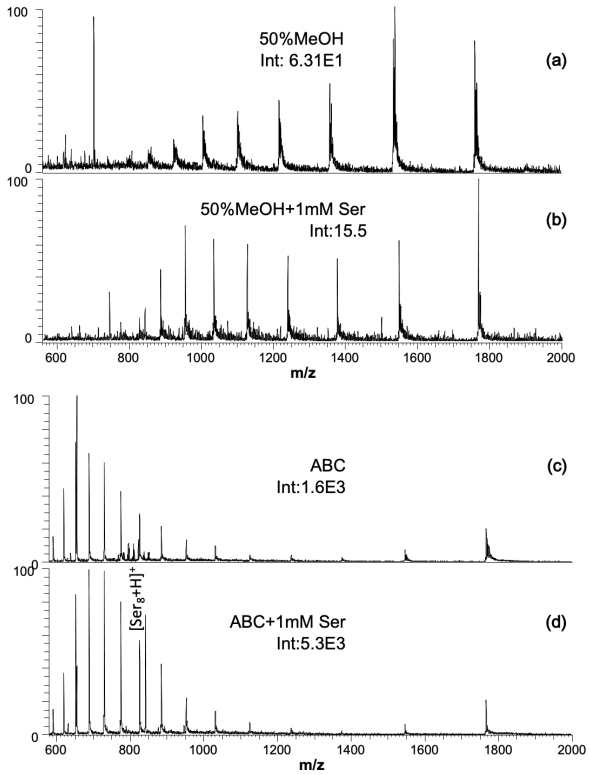

Figure 3.2. Full Spectra of cytochrome *c* sprayed with different desorption sprays. A) 50% MeOH:H_2O, b) 50% MeOH:H_2O and 1mM Ser, c) 200 mM ammonium bicarbonate (ABC) in 50% MeOH:H_2O, d) 200 mM ABC with 1mM Ser in 50% MeOH:H_2O. Int: intensity of highest intensity charge state (HICS).

Cytochrome *c* with added sodium chloride. Aqueous solutions of cytochrome *c* (80 μM) containing 1 mM and 10 mM NaCl were spray-deposited on PE, and the effects of analyzing these samples with 1 mM and 10 mM serine in 50% MeOH:H_2O as desorption spray were investigated (Figure 3.3). With 1 mM NaCl (Figure 3.3 (a)), the signal was considerably deteriorated compared to cytochrome *c* without added salt (Figure 3.2 (a)). However, protein peaks could still be detected with S/N>10. With 10 mM NaCl, protein peaks were hardly detectable (Figure 3.3 (b)).

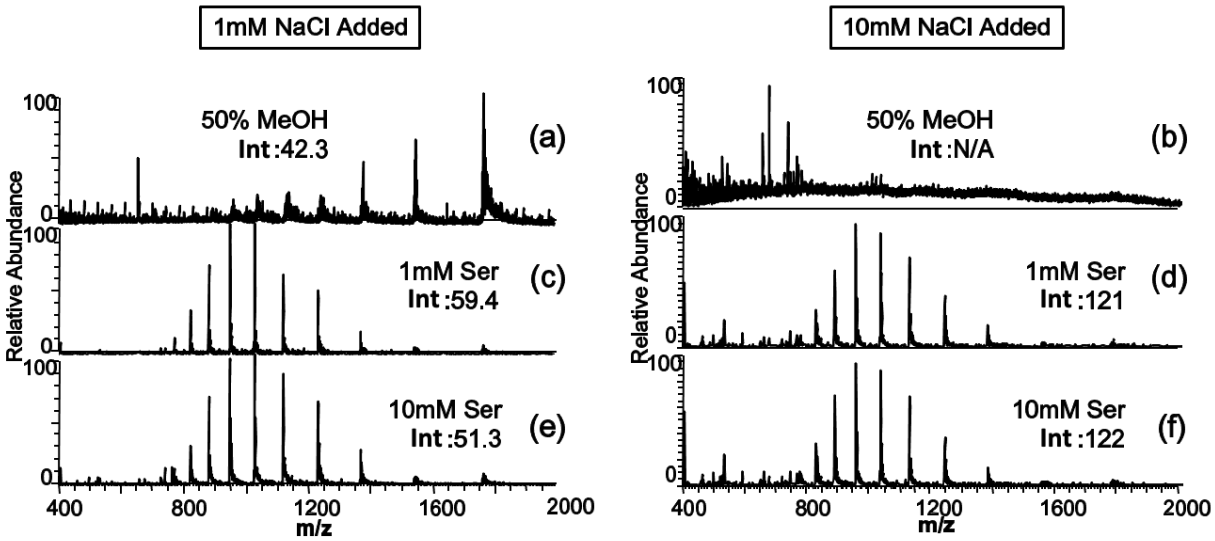

Figure 3.3. Representative DESI-MS spectra of cytochrome *c* spiked with 1 mM NaCl (left) and spiked with 10 mM NaCl (right) when analyzed by methanol-water desorption spray and serine in DESI-MS. (a) and (b) 50% MeOH:H_2O (no additive), (c) and (d) 1 mM Ser in 50% MeOH:H_2O, (e) and (f) 10 mM Ser in 50% MeOH:H_2O. (Int: absolute intensity of protein highest intensity charge state).

By adding 1 mM serine to desorption spray, the protein signal was significantly improved for both samples. The charge states also shifted from mostly native state like to higher values indicative of protein unfolding (Figure 3.3 (c) and Figure 3.3 (d)) as was also previously reported

for a variety of proteins when analyzed by ESI.[158] Unlike the results shown on the analysis of cytochrome *c* with no added NaCl, 10 mM serine in desorption spray did not suppress protein signal and in fact, gave a signal intensity improvement close to the one obtained by addition of 1 mM serine (Figure 3.3 (e) and Figure 3.3 (f)). This suggested that the optimal concentration of serine and the tolerance for the amount of serine in desorption spray could also be dependent on the amount of sodium present in the sample.

The exact ratio of serine to sodium ion concentration is more complicated to determine in DESI compared to ESI, as it is dependent on the size of the desorption footprint of the DESI spray, the exact composition of the primary solvent droplet as it reaches the surface, the final concentration of serine in the droplet, and surface concentration of sodium. A rough estimation of the ratios can, however, be attempted based on simple calculations: For a sample stage scan speed of 150 μm/s and an estimated 200 μm diameter DESI desorption footprint, approx. 1.80 mm^2 of a sample surface is analyzed per minute. When 80 μM protein sample is spiked with 10 mM NaCl and sprayed onto a PE surface, samples with surface concentrations of 25 pmol/mm^2 protein and 330 pmol/mm^2 NaCl were prepared. This leads to an estimated 6000 pmol salt present during the DESI analysis per minute, assuming complete removal from within the DESI footprint. For cytochrome *c* spiked with 1 mM NaCl, 600 pmol salt was analyzed under the same conditions per minute. The amount of serine delivered by DESI droplets when 1 mM or 10 mM serine was added into the 5 μL/min spray is estimated to be 5000 pmol and 50,000 pmol per minute, respectively.

It was previously shown that serine desalts native proteins during ESI-MS.[176] A decrease in the amount of sodium adduction with DESI-MS (as seen in Figure 3.3 and Figure 3.4) was expected as it is widely believed DESI and ESI share a similar ionization mechanism. In the

same study, the optimal ratio between serine and sodium ion was reported to be 10:1. However, their approach was described to be less effective for sodium concentrations above 2 mM. Although not directly comparable, when considering the sodium ion concentration in the original sample solution before deposition, serine in DESI is capable of removing higher concentrations of salt from proteins compared to ESI.

The same study also suggested that the sodium removal effect is due to the direct binding of free amino acids to sodium ions. This conclusion was derived from comparing the sodium removal effect of five different amino acids with empirical findings on sodium affinity of amino acids. Amino acid sodium affinities increase in the following order: **Gly**, **Ala**, Cys, Val, (Leu, lle), **Ser**, Met, Thr, (Phe, Pro), Asp, Tyr, (Glu, **Lys**), Trp, Asn, Gln, **His**,[188] where the amino acids studied by Clarke *et al.*[176] are highlighted in bold. Both alanine and glycine in the study by Clarke *et al.* were less successful than histidine, lysine, and serine in sodium removal. During DESI experiments, sodiated serine ion was observed in the spectrum. Curiously, at higher serine concentrations, when serine dimers and octamers were also observed during experiments, only protonated clusters were present.

Another important consideration of amino acid behavior in electrospray is proton affinity, as it can affect the ionization of proteins by competing for available protons in the electrospray with protein molecules during the ionization process. Proton affinity of 20 common α-amino acids has been computationally calculated[189-190] and compared.[191] As reported by Clarke *et al*., the shift in charge state distribution when histidine or lysine was added to the electrospray is evidence of the competition for charge between these amino acid additives and protein. With DESI, the data presented in Figure 3.2 and Figure 3.3 showed a shift to the higher charge states in the bimodal distribution of protein peaks with the addition of serine to 50% MeOH:H_2O in

desorption spray. However, for already denatured protein envelopes, such as those obtained when ammonium bicarbonate was also present in the desorbing solvent system, a slight decrease in HICS (highest intensity charge state) or HOCS (highest observed charge state) were observed (Figure 3.2).

For protein standards deposited out of solutions containing high NaCl concentrations, when analyzed together with 200 mM ammonium bicarbonate as desorbing spray additive in Figure 3.4 (e) and (f), improvements relative to the spectra shown in Figure 3.3 (a) and (b) are already evident, since ammonium bicarbonate also aids in sodium adduct removal, as described in our earlier paper.[181] However, the addition of 1 mM serine further improved the intensities of the protein HICS when 1 mM or 10mM NaCl was present (Figure 3.4 (a) and (d)). Since, with this denaturing desorption solvent composition, most of the signal is concentrated in higher, less adducted charge states, it appears that serine does so through a mechanism different from sodium adduction removal.

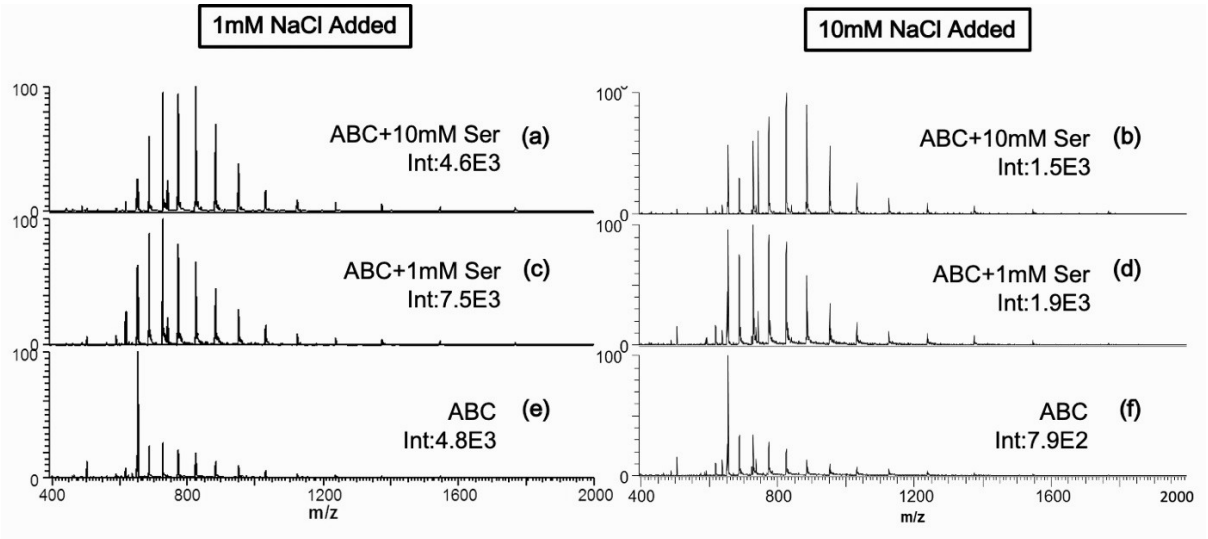

Figure 3.4. Cytochrome *c* spiked with 1 mM NaCl (left) and 10 mM NaCl (right), sprayed with 200 mM ammonium bicarbonate (ABC) in 50% MeOH:H_2O and 1 mM serine and 10 mM Ser as additive. Int: intensity of HICS.

3.3.2 Effect of serine on increasing signal intensity

As seen in Figure 3.4, another interesting effect was observed when serine was added to a solution also containing the denaturing additive ammonium bicarbonate, where its presence caused significant improvement in signal intensity in DESI-MS. Contrary to native-state conserving spray where the signal stays constant or is even slightly reduced (Figure 3.2), a significant improvement in signal intensity of HICS and integrated signal intensity of deconvoluted protein peak was observed for proteins under denaturing conditions of 200 mM ammonium bicarbonate. To study this effect further, 0.1% formic acid was also used as a denaturing co-additive on multiple proteins and compared to when ammonium bicarbonate and serine was present (Figure 3.5).

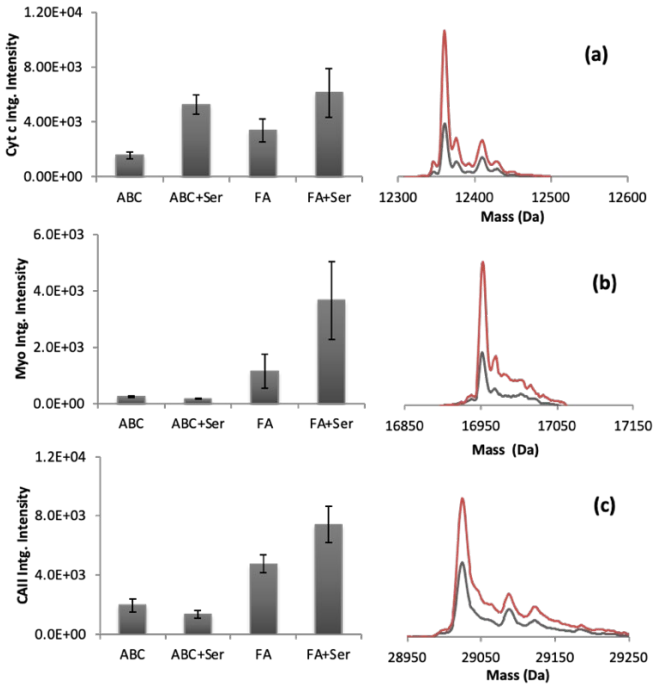

Figure 3.5. Effect of 1 mM serine with different co-additives on integrated signal intensity in DESI-MS of proteins. Error bars represent ± mean standard deviation. Deconvoluted spectra compare the protein signal when serine is added to the solvent system (red) to when there is no serine (black). Solvent systems are 50% MeOH with 200mM ammonium bicarbonate (ABC), or 0.1% formic acid (FA). The proteins are (a) cytochrome *c*, (b) myoglobin and (c) carbonic anhydrase II.

Under denaturing conditions much less adduction is usually observed since additives such as formic acid and ammonium bicarbonate both reduce adduction and due to the denatured state of the protein less adduction is typically observed for higher charge states. From the deconvoluted spectra in Figure 3.5, it can be observed that the overall extent of adduction did not change much with addition of 1 mM serine, relative to solutions that already contain formic acid or ammonium bicarbonate. This suggests that signal intensity improvement is not only related to adduct removal. The improvement was dependent on protein pI and solvent system composition. For high pI protein (cytochrome *c*), improvement was achieved with both formic acid and ammonium bicarbonate. On the other hand, low pI proteins (myoglobin and carbonic anhydrase) only showed an improvement with serine and formic acid, but when used with ammonium bicarbonate, a reduction in signal was observed. Representative spectra are presented in Figure 3.6.

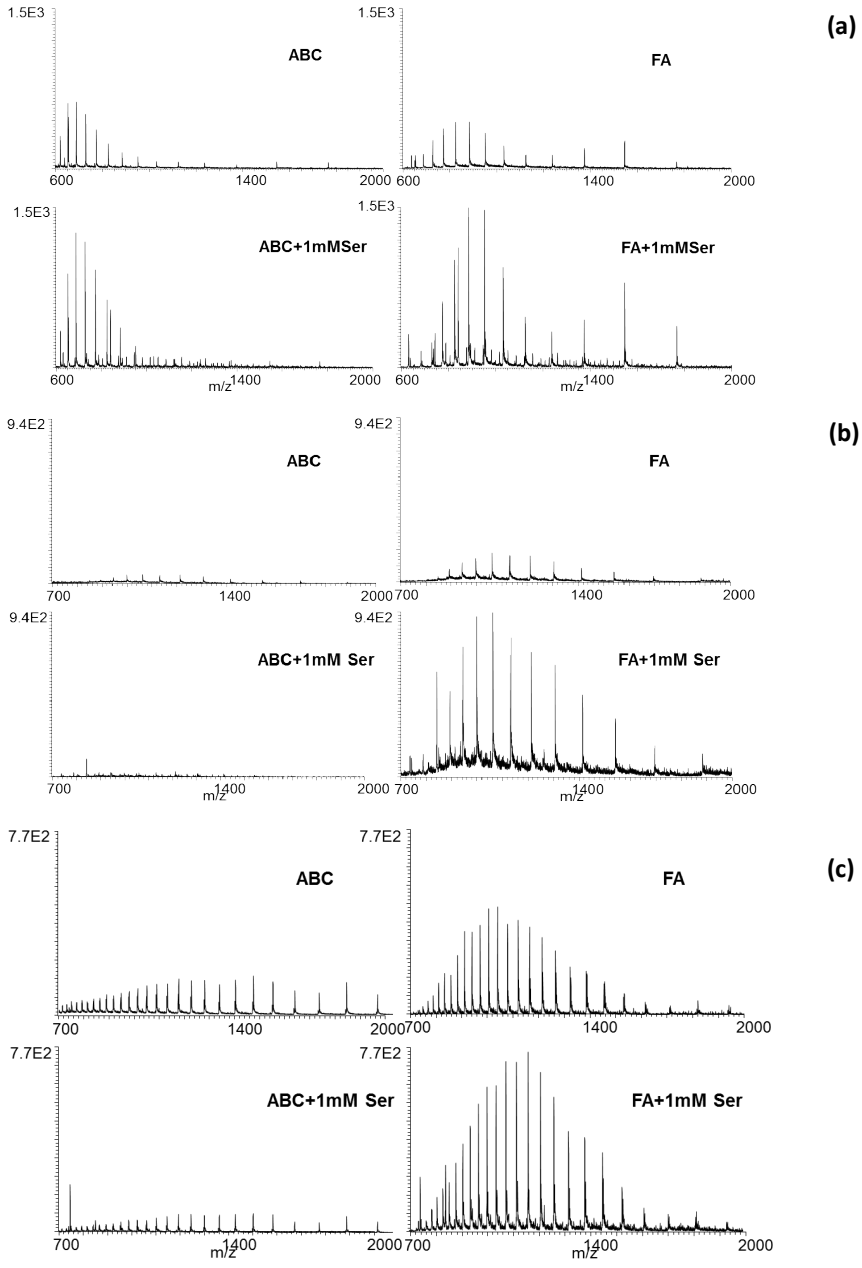

Figure 3.6. Representative MS spectra of proteins in Figure 3 with denaturing additives formic acid (FA) and ammonium bicarbonate (ABC) and 1 mM serine. (a) Cytochrome *c*, (b) Myoglobin and (c) Carbonic anhydrase II**.** Each panel in (a), (b) and (c) is normalized to the highest intensity charge state achieved for the best additive.

Similarly, bovine serum albumin (BSA) spectra were also only improved with serine and formic acid in the solvent system (Figure 3.7). The relationship between additives and protein pI has been reported and investigated before. Pan *et al.*[183] demonstrated that the maximum signal in positive mode is obtained when solution pH is about 3 units below the protein pI. Moreover, our previous publication also showed that proteins with high pI yield more improvement with ammonium bicarbonate in DESI compared to low pI proteins.[181]

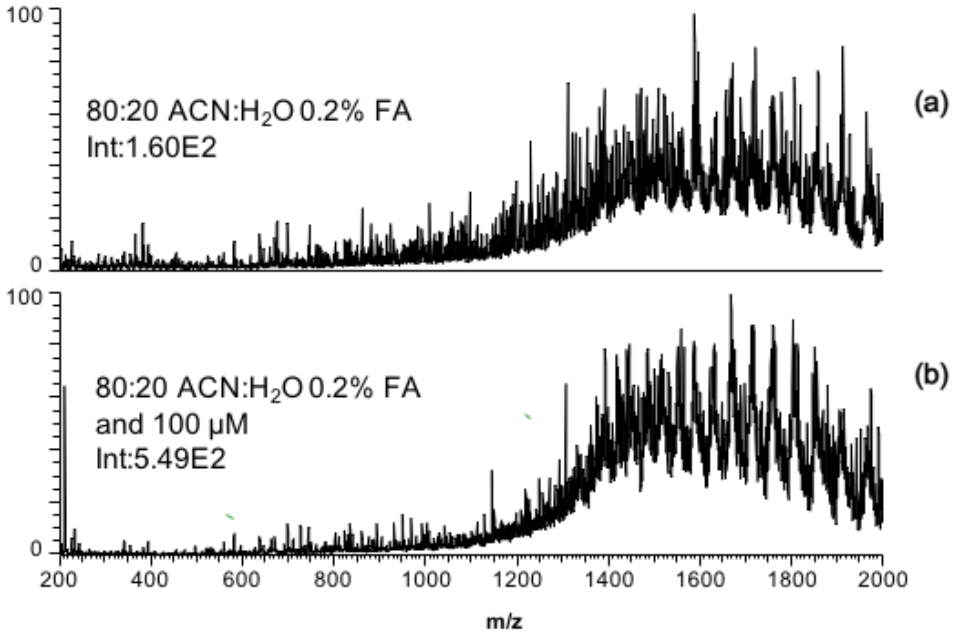

Figure 3.7. DESI-MS spectra of Bovine serum albumin (BSA), a low pI protein with molecular weight of 66 kDa, with and without serine in solvent system. Int: intensity of highest intensity BSA peak.

Indeed, several studies show that solvent pH and protein pI influence protein ionization in charge residue model (CRM) of electrospray ionization process.[164, 183] The isoelectric point of carbonic anhydrase II and myoglobin (pI = 4.7 and 6.8 respectively) are higher than the pH of 0.1% formic acid (pH=2.5) but lower than the pH of ammonium bicarbonate solution (pH=6.7), while cytochrome *c* pI (10.8) is higher than the pH of the ammonium bicarbonate solution. While

it can be argued that the improvement in integrated protein signal intensity from the addition of serine to denaturing additives could be a result of adduct removal from lower charge states, it should be kept in mind that the contribution of these charge states to the overall signal intensity of protein (i.e., integrated intensity values shown in bar graphs of Figure 3.5) is minor. Preliminary data showed significant improvement in the signal of myoglobin when analyzed from an untreated raw meat imprint, analyzed with 100 µM serine in 80:20 ACN:H_2O and 0.2% formic acid (Figure 3.8), suggesting the potential of serine as an additive for improving protein detection from biological tissues. This effect was further explored by additional experiments discussed in the next section.

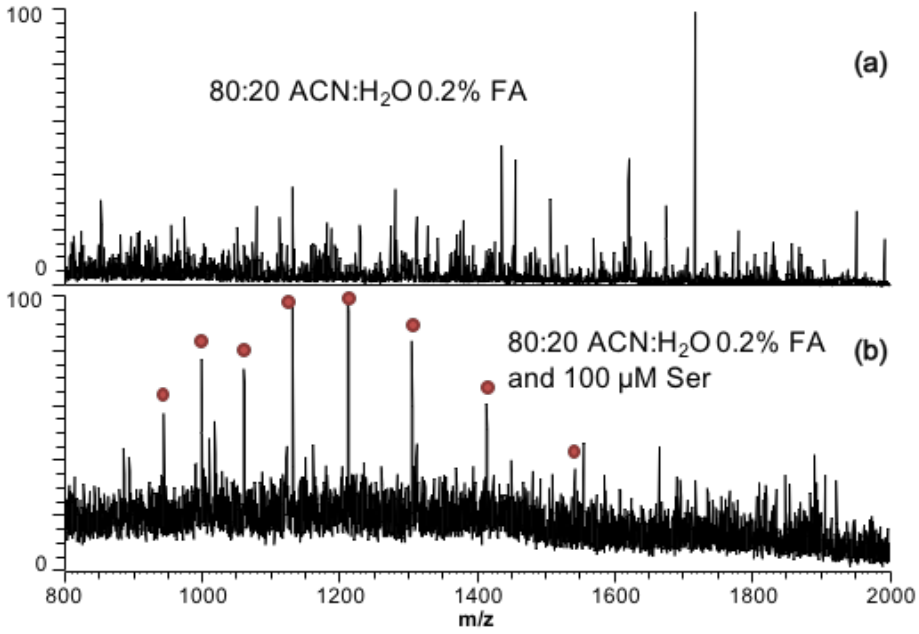

Figure 3.8. DESI-MS analysis of raw meat extract on absorbent fabric with a) 80:20 ACN:H_2O and 0.2% formic acid, b) 100 µM Ser in 80:20 ACN:H_2O and 0.2% formic acid. Myoglobin protonated charge states are indicated with red dots.

3.3.3 Concentration dependency of signal improvement in DESI

Different concentrations between 1 µM to 10 mM of serine in 50% MeOH:H_2O with 200 mM ammonium bicarbonate for cytochrome *c* and 0.1% formic acid for carbonic anhydrase were used as DESI solvent. The protein samples were analyzed without the addition of NaCl to highlight the improvements in signal intensity through a mechanism believed to be distinct from adduct removal. As can be observed in Figure 3.9 (a) and 3.9 (c), with increasing amounts of serine there was an increase in protein peak intensity up to the point that non-volatile clusters and serine adducts induced ion suppression and decreased protein signal. With DESI, the signal improvement vs. serine concentration followed a similar trend for both cytochrome *c* and carbonic anhydrase (Figure 3.9 (a) and 3.9 (c)).

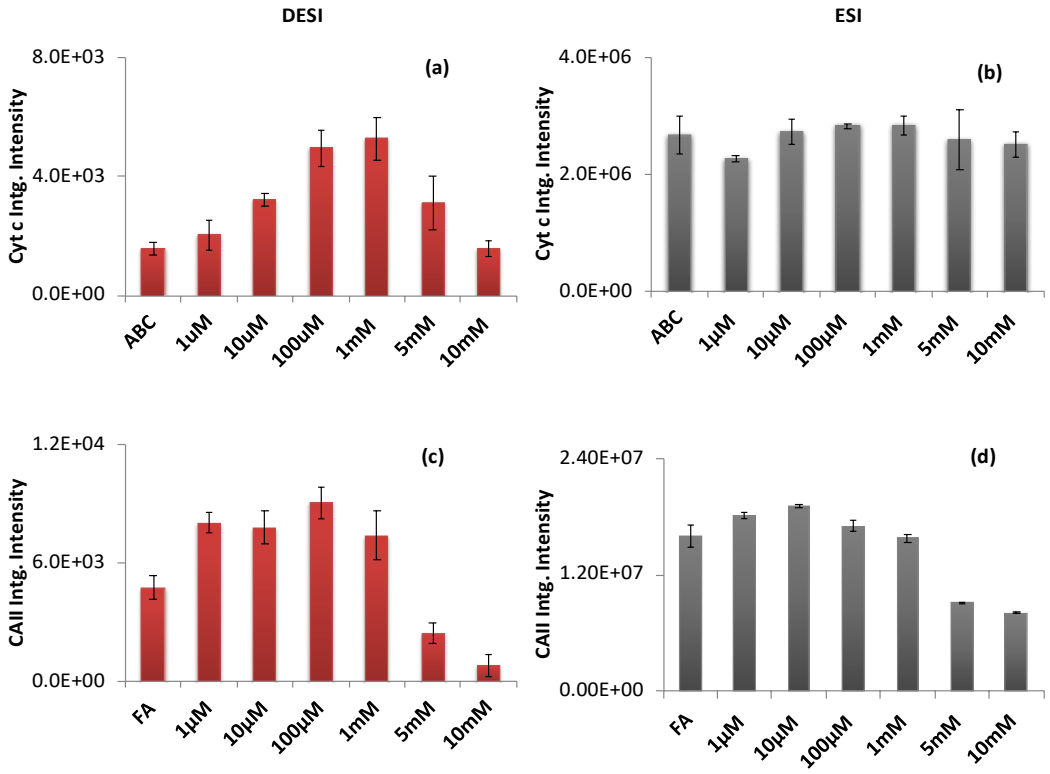

Figure 3.9. Integrated signal intensity for deconvoluted spectra with various concentrations of serine. The intensities for (a) cyt *c* and (c) CAII by DESI improve with serine addition, while the intensities of (b) cyt *c* and (d) CAII by ESI do not improve.

Micromolar concentrations appeared more effective at signal improvement, and high concentrations (5 mM and 10 mM) significantly decreased signal intensity due to ion suppression that is presumably caused by serine clusters. In concentrations above 1 mM, protonated serine dimer $[Ser_2+H]^+$ at m/z 211 and protonated serine octamer $[Ser_8+H]^+$ at m/z 840 became the most abundant species, strongly dominating the spectra (Figure 3.10 (c)).

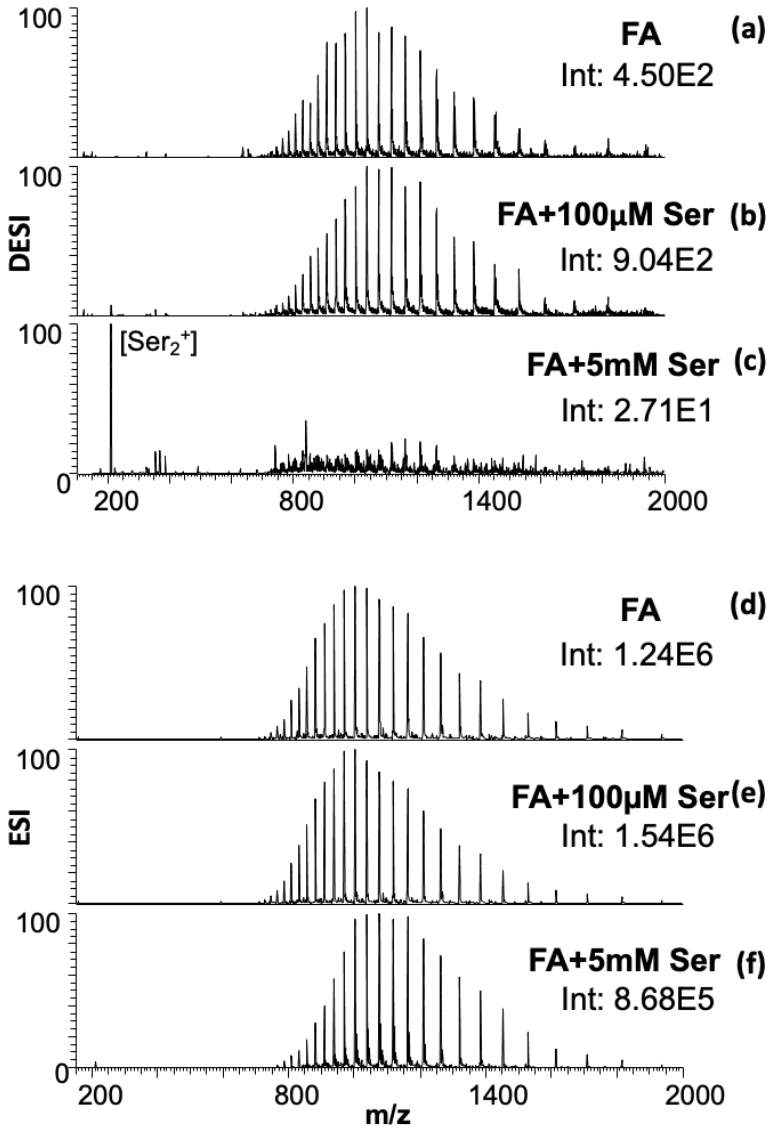

Figure 3.10. Comparison between representative spectra of DESI (panel a-c) and ESI (panel d-f) with different concentrations of serine additive in 0.1% formic acid for analyzing carbonic anhydrase II, (Int: absolute intensity of protein HICS).

Another interesting observation was the formation of protein–serine adducts that spread the protein signal into multiple peaks, thus decreasing signal intensity for carbonic anhydrase (Figure 3.10 (c)) and for cytochrome *c* (Figure 3.11 (c)). A concentration in the range of high micromolar up to 1 mM serine improved signal effectively without inducing adducts and suppressing protein ions. Looking at the spectra in Figure 3.10 and Figure 3.11, the intensity of many charge states, including HICS were increased by the addition of different amounts of serine to the DESI spray. Interestingly, contrary to native-like conditions where the addition of serine caused protein unfolding (Figure 3.3), in denaturing solutions increasing concentrations of serine caused a shift to lower charge states in both DESI and ESI, as observed in Figure 3.10 for carbonic anhydrase and Figure 3.11 for cytochrome *c*.

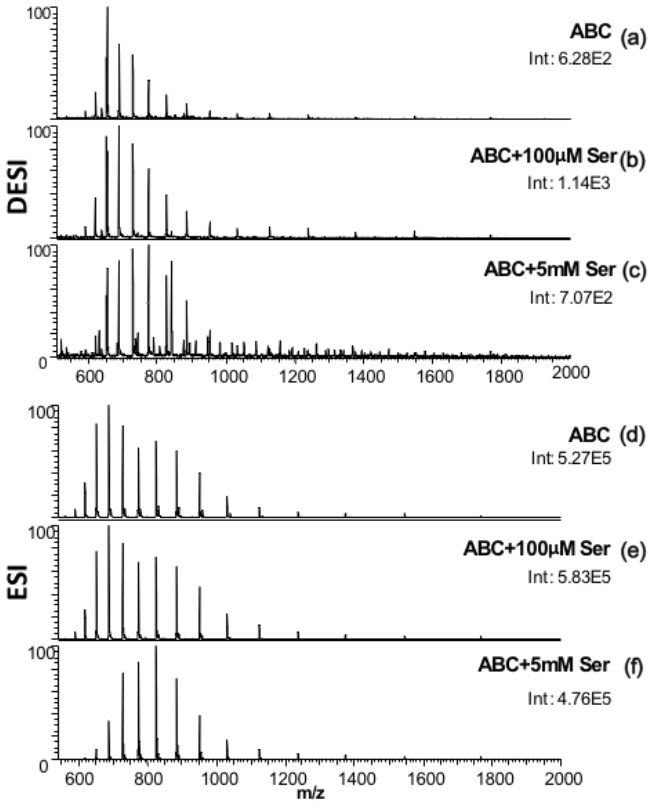

Figure 3.11. DESI vs. ESI of cytochrome *c*, analyzed with 200 mM ammonium bicarbonate (ABC) and different concentrations of Ser. Int: intensity of HICS.

Other amino acids were previously shown to have a stabilizing effect on protein in high concentrations.[148] Figure 3.12 shows the analysis of hemoglobin and cytochrome *c* with 0.1% formic acid in 50% MeOH:H_2O and equimolar concentrations of arginine (Arg) and glutamic acid (Glu) in the desorption spray of DESI. This suggests that the signal intensity improvement is not specific to serine and further supports the role of the solution stabilizing effect in the observed signal improvements.

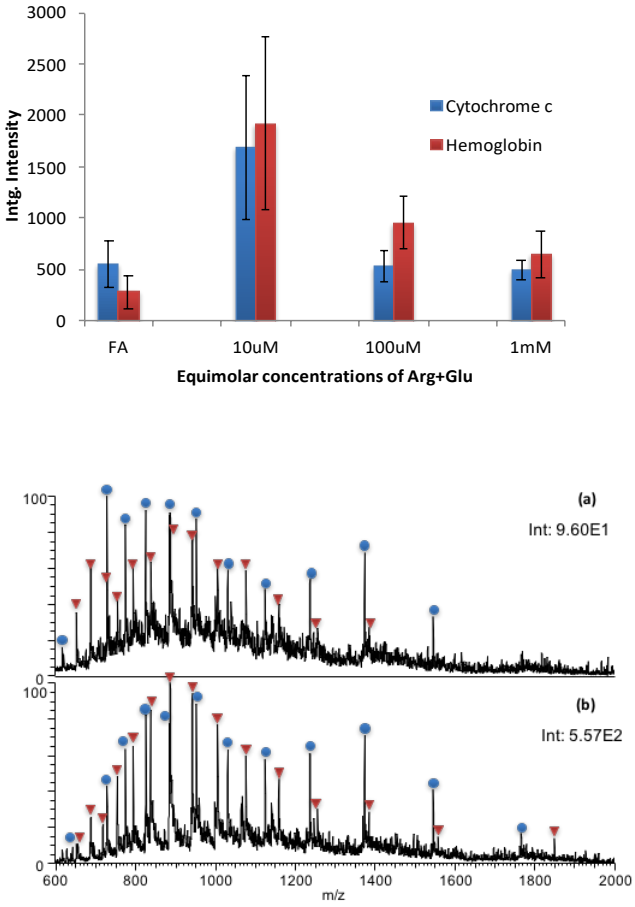

Figure 3.12. A mixture of 50 pmol/mm^2 each of hemoglobin and cytochrome *c* natively deposited out of water and analyzed by DESI with 0.1% formic acid in 50% MeOH:H_2O and various concentrations of an equimolar mixture of arginine (Arg) and glutamic acid (Glu). Representative spectra of (a) 0.1% formic acid in 50% MeOH:H_2O (no amino acid additive) and (b) 10 µM Arg+Glu in 0.1% formic acid in 50% MeOH:H_2O. Charge states of two proteins are marked with red triangles (hemoglobin) and blue circles (cytochrome *c*). Int= highest intensity charge state.

3.3.4 DESI vs. ESI and signal improvement

Interestingly, this improvement in integrated signal intensity was not detected with ESI. Figure 3.9 presents the results of 10 μM cytochrome *c* with different concentrations of serine in 200 mM ammonium bicarbonate and 10 μM carbonic anhydrase with 0.1% formic acid when directly analyzed by micro-ESI using a similar emitter as used for DESI but pointed directly at the inlet. In ESI, unlike DESI, no significant signal improvement was observed with the addition of serine. However, similar to DESI, at higher concentrations of 5 mM and 10 mM serine, signal suppression was an issue, especially for carbonic anhydrase (Figure 3.9 (c) and 3.9 (d)). The signal improvement was not observed in ESI under similar conditions (with similar concentrations of ammonium bicarbonate for cytochrome *c* and formic acid for carbonic anhydrase II).

This also supports the hypothesis that serine could play a facilitating role in the desorption or 'droplet pickup' mechanism of DESI, rather than through adduct removal or some other process relating to ionization. This signal improvement by serine in DESI can originate from either increasing dissolution or solubility during the droplet pick-up process, an effect that plays no role in ESI. Previous studies were able to show an improvement in DESI ion signal by adding very low concentrations of surfactants to standard 50% MeOH:H_2O solvent spray.[192] As mentioned previously, multiple studies have highlighted the role of amino acids in improving protein solubility and keeping proteins in solution by inhibiting aggregation.[148, 150, 154] It seems likely that there is a link between inhibition of protein aggregation and improving protein signal in DESI. Based on the data, serine improves protein solubility in the micro-localized liquid layer formed on the surface during the desorption step of DESI. This effect could be caused by reducing denaturation-induced aggregation by inhibition of nonspecific interaction of exposed

hydrophobic cores of unfolded proteins, based on a mechanism previously suggested for other amino acids and their role in improving protein solubility.[193]

3.4. Conclusion

Similar to previous ESI results, serine is a successful additive in significantly reducing sodium adduction from natively analyzed protein in DESI. Interestingly, serine was successful in the removal of 10 mM sodium from cytochrome *c*, whereas in ESI, only concentrations up to 1 mM seemed to benefit from the addition of serine to the ESI working solution. Other than salt removal, significant signal improvement was achieved when a suitable denaturing co-additive was combined with serine in the desorption spray. The effect was dependent on matching protein pI and solvent system pH. The combination of micromolar concentrations of serine with formic acid seems to be most effective in improving the protein signal for both low and high pI proteins. In cases where an acidic solution is not desirable, ammonium bicarbonate can also improve the signal intensity of high pI proteins. Since this enhancement in signal intensity of denatured proteins was not observed by similar ESI experiments, we propose that serine improves the dissolution of dried protein spots during formation of the micro-localized liquid layer in DESI by increasing protein solubility. A possible mechanism of this effect based on previous studies through inhibition of protein aggregation during denaturing conditions seems likely. Overall, serine was shown to be an effective additive for improving detection of proteins with DESI by enhancing signal intensity and S/N.

3.5. References

1. Cooks, R. G.; Ouyang, Z.; Takats, Z.; Wiseman, J. M., Ambient Mass Spectrometry. *Science* **2006,** *311* (5767), 1566-1570.
2. Ifa, D. R.; Wu, C.; Ouyang, Z.; Cooks, R. G., Desorption Electrospray Ionization and Other Ambient Ionization Methods: Current Progress and Preview. *Analyst* **2010,** *135* (4), 669-681.

3. Tao, A. W.; Cooks, R. G., Rapid Ambient Mass Spectrometric Profiling of Intact, Untreated Bacteria Using Desorption Electrospray Ionization. *Chemical Communications* **2007,** (1), 61-63.
4. Meetani, M. A.; Shin, Y. S.; Zhang, S.; Mayer, R.; Basile, F., Desorption Electrospray Ionization Mass Spectrometry of Intact Bacteria. *Journal of Mass Spectrometry* **2007,** *42* (9), 1186-1193.
5. Song, Y.; Talaty, N.; Datsenko, K.; Wanner, B. L.; Cooks, R. G., In Vivo Recognition of Bacillus Subtilis by Desorption Electrospray Ionization Mass Spectrometry (Desi-Ms). *Analyst* **2009,** *134* (5), 838-841.
6. Tata, A.; Perez, C.; Campos, M. L.; Bayfield, M. A.; Eberlin, M. N.; Ifa, D. R., Imprint Desorption Electrospray Ionization Mass Spectrometry Imaging for Monitoring Secondary Metabolites Production During Antagonistic Interaction of Fungi. *Analytical Chemistry* **2015,** *87* (24), 12298-12305.
7. Tata, A.; Perez, C. J.; Hamid, T. S.; Bayfield, M. A.; Ifa, D. R., Analysis of Metabolic Changes in Plant Pathosystems by Imprint Imaging Desi-Ms. *Journal of the American Society for Mass Spectrometry* **2015,** *26* (4), 641-648.
8. Talaty, N.; Gong, H. H.; Koeniger, S.; Vogt, A.; Pheil, M.; Fruehan, P.; Neilly, J.; Lopour, M.; Johnson, R. W., From Discovery to Finished Products: Innovative Applications of Surface Mass Spectrometry in Pharmaceutical Industry. *Microscopy and Microanalysis* **2014,** *20* (S3), 1412-1413.
9. Chen, H.; Talaty, N. N.; Takáts, Z.; Cooks, R. G., Desorption Electrospray Ionization Mass Spectrometry for High-Throughput Analysis of Pharmaceutical Samples in the Ambient Environment. *Analytical Chemistry* **2005,** *77* (21), 6915-6927.
10. Williams, J. P.; Scrivens, J. H., Rapid Accurate Mass Desorption Electrospray Ionisation Tandem Mass Spectrometry of Pharmaceutical Samples. *Rapid Communications in Mass Spectrometry* **2005,** *19* (24), 3643-3650.
11. Harry, E. L.; Reynolds, J. C.; Bristow, A. W.; Wilson, I. D.; Creaser, C. S., Direct Analysis of Pharmaceutical Formulations from Non-Bonded Reversed-Phase Thin-Layer Chromatography Plates by Desorption Electrospray Ionisation Ion Mobility Mass Spectrometry. *Rapid Communications in Mass Spectrometry* **2009,** *23* (17), 2597-2604.
12. Kauppila, T. J.; Wiseman, J. M.; Ketola, R. A.; Kotiaho, T.; Cooks, R. G.; Kostiainen, R., Desorption Electrospray Ionization Mass Spectrometry for the Analysis of Pharmaceuticals and Metabolites. *Rapid Communications in Mass Spectrometry* **2006,** *20* (3), 387-392.
13. Van Berkel, G. J.; Ford, M. J.; Deibel, M. A., Thin-Layer Chromatography and Mass Spectrometry Coupled Using Desorption Electrospray Ionization. *Analytical Chemistry* **2005,** *77* (5), 1207-1215.
14. Kauppila, T. J.; Talaty, N.; Salo, P. K.; Kotiaho, T.; Kostiainen, R.; Cooks, R. G., New Surfaces for Desorption Electrospray Ionization Mass Spectrometry: Porous Silicon and Ultra-Thin Layer Chromatography Plates. *Rapid Communications in Mass Spectrometry* **2006,** *20* (14), 2143-2150.
15. Paglia, G.; Ifa, D. R.; Wu, C.; Corso, G.; Cooks, R. G., Desorption Electrospray Ionization Mass Spectrometry Analysis of Lipids after Two-Dimensional High-Performance Thin-Layer Chromatography Partial Separation. *Analytical Chemistry* **2010,** *82* (5), 1744-1750.
16. Cheng, S.-C.; Huang, M.-Z.; Shiea, J., Thin Layer Chromatography/Mass Spectrometry. *Journal of Chromatography A* **2011,** *1218* (19), 2700-2711.
17. Wiseman, J. M.; Ifa, D. R.; Song, Q.; Cooks, R. G., Tissue Imaging at Atmospheric Pressure Using Desorption Electrospray Ionization (Desi) Mass Spectrometry. *Angewandte Chemie International Edition* **2006,** *45* (43), 7188-7192.
18. Wiseman, J. M.; Ifa, D. R.; Zhu, Y.; Kissinger, C. B.; Manicke, N. E.; Kissinger, P. T.; Cooks, R. G., Desorption Electrospray Ionization Mass Spectrometry: Imaging Drugs and Metabolites in Tissues. *Proceedings of the National Academy of Sciences* **2008,** *105* (47), 18120-18125.
19. Banerjee, S.; Zare, R. N.; Tibshirani, R. J.; Kunder, C. A.; Nolley, R.; Fan, R.; Brooks, J. D.; Sonn, G. A., Diagnosis of Prostate Cancer by Desorption Electrospray Ionization Mass Spectrometric Imaging of Small Metabolites and Lipids. *Proceedings of the National Academy of Sciences* **2017,** *114* (13), 3334-3339.

20. Perez, C. J.; Tata, A.; de Campos, M. L.; Peng, C.; Ifa, D. R., Monitoring Toxic Ionic Liquids in Zebrafish (Danio Rerio) with Desorption Electrospray Ionization Mass Spectrometry Imaging (Desi-Msi). *Journal of the American Society for Mass Spectrometry* **2017,** *28* (6), 1136-1148.
21. Garza, K. Y.; Feider, C. L.; Klein, D. R.; Rosenberg, J. A.; Brodbelt, J. S.; Eberlin, L. S., Desorption Electrospray Ionization Mass Spectrometry Imaging of Proteins Directly from Biological Tissue Sections. *Analytical Chemistry* **2018,** *90* (13), 7785-7789.
22. Towers, M. W.; Karancsi, T.; Jones, E. A.; Pringle, S. D.; Claude, E., Optimised Desorption Electrospray Ionisation Mass Spectrometry Imaging (Desi-Msi) for the Analysis of Proteins/Peptides Directly from Tissue Sections on a Travelling Wave Ion Mobility Q-Tof. *Journal of the American Society for Mass Spectrometry* **2018**, *29* (12), 2456-2466.
23. Chernetsova, E. S.; Morlock, G. E., Ambient Desorption Ionization Mass Spectrometry (Dart, Desi) and Its Bioanalytical Applications. *Bioanalytical Reviews* **2011,** *3* (1), 1-9.
24. Ferguson, C. N.; Benchaar, S. A.; Miao, Z.; Loo, J. A.; Chen, H., Direct Ionization of Large Proteins and Protein Complexes by Desorption Electrospray Ionization-Mass Spectrometry. *Analytical Chemistry* **2011,** *83* (17), 6468-6473.
25. Honarvar, E.; Venter, A. R., Comparing the Effects of Additives on Protein Analysis between Desorption Electrospray (Desi) and Electrospray Ionization (Esi). *Journal of the American Society for Mass Spectrometry* **2018**, *29* (12) 2443-2455.
26. Venter, A.; Sojka, P. E.; Cooks, R. G., Droplet Dynamics and Ionization Mechanisms in Desorption Electrospray Ionization Mass Spectrometry. *Analytical Chemistry* **2006,** *78* (24), 8549-8555.
27. Douglass, K. A.; Jain, S.; Brandt, W. R.; Venter, A. R., Deconstructing Desorption Electrospray Ionization: Independent Optimization of Desorption and Ionization by Spray Desorption Collection. *Journal of the American Society for Mass Spectrometry* **2012,** *23* (11), 1896-1902.
28. Jain, S.; Heiser, A.; Venter, A. R., Spray Desorption Collection: An Alternative to Swabbing for Pharmaceutical Cleaning Validation. *Analyst* **2011,** *136* (7), 1298-1301.
29. Hamada, H.; Arakawa, T.; Shiraki, K., Effect of Additives on Protein Aggregation. *Current Pharmaceutical Biotechnology* **2009,** *10* (4), 400-407.
30. Shiraki, K.; Kudou, M.; Fujiwara, S.; Imanaka, T.; Takagi, M., Biophysical Effect of Amino Acids on the Prevention of Protein Aggregation. *The Journal of Biochemistry* **2002,** *132* (4), 591-595.
31. Kumat, T.; Samuel, D.; Jayaraman, G.; Srimathi, T.; Yu, C., The Role of Proline in the Prevention of Aggregation During Protein Folding in Vitro. *IUBMB Life* **1998,** *46* (3), 509-517.
32. Samuel, D.; Kumar, T. K. S.; Ganesh, G.; Jayaraman, G.; Yang, P.-W.; Chang, M.-M.; Trivedi, V. D.; Wang, S.-L.; Hwang, K.-C.; Chang, D.-K., Proline Inhibits Aggregation During Protein Refolding. *Protein Science* **2000,** *9* (2), 344-352.
33. Xia, Y.; Park, Y.-D.; Mu, H.; Zhou, H.-M.; Wang, X.-Y.; Meng, F.-G., The Protective Effects of Osmolytes on Arginine Kinase Unfolding and Aggregation. *International Journal of Biological Macromolecules* **2007,** *40* (5), 437-443.
34. Meng, F.-G.; Park, Y.-D.; Zhou, H.-M., Role of Proline, Glycerol, and Heparin as Protein Folding Aids During Refolding of Rabbit Muscle Creatine Kinase. *The International Journal of Biochemistry & Cell Biology* **2001,** *33* (7), 701-709.
35. Kim, S.-H.; Yan, Y.-B.; Zhou, H.-M., Role of Osmolytes as Chemical Chaperones During the Refolding of Aminoacylase. *Biochemistry and Cell Biology* **2006,** *84* (1), 30-38.
36. Reddy K, R. C.; Lilie, H.; Rudolph, R.; Lange, C., L-Arginine Increases the Solubility of Unfolded Species of Hen Egg White Lysozyme. *Protein Science* **2005,** *14* (4), 929-935.
37. Hevehan, D. L.; De Bernardez Clark, E., Oxidative Renaturation of Lysozyme at High Concentrations. *Biotechnology and Bioengineering* **1997,** *54* (3), 221-230.
38. Katayama, D. S.; Nayar, R.; Chou, D. K.; Valente, J. J.; Cooper, J.; Henry, C. S.; Vander Velde, D. G.; Villarete, L.; Liu, C.; Manning, M. C., Effect of Buffer Species on the Thermally Induced Aggregation of Interferon-Tau. *Journal of Pharmaceutical Sciences* **2006,** *95* (6), 1212-1226.
39. Mehta, A. D.; Seidler, N. W., B-Alanine Suppresses Heat Inactivation of Lactate Dehydrogenase. *Journal of Enzyme Inhibition and Medicinal Chemistry* **2005,** *20* (2), 199-203.

40. Zhang, H.; Lu, H.; Chingin, K.; Chen, H., Stabilization of Proteins and Noncovalent Protein Complexes During Electrospray Ionization by Amino Acid Additives. *Analytical Chemistry* **2015,** *87* (14), 7433-7438.
41. Cech, N. B.; Enke, C. G., Practical Implications of Some Recent Studies in Electrospray Ionization Fundamentals. *Mass Spectrometry Reviews* **2001,** *20* (6), 362-387.
42. Chen, Y.; Mori, M.; Pastusek, A. C.; Schug, K. A.; Dasgupta, P. K., On-Line Electrodialytic Salt Removal in Electrospray Ionization Mass Spectrometry of Proteins. *Analytical Chemistry* **2010,** *83* (3), 1015-1021.
43. Zhou, S.; Cook, K. D., A Mechanistic Study of Electrospray Mass Spectrometry: Charge Gradients within Electrospray Droplets and Their Influence on Ion Response. *Journal of the American Society for Mass Spectrometry* **2001,** *12* (2), 206-214.
44. Wang, G.; Cole, R. B., Effect of Solution Ionic Strength on Analyte Charge State Distributions in Positive and Negative Ion Electrospray Mass Spectrometry. *Analytical Chemistry* **1994,** *66* (21), 3702-3708.
45. Koszinowski, K.; Lissy, F., Counter-Ion and Solvent Effects in Electrospray Ionization of Solutions of Alkali Metal and Quaternary Ammonium Salts. *International Journal of Mass Spectrometry* **2013,** *354*, 219-228.
46. Pan, P.; McLuckey, S. A., The Effect of Small Cations on the Positive Electrospray Responses of Proteins at Low Ph. *Analytical Chemistry* **2003,** *75* (20), 5468-5474.
47. Sterling, H. J.; Batchelor, J. D.; Wemmer, D. E.; Williams, E. R., Effects of Buffer Loading for Electrospray Ionization Mass Spectrometry of a Noncovalent Protein Complex That Requires High Concentrations of Essential Salts. *Journal of the American Society for Mass Spectrometry* **2010,** *21* (6), 1045-1049.
48. Metwally, H.; McAllister, R. G.; Konermann, L., Exploring the Mechanism of Salt-Induced Signal Suppression in Protein Electrospray Mass Spectrometry Using Experiments and Molecular Dynamics Simulations. *Analytical Chemistry* **2015,** *87* (4), 2434-2442.
49. Iavarone, A. T.; Udekwu, O. A.; Williams, E. R., Buffer Loading for Counteracting Metal Salt-Induced Signal Suppression in Electrospray Ionization. *Analytical Chemistry* **2004,** *76* (14), 3944-3950.
50. Flick, T. G.; Merenbloom, S. I.; Williams, E. R., Anion Effects on Sodium Ion and Acid Molecule Adduction to Protein Ions in Electrospray Ionization Mass Spectrometry. *Journal of the American Society for Mass Spectrometry* **2011,** *22* (11), 1968-1977.
51. Pan, J.; Xu, K.; Yang, X.; Choy, W.-Y.; Konermann, L., Solution-Phase Chelators for Suppressing Nonspecific Protein− Metal Interactions in Electrospray Mass Spectrometry. *Analytical Chemistry* **2009,** *81* (12), 5008-5015.
52. Cassou, C. A.; Williams, E. R., Desalting Protein Ions in Native Mass Spectrometry Using Supercharging Reagents. *Analyst* **2014,** *139* (19), 4810-4819.
53. DeMuth, J. C.; McLuckey, S. A., Electrospray Droplet Exposure to Organic Vapors: Metal Ion Removal from Proteins and Protein Complexes. *Analytical Chemistry* **2014,** *87* (2), 1210-1218.
54. Niessen, W. M., *Liquid Chromatography-Mass Spectrometry*. CRC Press: 2006.
55. Apffel, A.; Fischer, S.; Goldberg, G.; Goodley, P. C.; Kuhlmann, F. E., Enhanced Sensitivity for Peptide Mapping with Electrospray Liquid Chromatography-Mass Spectrometry in the Presence of Signal Suppression Due to Trifluoroacetic Acid-Containing Mobile Phases. *Journal of Chromatography A* **1995,** *712* (1), 177-190.
56. Temesl, D.; Law, B., The Effect of Lc Eluent Composition on Ms Responses Using Electrospray Ionization. *LC GC* **1999,** *17* (7), 626-632.
57. Garcia, M., The Effect of the Mobile Phase Additives on Sensitivity in the Analysis of Peptides and Proteins by High-Performance Liquid Chromatography–Electrospray Mass Spectrometry. *Journal of Chromatography B* **2005,** *825* (2), 111-123.
58. Clarke, D. J.; Campopiano, D. J., Desalting Large Protein Complexes During Native Electrospray Mass Spectrometry by Addition of Amino Acids to the Working Solution. *Analyst* **2015,** *140* (8), 2679-2686.

59. Jackson, A. U.; Talaty, N.; Cooks, R. G.; Van Berkel, G. J., Salt Tolerance of Desorption Electrospray Ionization (Desi). *Journal of the American Society for Mass Spectrometry* **2007,** *18* (12), 2218-2225.
60. Green, F.; Salter, T.; Gilmore, I.; Stokes, P.; O'Connor, G., The Effect of Electrospray Solvent Composition on Desorption Electrospray Ionisation (Desi) Efficiency and Spatial Resolution. *Analyst* **2010,** *135* (4), 731-737.
61. Cotte-Rodríguez, I.; Takáts, Z.; Talaty, N.; Chen, H.; Cooks, R. G., Desorption Electrospray Ionization of Explosives on Surfaces: Sensitivity and Selectivity Enhancement by Reactive Desorption Electrospray Ionization. *Analytical Chemistry* **2005,** *77* (21), 6755-6764.
62. Nyadong, L.; Hohenstein, E. G.; Galhena, A.; Lane, A. L.; Kubanek, J.; Sherrill, C. D.; Fernández, F. M., Reactive Desorption Electrospray Ionization Mass Spectrometry (Desi-Ms) of Natural Products of a Marine Alga. *Analytical and Bioanalytical Chemistry* **2009,** *394* (1), 245-254.
63. Liu, Y.; Miao, Z.; Lakshmanan, R.; Loo, R. R. O.; Loo, J. A.; Chen, H., Signal and Charge Enhancement for Protein Analysis by Liquid Chromatography–Mass Spectrometry with Desorption Electrospray Ionization. *International Journal of Mass Spectrometry* **2012,** *325*, 161-166.
64. Honarvar, E.; Venter, A. R., Ammonium Bicarbonate Addition Improves the Detection of Proteins by Desorption Electrospray Ionization Mass Spectrometry. *Journal of the American Society for Mass Spectrometry* **2017**, *28* (6), 1109-1117.
65. Takáts, Z.; Wiseman, J. M.; Gologan, B.; Cooks, R. G., Electrosonic Spray Ionization. A Gentle Technique for Generating Folded Proteins and Protein Complexes in the Gas Phase and for Studying Ion−Molecule Reactions at Atmospheric Pressure. *Analytical Chemistry* **2004,** *76* (14), 4050-4058.
66. Zhang, Z.; Marshall, A. G., A Universal Algorithm for Fast and Automated Charge State Deconvolution of Electrospray Mass-to-Charge Ratio Spectra. *Journal of The American Society for Mass Spectrometry* **1998,** *9* (3), 225-233.
67. Pan, P.; Gunawardena, H. P.; Xia, Y.; McLuckey, S. A., Nanoelectrospray Ionization of Protein Mixtures: Solution Ph and Protein P I. *Analytical Chemistry* **2004,** *76* (4), 1165-1174.
68. Flick, T. G.; Cassou, C. A.; Chang, T. M.; Williams, E. R., Solution Additives That Desalt Protein Ions in Native Mass Spectrometry. *Analytical Chemistry* **2012,** *84* (17), 7511-7517.
69. Myung, S.; Wiseman, J. M.; Valentine, S. J.; Takats, Z.; Cooks, R. G.; Clemmer, D. E., Coupling Desorption Electrospray Ionization with Ion Mobility/Mass Spectrometry for Analysis of Protein Structure: Evidence for Desorption of Folded and Denatured States. *The Journal of Physical Chemistry B* **2006,** *110* (10), 5045-5051.
70. Koch, K. J.; Gozzo, F. C.; Zhang, D.; Eberlin, M. N.; Cooks, R. G., Serine Octamer Metaclusters: Formation, Structure Elucidation and Implications for Homochiral Polymerization. *Chemical Communications* **2001,** (18), 1854-1855.
71. Takats, Z.; Nanita, S. C.; Cooks, R. G.; Schlosser, G.; Vekey, K., Amino Acid Clusters Formed by Sonic Spray Ionization. *Analytical Chemistry* **2003,** *75* (6), 1514-1523.
72. Bojesen, G.; Breindahl, T.; Andersen, U. N., On the Sodium and Lithium Ion Affinities of Some A-Amino Acids. *Journal of Mass Spectrometry* **1993,** *28* (12), 1448-1452.
73. Gorman, G. S.; Speir, J. P.; Turner, C. A.; Amster, I. J., Proton Affinities of the 20 Common. Alpha.-Amino Acids. *Journal of the American Chemical Society* **1992,** *114* (10), 3986-3988.
74. Harrison, A., The Gas-Phase Basicities and Proton Affinities of Amino Acids and Peptides. *Mass Spectrometry Reviews* **1997,** *16* (4), 201-217.
75. Gronert, S.; Simpson, D. C.; Conner, K. M., A Reevaluation of Computed Proton Affinities for the Common A-Amino Acids. *Journal of the American Society for Mass Spectrometry* **2009,** *20* (11), 2116-2123.
76. Badu-Tawiah, A.; Cooks, R. G., Enhanced Ion Signals in Desorption Electrospray Ionization Using Surfactant Spray Solutions. *Journal of the American Society for Mass Spectrometry* **2010,** *21* (8), 1423-1431.

77. Chi, E. Y.; Krishnan, S.; Randolph, T. W.; Carpenter, J. F., Physical Stability of Proteins in Aqueous Solution: Mechanism and Driving Forces in Nonnative Protein Aggregation. *Pharmaceutical Research* **2003,** *20* (9), 1325-1336.

Chapter 4

4. EFFECTS OF AMINO ACID ADDITIVES ON PROTEIN SOLUBILITY - INSIGHTS FROM DESORPTION AND DIRECT ELECTROSPRAY IONIZATION MASS SPECTROMETRY

Reprinted (adapted) from

Roshan Javanshad, Andre R. Venter

Analyst, **2021,** 146**,** 6592-6604

4.1. Introduction

Understanding the mechanisms governing protein solubility and aggregation at the molecular level is of great importance to many fields including biochemistry, pharmaceutical sciences, and clinical studies.[1-3] Osmolytes are a diverse group of small molecules naturally selected to protect proteins against different stress factors while maintaining protein function[4-5] and have widespread applications in many fields.[6-7] Naturally occurring amino acids are amongst the osmolytes that have been studied for nearly four decades[8] for enhancing protein solubility and reducing protein aggregation.[9-11] The effect of arginine (Arg)[12] on suppressing protein aggregation[13] and the stabilizing effect of several other amino acids, including glycine (Gly),[14-15] proline (Pro),[16-20] histidine (His),[21] alanine (Ala),[22] glutamic acid (Glu) - arginine mixtures,[23] and

small amines[24-25] have demonstrated the ability of amino acid additives to stabilize proteins under stress conditions and to improve protein solubility by suppressing aggregation.

Despite decades of extensive studies, there is no unified theory that can explain how amino acids inhibit protein aggregation.[26] Progress has been made to successfully differentiate between the effects of additives on native versus unfolded or denatured structures.[27] Some additives help stabilize the structure of native proteins and therefore improve stability, whereas others may destabilize the native structure or show little effect on protein structure but effectively suppress aggregation.[28-32] Amongst the proposed mechanisms, preferential interaction theory,[33-36] the crowding effect[37-38] and/or the gap effect[39] have been widely studied. These proposed mechanisms have predominantly been examined or modeled at high concentrations of additives (in 50 mM range) in bulk solution by conventional biophysical techniques,[31, 40-42] and have not yet been studied at micro-scale with techniques that can operate at lower quantities and concentrations.

Desorption electrospray ionization mass spectrometry (DESI-MS) couples extractive-desorption of the samples with electrospray ionization.[43] The analysis of samples in DESI occurs via the droplet pickup mechanism,[44] where charged droplets of solvent impact the sample, and a thin, localized solvent layer is formed on the surface, dissolving the analytes. Progeny droplets containing the extracted analyte are formed via subsequent droplet collisions and undergo electrospray ionization processes.

DESI provides similar spectral information of proteins to what is obtained with ESI-MS[45-47] albeit at lower intensities, and the technique especially struggles with larger proteins.[45, 48] Various approaches have been developed to improve DESI analysis of proteins. For example,

coupling ion mobility separation with DESI,[49-50] creating a very short sampling pathway[51] and using a pre-wetting technique.[52] By deconstructing DESI and independently investigating protein desorption and ionization, we confirmed that inefficient protein dissolution during the short timescale of DESI is a major contributor to the lower protein signal.[48, 53]

Non-specific protein aggregates in concentrated solutions or droplets, such as those generated by electrospray are prevalent, and the formation of aggregates in both bulk solution and droplets due to weak non-covalent interactions is well-established.[54-55] Aggregate numbers close to 20 were observed in the subpopulation of droplets with apparent diameters near 220 nm and protein concentration of 4 μM, and the probability of higher aggregate numbers increase with higher protein concentrations and larger droplet sizes.[56] Considering the thin, micro-localized solvent layer on the sample surface, into which proteins are dissolved, and the size of DESI progeny droplets (average 1-4 μm),[57] aggregates can form extensively due to the high concentration of unfolding protein, resulting in protein signal reduction. The solubility of proteins in the desorption solvent and aggregate formation directly affects the efficacy of protein dissolution[58] in the desorbing solvent during the short DESI time frame,[59] which provides a reasonable explanation of why the analysis of proteins by DESI-MS is inherently more difficult than small molecules.[45, 48]

Additives have been a convenient approach for improving protein solubility in DESI. We previously explored approaches such as gas-phase additives, for example vapors of ethyl acetate,[60] and solution-phase additives such as ammonium bicarbonate[61] and the amino acid L-serine[62] in order to enhance protein analysis by DESI-MS.

Applications of amino acid additives in ESI-MS of proteins have been explored relatively recently. The stabilizing effect of amino acids against thermal denaturation of non-covalent protein complexes in ESI-MS was reported and contributed to ion ejection and reduced columbic repulsion.[63] The stabilizing effect of amino acids and imidazole on protein-ligand ions against in-source fragmentation during ESI-MS has also been studied and reported as highly dependent on ESI conditions and instrumentation[64] and likely related to an evaporative cooling mechanism.[65]

It has been shown that amino acid additives, L-serine in particular, can improve protein analysis by removing sodium adducts from high NaCl concentration in the protein sample during native ESI[66] and DESI.[62] Since DESI progeny droplets follow the same ionization process as ESI droplets,[44] the desalting effect of L-serine, which was observed in both types of experiment, is likely related to the electrospray ionization process. On the other hand, L-serine also increased signal intensity of purified proteins in DESI-MS when combined with formic acid or ammonium bicarbonate as co-additives, but no such effect was observed in ESI-MS of similar protein solutions, indicating that this effect is independent of electrospray ionization processes and related to protein dissolution and desorption.

With DESI-MS and ESI-MS the analysis of proteins occurs via the same ionization mechanisms, therefore, relative changes in signal between these two techniques provide a window into studying protein dissolution and desorption.[48,53] With DESI, the short but controllable interaction time of proteins with denaturing solvents and additives before detection allows one the unique opportunity to study protein unfolding during dissolution, while in non-native ESI, unfolding has already occurred during sample preparation, long before protein detection. In this study, we interpret relative changes in protein signal intensities as protein

dissolution effects, after controlling for possible ionization differences using comparable experiments in ESI. We demonstrate that mechanistic insights into the effects of solution-phase additives on proteins can be obtained at much lower additive concentrations and protein amounts, compared to most biophysical techniques that are commonly used for this purpose.

4.2 Experimental

4.2.1 Materials

Lyophilized equine heart cytochrome *c* (Cyt *c*, 12.3 kDa, pI=10.3) and equine muscle myoglobin (Myo, 17.5 kDa for holo-myoglobin, pI=7.4) were purchased from Sigma-Aldrich (St. Louis, MO). Proteins were at 95% purity and were used without further purification. BioUltra grade ammonium bicarbonate (ABC), ammonium acetate (NH_4OAc), A.C.S. grade ammonium hydroxide (NH_4OH), HPLC-MS grade methanol (MeOH), LC-MS grade formic acid (FA) and all amino acids (98%) were purchased from Sigma-Aldrich (St. Louis, MO) except N-acetyl L-serine which was purchased from Carbosynth (Berkshire, UK). Milli Q water was obtained from a Thermo-Barnstead Water Polisher. Fused silica capillaries were purchased from Trajan Scientific (Ringwood, Australia). Porous polyethylene surfaces (PE) with an average pore size of 15-45 μm (POREX-4900) were purchased from Interstate Specialty Products (Sutton, MA). PTFE plates were purchased from Prosolia Inc (Indianapolis, IN).

4.2.2 Sample preparation and solvent systems

Stock solutions of each protein were made by dissolving the lyophilized protein powder in Milli Q water to a final concentration of 800 μM or 80 μM depending on the desired surface concentration. Protein solutions were sprayed on the surface with a pneumatically-assisted

nebulizer spray made of two coaxial fused silica capillaries similar to an ESSI sprayer.[67] The sprayer was orthogonally positioned at 3 mm above the surface. Nebulizing gas pressure and flow rates were 100 psi and 3 µl/min respectively, and the stage was moved at 150 µm/s, resulting in long homogenous protein lines deposited with 1.1 ± 0.1 mm widths. The average surface concentration of these protein lines was approximately 22 pmol/mm^2 for all DESI experiments with the exception of spectra in Figure 4.1 and Figure 4.2 which were obtained from protein lines with an approximate surface concentration of 10X higher (222 pmol/mm^2) in order to obtain clear and comparable spectra for all different solvent systems regardless of the inherently lower sensitivity of the non-acidic solvents. For PTFE slides, 3 µl volumes of 20 µM aqueous protein solutions were micro pipetted on the slide and dried under vacuum for 30 minutes at approximately 85 kPa. The diameter of the dried spot was approximately 1.2 mm, resulting in average protein surface concentration of 24 pmol/mm^2. ESI experiments used 10 µM protein in the appropriate solvent systems.

All DESI desorption solvent systems were made in 50% MeOH:H_2O. Aqueous stock solutions of 2.0 M ammonium bicarbonate and 2.0 M ammonium acetate were used to prepare 200 mM dilutions in 50% MeOH (approximately pH 8.0 and 7.3, respectively). LC-MS grade formic acid and ammonium hydroxide were used to prepare 0.1% (v/v) formic acid and 1% (v/v) ammonium hydroxide in 50% MeOH (approximately pH 3.0 and 10, respectively). Serial dilutions from aqueous amino acid stock solutions were used to make 100 µM amino acid in the solvent system. The pH of aqueous solutions was measured at room temperature with a Mettler Toledo Seven Easy pH meter (Columbus, OH) equipped with an InLab Expert pH electrode.

Similar to previous relevant studies,[68] the reported pH values were not corrected for the influence of MeOH as it was deemed inconsequential to the experiments.

4.2.3 Instrumentation and experimental parameters

A linear ion trap mass spectrometer, LTQ (Thermo Scientific, Waltham, MA, USA) was combined with a 3-dimensional translational stage (Purdue University, West Lafayette, IN, USA) for DESI analyses. An extended ion sampling capillary with a 5 cm extension was purchased from Scientific Instruments Inc. An electrospray emitter and desorption sprayer was prepared from a Swagelok T-piece and two pieces of coaxial fused silica capillary tubing.[67] The outer capillary (for sheath gas) was approximately 20 mm in length with an outer diameter of 430 μm and an inner diameter of 320 μm. The internal capillary (for solvent) had an outer diameter of 220 μm, and an inner diameter of 50 μm. The solvent capillary extended through the T-piece and was connected to a syringe pump which delivered the solvent.

DESI sprayer incident angle was 54°. The distance between the desorption sprayer and heated extended capillary was 4 mm. The tip of the desorption sprayer was 1 mm above the surface. ESI experiments were performed under the same conditions as DESI, but protein solutions were directly sprayed towards the heated extended capillary using the same sprayer.

Spray potential was set at 4.0 kV and was applied to the liquid junction of a stainless-steel syringe needle which delivered solvent at a flow rate of 5 μL/min, with N_2 as nebulizing gas at 100 psi. Capillary temperature was set at 250°C. LTQ ion optic parameters were optimized by LTQ TunePlus automatic tuning feature for each protein highest intensity charge state (HICS) peak, using direct infusion of 5 μM protein in each solvent system.

4.2.4 Data analysis

Mass spectra were collected and viewed in Xcalibur Qual Browser (2.0.7). At least three independent trials were collected for each solvent system. In each trial three protein sample lines or spots were perpendicularly scanned and averaged. Signal intensities were calculated as the average of three trials and error bars represent ± mean standard deviation. MagTran software (1.03) was used for charge state deconvolution and calculation of integrated protein signal intensity and S/N as described by Zhang and Marshall.[69]

4.3 Results and discussion

4.3.1 Influence of solvent composition on protein signal increase by L-serine

Previously, we showed that the addition of low millimolar L-serine concentrations into 50% MeOH:H_2O desorption solvent can improve sensitivity for protein detection by DESI-MS in the presence of 1 mM and higher concentrations of NaCl,[62] similar to observations reported in native ESI-MS experiments.[66] However, L-serine also increased signal intensity of purified proteins in DESI-MS when combined with formic acid or ammonium bicarbonate as co-additives, but no such effect was observed in ESI-MS of similar protein solutions. To investigate the role of solvent composition on the mechanism governing increased protein signal in DESI-MS with addition of L-serine, the combination of L-serine with the following four solvent systems were compared: formic acid, ammonium acetate, ammonium bicarbonate, and ammonium hydroxide. All solvents were made in 50% MeOH:H_2O, and therefore 50% MeOH:H_2O was treated as the additive-free control. Out of the five different solvent systems, only the formic acid-containing solution showed an increase in protein signal with L-serine addition for both cytochrome *c* and myoglobin. However, L-serine was also able to increase the

signal intensity for cytochrome *c* in ammonium bicarbonate containing solutions, as seen in Figure 4.1. A complete set of representative spectra for all five solvent systems and changes in protein signal intensities with L-serine addition can be found in Figure 4.2 and Table 4.1.

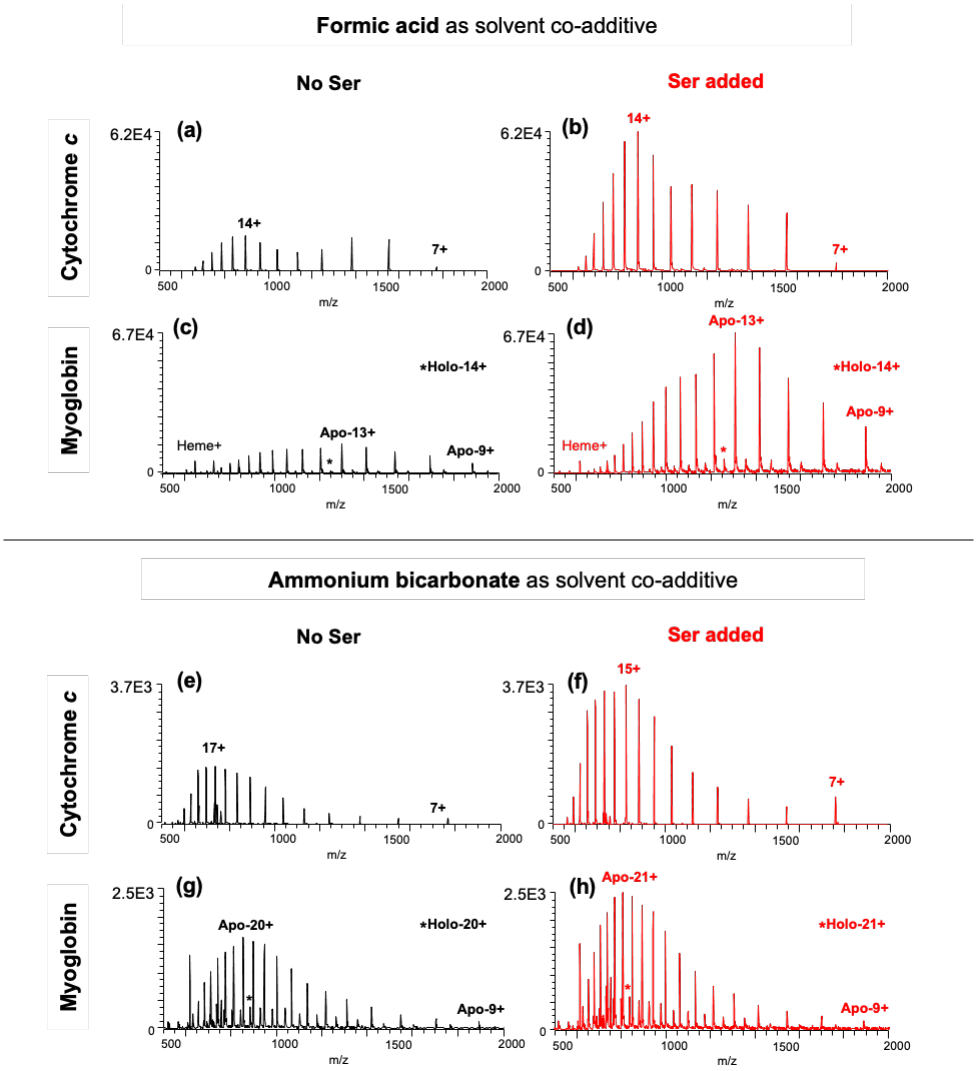

Figure 4.1. Representative DESI-MS spectra of natively deposited cytochrome *c* and myoglobin analyzed without L-serine and with 100 µM L-serine. DESI-MS spectra of natively deposited cytochrome *c* and myoglobin analyzed without L-serine (shown in black) and with 100 µM L-serine (shown in red). (a), (c) 0.1% formic acid in 50% MeOH without L-serine, and (b), (d) with 100 µM L-serine. (e), (g) 200 mM ammonium bicarbonate in 50% MeOH without L-serine, and (g), (h) with 100 µM L-serine. The absolute intensities reported are the average intensity of the highest observed charge state (HICS) for the protein in each desorbing solvent system.

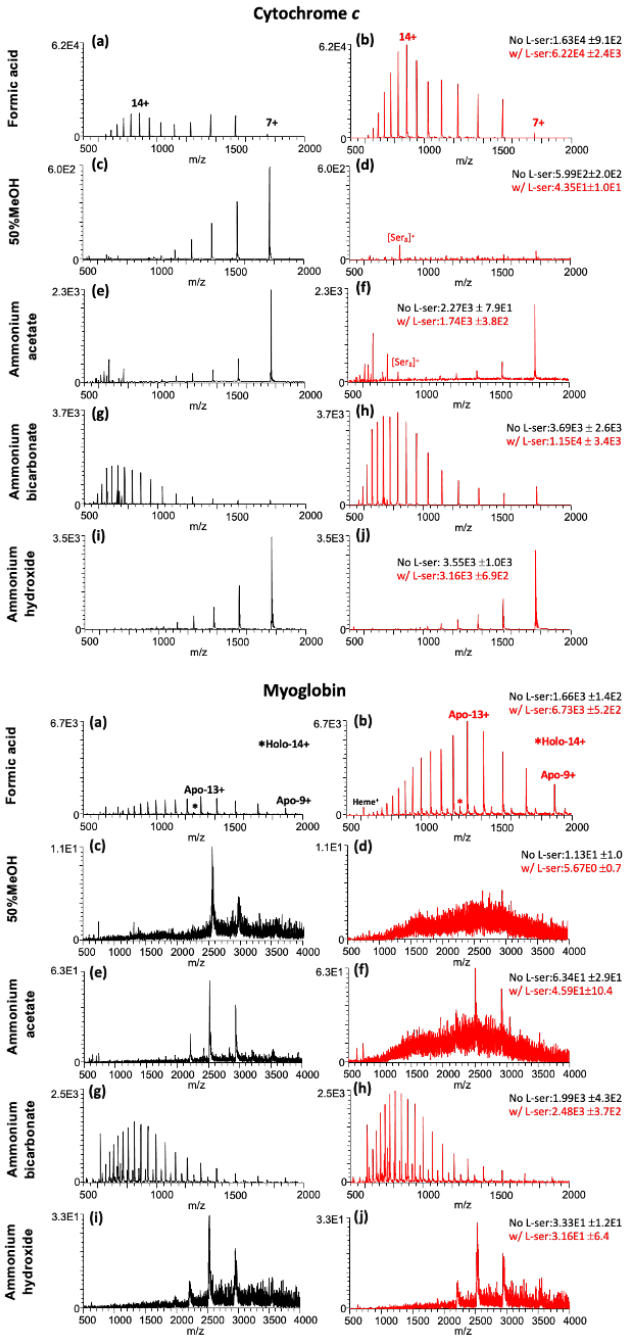

Figure 4.2. Representative DESI-MS spectra of natively deposited cytochrome *c* and myoglobin analyzed with five different desorption solvent systems with 100 μM L-serine. Solvent systems containing L-serine (shown in red) and without it (shown in black) are arranged by increasing pH. (a), (b) 0.1% formic acid in 50% MeOH. (c), (d) 50% MeOH. (e), (f) 200 mM ammonium acetate in 50% MeOH. (g), (h) 200 mM ammonium bicarbonate in 50% MeOH. (i), (j) 1% ammonium hydroxide in 50%MeOH. The intensities reported are the average intensity of the highest observed charge state (HICS) of the protein in each solvent system with L-serine (in red) and without it (in black).

Table 4.1. Improvement in signal intensity for each protein with addition of L-serine to the five different solvent systems.

	pH	Average fold change Cyt *c* HICS Intensity	Average fold change Cyt *c* Integrated Intensity	Average fold change apo-Myo HICS Intensity	Average fold change Apo-myo Integrated Intensity	Average fold change holo-Myo HICS Intensity	Average fold change Holo-myo Integrated Intensity
Formic acid	2.99	3.8±0.1	3.1±0.4	4.3± 0.3	3.7± 0.2	3.5± 0.3	3.31±0.3
50% MeOH	5.75	0.1± 0.02	0.4±0.02	N/A	N/A	0.5± 0.05	N/A
Ammonium acetate	7.32	0.8± 0.2	0.7±0.1	N/A	N/A	0.7±0.2	N/A
Ammonium bicarbonate	7.97	3.1± 0.2	3.1±0.3	1.4± 0.2	1.2± 0.2	1.3± 0.2	1.3± 0.2
Ammonium hydroxide	10.02	0.9± 0.2	0.8±0.2	N/A	N/A	0.9± 0.2	N/A

An important consequence of changing solvent additives is the solution pH and the effect this can have on the protonation state of sample species. Serine was added into solvent systems that spanned a pH range of 3 to 10. The estimated protonation populations of serine and the protein net charge in the different pH ranges can be found in Table 4.2. Although the solution pH can affect serine protonation state, and therefore population ratios of different serine species in the solution, in all solvent systems except ammonium hydroxide, zwitterionic serine is the predominant form. No correlation between desorption solvent pH and increased protein signal intensities with L-serine was observed.

Table 4.2. Approximate net charge on protein and serine in different solvent systems.

Cytochrome *c*						
Solvent	**Intensity Fold Change**	**≈pH**	**Protein Net Charge (pI 10.3)**	**Serine Population**	**pH-pka$_1$ (2.21)**	**pH-pka$_2$ (9.15)**
Formic acid	3.1	3	+	60-70% zwitterion 30-40% positive	0.79	
50% MeOH	0.8	6	+	100% zwitterion	3.79	
Ammonium acetate	0.8	7	+	99% zwitterion 1% negative		-2.15
Ammonium bicarbonate	3.1	8	+	92-94% zwitterion 6-8% negative		-1.15
Ammonium hydroxide	0.9	10	-	10-20% zwitterion 80-90% negative		0.85

Myoglobin						
Solvent	**Intensity Fold Change**	**≈pH**	**Protein Net Charge (pI 7.4)**	**Serine Population**	**pH-pka$_1$ (2.21)**	**pH-pka$_2$ (9.15)**
Formic acid	3.7	3	+	60-70% zwitterion 30-40% positive	0.79	
50% MeOH	0.5	6	+	100% zwitterion	3.79	
Ammonium acetate	0.7	7	-	99% zwitterion 1% negative		-2.15
Ammonium bicarbonate	1.2	8	-	92-94% zwitterion 6-8% negative		-1.15
Ammonium hydroxide	0.9	10	-	10-20% zwitterion 80-90% negative		0.85

The other important consequence of changing solvent composition is protein conformational changes. Lower charge states, indicative of more folded protein conformations, were observed with desorbing solvents containing 50% MeOH, and when ammonium acetate or ammonium hydroxide was added into this solvent (Figure 4.2). In ammonium acetate and ammonium hydroxide the change in protein signal intensities with serine addition was not statistically significant (p-value>0.05) and in the additive-free solvent system the signal even deteriorated. Signal suppression in the additive-free solvent system is likely due to extensive

formation of nonspecific adducts and spreading of the protein signal over multiple peaks which causes a reduction in the signal intensity of the highest intensity charge state (HICS). As can be observed in Figure 4.2 (d) and (f) for myoglobin, the extensive overlapping peaks resemble non-specific adduction of small molecules to proteins.[70-71]

In contrast, protein signal intensities increased by a factor of 3.8±0.1 for cytochrome *c*, and by a factor of 4.3±0.3 and 3.5±0.2 for apo-myoglobin and holo-myoglobin, respectively, with addition of L-serine to the desorption solvent containing 0.1% formic acid (Figure 4.1 (c,d)). Similarly, with the addition of L-serine to 200 mM ammonium bicarbonate as desorption solvent, cytochrome *c* signal intensity increased by a factor of 3.1±0.2 (Figure 4.1 (e,f)). The signal intensity for myoglobin, on the other hand, increased only by a factor of 1.2±0.2 (Figure 4.1 (g,h)), which was not statistically significant (p-value>0.05). Extensive unfolding was also observed for both proteins, despite the near-neutral pH of the solvent system and buffering by ammonium bicarbonate. It was previously proposed that protein unfolding with ammonium bicarbonate containing solutions during ESI is likely due to protein destabilization inside the heated electrospray droplets, either because of an increase in hydrophobic surface area by bubble formation, or due to electrothermal supercharging.[61, 72-73]

A comparison between the two proteins suggests that this difference could be related to protein net charge in solution. Cytochrome *c* and myoglobin are both single-chain peptides of similar size (12.3 kDa and 16.9 kDa, respectively), but their isoelectric points are approximately 10.3[74] and 7.4,[75] respectively. This difference in isoelectric points results in myoglobin having a negative to near neutral net charge in ammonium bicarbonate solution, whereas cytochrome *c*

has a positive net charge. Likewise, protein net charge is an important factor in determining the effect of Hofmeister series and osmolytes on protein solubility.[76-77]

Therefore, as evident from a comparison between the behaviors of the two proteins in the four desorbing solvent systems, a denaturing desorbing solvent and protein with a net positive charge are key factors in the mechanism governing the substantial improvement in protein signal with L-serine.

4.3.2 Role of protein conformational change and serine addition timepoint

To investigate the role of protein conformation prior to the interaction with L-serine, cytochrome *c* and myoglobin were spray-deposited out of aqueous solution (native-like conformation) or out of 0.1% formic acid solution (unfolded conformation) and analyzed with a desorption spray solvent containing 0.1% formic acid in 50% MeOH in the presence or absence of 100 μM L-serine. As seen in Figure 4.3, for both cytochrome *c* and myoglobin, signal intensities of proteins deposited in native conformation (top panel) increased more with serine addition than when proteins were already unfolded before serine addition (bottom panel). The signal intensity for natively deposited cytochrome *c* and apo-myoglobin increased by a factor of 2.6±0.3 and 3.8±0.8, respectively. Despite using 50% MeOH and formic acid as the desorbing spray solvent, holo-myoglobin signal was also observed for the natively deposited sample and increased by a factor of 3.5±0.2 with serine addition, as seen in Figure 4.3 (b). When the samples were deposited out of denaturing solution, serine addition achieved only mild increases in the signal of 1.3±0.3 and 1.5±0.4 for cytochrome *c* and apo-myoglobin with *p*-values 0.098 and 0.042, respectively (Figure 4.3 (g,h)).

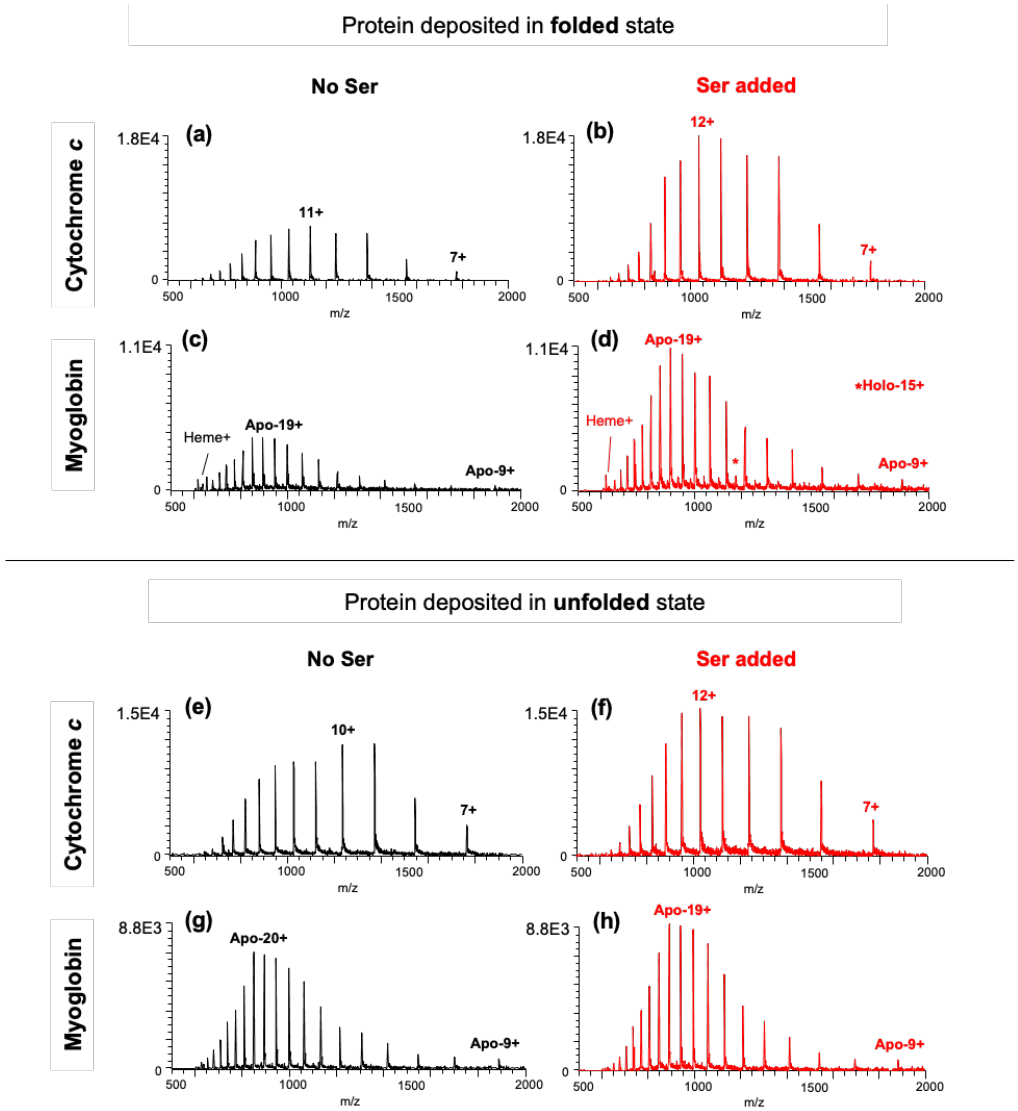

Figure 4.3. Representative DESI-MS spectra of cytochrome *c* and myoglobin deposited from (a-d) aqueous solution vs. (e-h) acidic solution, analyzed with 0.1% formic acid in 50%MeOH (shown in black) or with 100 μM L-serine (shown in red). The intensities are scaled to the average intensity of highest observed charge state (HICS) for each protein when analyzed with 100 μM L-serine.

In the previous section we showed the importance of denaturing solvent systems for the beneficial effect of serine addition on signal intensities. The difference in relative improvements

between native and unfolded protein prior to analysis further indicates that serine should be present during the unfolding process.

A similar increase in signal intensity does not occur under denaturing conditions upon the addition of L-serine when proteins are analyzed in solution using direct ESI infusion.[62] Figure 4.4 shows 10 μM of each protein, electrosprayed out of the exact solvent systems as for the DESI results in Figure 4.1 (a) and (b) and Figure 4.3 (0.1% formic acid in 50%MeOH). The order of adding formic acid and L-serine was also alternated to measure the effect of unfolding in bulk solution in the presence of L-serine. The addition of 100 μM L-serine to the working solution before and after protein unfolding through acidification made no meaningful difference in protein ESI signal intensity, although the changes in absolute signal intensity between adding serine first was statistically significant (p-value<0.05) for cytochrome *c*. Adding L-serine prior to acidification in bulk solution increased the signal for cytochrome *c* by a mere 1.3 times compared to when it was not present (p-value=0.001). On the other hand, when serine was added after formic acid addition to the cytochrome *c* solution, there was no statistically significant change compared to not having serine in the solution at all (p-value>0.05). In the case of myoglobin, addition of serine reduced the absolute signal intensity compared to no serine present, and there was no statistical difference between adding serine before or after formic acid (p-value=0.56), as seen in Figure 4.4.

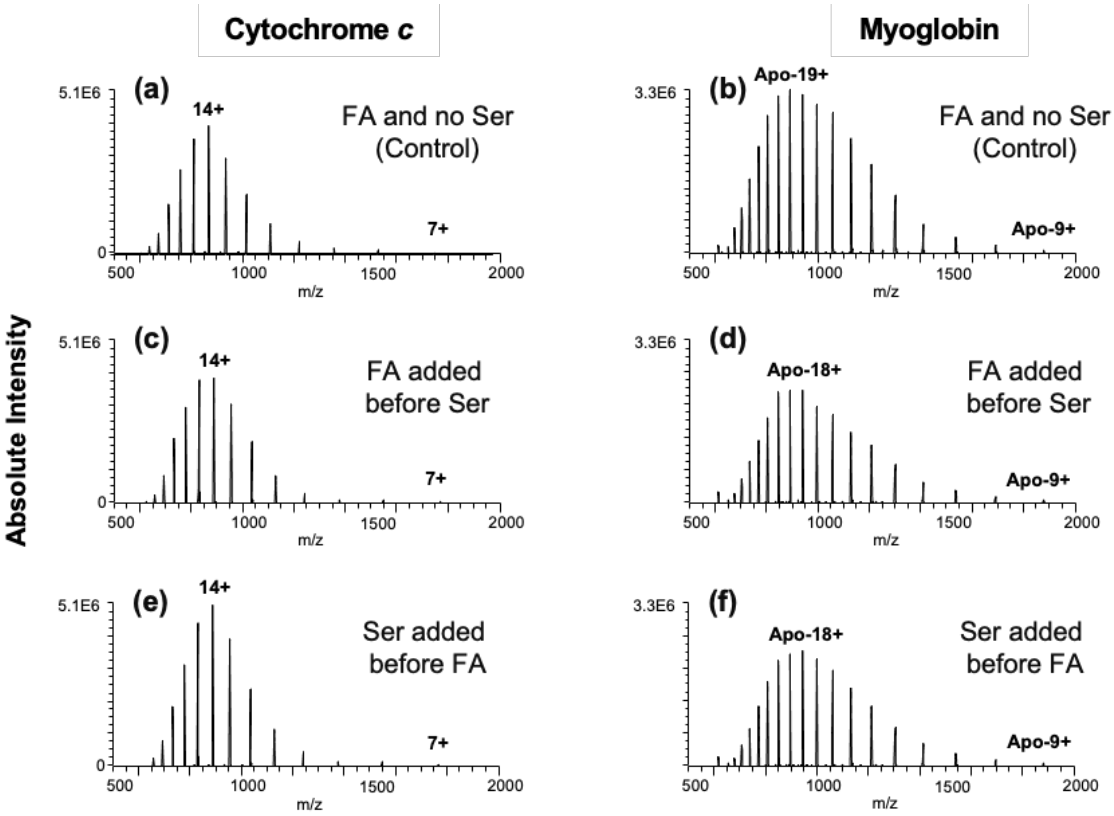

Figure 4.4. Representative ESI spectra of cytochrome *c* and myoglobin unfolding in bulk solution. Bulk solution containing (a), (b) 0.1% formic acid only, (c), (d) containing 0.1% formic acid and 100 μM L-serine with formic acid added first followed by serine after mixing to the protein solution, and (e), (f) containing 0.1% formic acid and 100 μM L-serine with L-serine added first to the protein solution followed by formic acid.

The lack of improvement in protein signal intensity in ESI reiterates that the improvement in protein signal intensity in DESI is likely related to the dissolution of proteins during desorption. We have previously shown that proteins desorb equally well from the surface in DESI, and poor dissolution, rather than physical desorption or ionization problems are the major contributor to poor DESI-MS signals for protein.[48, 53] The lack of improvement in protein signal with L-serine in ESI (Figure 4.4) and the difference between timescales of unfolding and dissolution to ion detection in DESI versus ESI possibly point towards serine affecting the kinetics of dissolution, rather than a thermodynamic effect on solubility. These observations

together imply that dissolution of native proteins in denaturing solvents is positively influenced in the presence of L-serine as a solution additive, manifested by an increase in protein signal intensity measured by DESI-MS.

4.3.3 Relating DESI observations with known models for suppression of protein aggregation by amino acids

One of the most consequential repercussions of protein unfolding is aggregation. Mechanisms of protein unfolding and subsequent aggregation can involve non-covalent weak interactions such as hydrophobic and electrostatic interactions, hydrogen bonding, Van der Waals interactions, or covalent disulfide bonds.[78] Many studies support the proposed mechanism that amino acid additives can improve protein solubility by suppressing aggregation of unfolded species or partially unfolded intermediates.[79-80] This has been demonstrated using in-vitro and in-silico studies, by NMR, X-ray spectroscopy, and crystallography, often implicating direct binding to folding intermediates.[12, 41, 81-83]

The exact mechanism of action for the prevention of aggregation by additives including amino acids is yet under debate,[84] but here we place our observations from DESI-MS and ESI-MS experiments into the context of two widely studied theories on additive effects on protein solubility. Preferential interaction theory[33-36] measures changes in thermodynamic properties such as the interaction of protein surface with additive and water in bulk solution. Based on this model, additives that stabilize protein, such as most osmolytes, including a number of amino acids, are preferentially excluded from the protein surface and can influence protein folding equilibrium.[85] Other additives, such as urea and arginine that are not excluded from the surface of the protein and are weakly bound, do not stabilize native protein structure, but improve

protein solubility through aggregation suppression.[85-86] In our data, L-serine did not shift the protein charge state distribution to those representing more folded charge states, and also destabilized myoglobin (Figure 4.3). Chen *et al.* have reported similar observations in ESI-MS of myoglobin in 20 mM ammonium acetate buffer with L-serine.[63] Based on these observations and according to the preferential interaction theory, we propose that L-serine behaves as a destabilizing additive, and similar to arginine, binds to the protein through weak interactions to suppress protein aggregation.

The gap effect theory differentiates between reversible or irreversible aggregation and non-native or native aggregation and has been proposed based on results from computational models and molecular dynamic simulations.[39] Based on this model, as two protein molecules associate, a gap is formed in which an amino acid additive is considered neither preferentially bound nor completely excluded from the protein surface (known as a neutral crowder), while allowing water molecules to interact with proteins.[87] Such additives increase the free energy of protein−protein association and slow aggregation, not because of changes in thermodynamic properties but based on a kinetic effect on protein association during aggregation. Comparison between Figure 4.3 and Figure 4.4 supports the hypothesis that L-serine is perhaps affecting the kinetics of protein aggregation during unfolding, which can be captured due to the short timescale of protein dissolution in DESI compared to the time between sample preparation and analysis by direct ESI.

Recent studies have reported more evidence for direct interaction between amino acid additives and protein,[42, 88-89] including FTIR spectroscopy and molecular dynamic simulations that show a direct interaction between proline and lysozyme[42] and X-ray crystallography study

that show binding of glycine amide to hydrophobic residues of lysozyme.[81] Non-covalent binding of multiple amino acids to native and denatured cytochrome *c* in ESI-MS has also been reported.[90] It was proposed that the formation of stable non-covalent complexes with these amino acids depend on stable ionic interactions and successful formation of hydrogen bonds with specific charged residues of the protein, especially those with the least steric and electrostatic repulsion between amino acid additive and the protein. We also observed L-serine adducts with S/N>3 on charge states +7 to +12 at low temperatures (70ºC) in both ESI-MS and DESI-MS (Figure 4.5). The presence of L-serine adducts on protein peaks in the denaturing solvent 0.1% formic acid in 50% MeOH provides evidence that interaction between unfolding protein and L-serine is possible. In the following sections, we further explore the possible direct interactions between L-serine functional groups and the protein.

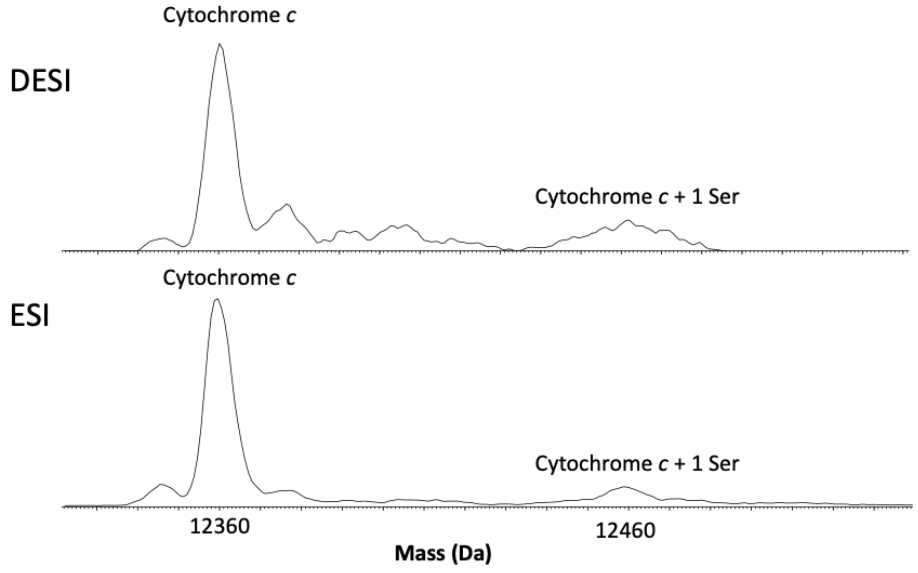

Figure 4.5. Representative deconvoluted spectra of cytochrome *c* shows presence of L-serine adducts on cytochrome *c* peaks that were detected at low temperature (70ºC) in DESI and ESI with 0.1% formic acid in 50% MeOH with 100 µM L-serine as desorption solution and working solution respectively.

4.3.4 Investigating serine-surface interactions involved in mechanism of signal enhancement

During the unfolding process, it is possible that the denaturing protein can bind more tightly with the surface as well as with other proteins in solution due to exposure of a larger surface area of either hydrophobic or polar amino acids from the protein core. To evaluate the potential role of serine disrupting protein-surface interactions, the more hydrophilic PE surface, that was used for the data presented in Figure 4.3 (a), was replaced with the more hydrophobic surface of porous PTFE, which has a different polarity and dielectric constant. As shown in Figure 4.6 (a), changing the identity of the surface to the more hydrophobic PTFE did not influence the extent of protein signal increase with the addition of L-serine to the solvent.

Additional evidence for eliminating surface interactions from contributing to the beneficial L-serine effect is demonstrated in Figure 4.6 (b). To evaluate the potential for L-serine to disrupt protein surface interactions, L-serine was added to the surface before protein deposition, after protein deposition and premixed into protein stock solution. As demonstrated in Figure 4.6 (b), there was no statistical difference between these different methods of serine application (p-value>0.05), although it could be argued that there is considerable mixing occurring on the sample surface during the turbulent DESI analysis. Based on these observations, it is unlikely that protein-surface interactions play a dominant role in the beneficial effect serine has on protein signal with DESI-MS. Moreover, since similar improvements were observed with serine either in the desorbing spray or when applied to the sample prior to desorption confirms that the improvement in signal intensity is not due to changes in physical parameters, such as surface tension of the bulk desorption solvent.

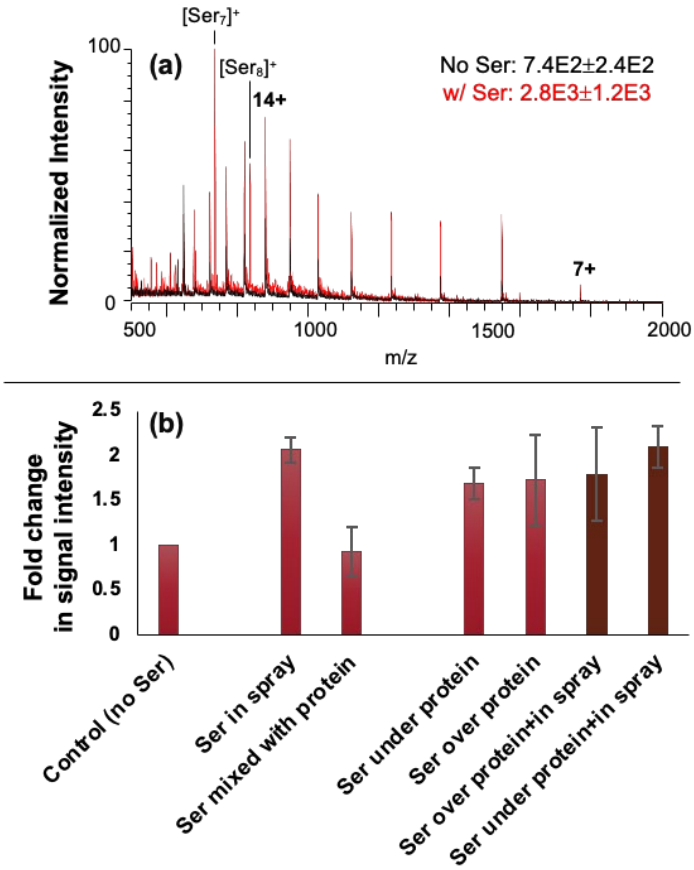

Figure 4.6. Effect of surface identity and relative position of serine to protein. (a) Representative DESI-MS spectra of aqueous cytochrome *c* deposited on PTFE slides and analyzed with 0.1% formic acid in 50% MeOH (shown in black), and with 100 μM L-serine (shown in red). The reported intensities are the average intensity of the highest intensity charge state (HICS) for cytochrome *c*. The equivalent PE data is found earlier in Figure 2 (a). (b) Signal intensity of cytochrome *c* on PE analyzed with 0.1% formic acid in 50% MeOH (control) and 100 μM L-serine in different places during the DESI-MS analysis.

Curiously, having L-serine in the aqueous protein stock solution prior to sample deposition did not yield any improvement in protein signal intensity. When L-serine is mixed with the protein stock solution prior to the analysis, similar to ESI experiments, L-serine comes into contact with protein in bulk solution (fully hydrated protein), whereas for every other sample in Figure 4.6 (b), the L-serine point of contact with protein starts with the dried protein

dissolving into the desorption spray micro-localized layer (during the hydration process). The observations from Figure 4.6 (b) suggest that interaction between L-serine and the unfolding protein during the dissolution process results in the observed increases in protein signal intensity.

4.3.5 Investigating possible intermolecular interactions of serine with protein during solvation of unfolding protein

After eliminating the possibility of L-serine interrupting protein-surface interactions, we investigated L-serine-protein interactions through modifying the L-serine structure, including stereochemistry of the side chain, and blocking the functional groups, as well as comparisons between similar L-amino acids with the hydroxyl group side chain.

The least benign modification could be changing the L enantiomer to D. As Shown in Figure 4.7, D-serine is not as effective as L-serine in improving protein signal, and the racemic mixture of serine was only slightly more effective than D-serine. This observation again suggests that the improvement in protein signal is not due to changes in the physical properties of the solvent, such as surface tension, but perhaps the consequence of direct interactions between the additive and protein. The role of stereoisomer also implies that a chiral interaction is part of the interaction between protein and L-serine. Chiral recognition has been shown to play a role in weak interactions and hydrogen bonding[91] and also with chiral solute-water interaction in solutions.[92] The chirality of L-serine can potentially affect the hydrogen bonding, especially with the peptide backbone of the protein, which has the greatest potential for hydrogen bonding and is sterically influenced by the chirality of the amino acids.[93]

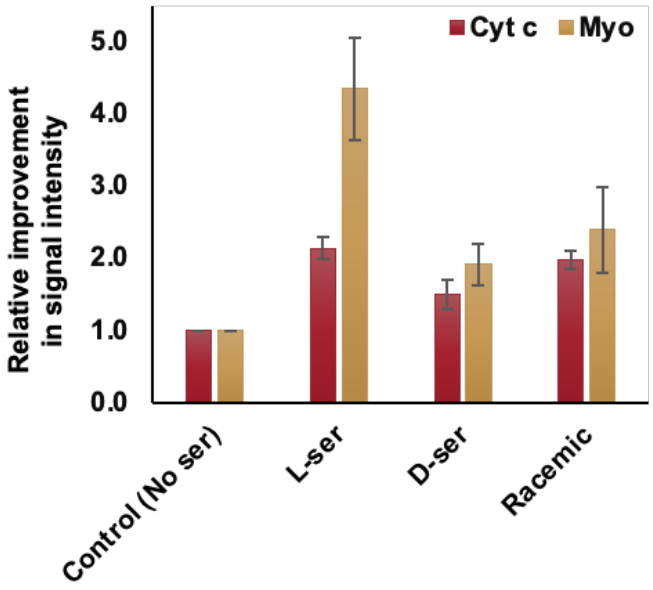

Figure 4.7. Comparison between serine enantiomers and the racemic mixture when used as solvent additives for analysis of natively deposited proteins with 0.1% formic acid in 50% MeOH.

Surprisingly the improvement in signal with a racemic mixture of serine was no more effective than D-serine, indicating that perhaps higher-order serine clusters are involved in the effect. Some precedent has been set for the role of clusters of both arginine and proline as protein aggregation suppressors.[82,94] It is a possibility that L-serine clusters can affect protein aggregation through modulating protein-protein interactions in a similar manner. Although in our experiments the peak intensities of these higher-order serine clusters were not dominant, it is fascinating that serine, to an extent not reached by any other amino acid, forms unusually stable clusters, in particular serine octamer, with a remarkable preference for homochirality.[95-96] Recent studies have validated that serine clusters indeed exist not only in the gas-phase, but also in solution, although at low concentrations.[97-98]

In Figure 4.8, the importance of each functional group on L-serine in its potential direct interaction with the unfolding proteins was investigated. We systematically modified the three functional groups on the serine molecular structure and compared the effects on protein analysis of these derivatives to L-serine. For both cytochrome *c* and myoglobin, any modifications on L-serine molecular structure resulted in a reduction of improvement in protein signal.

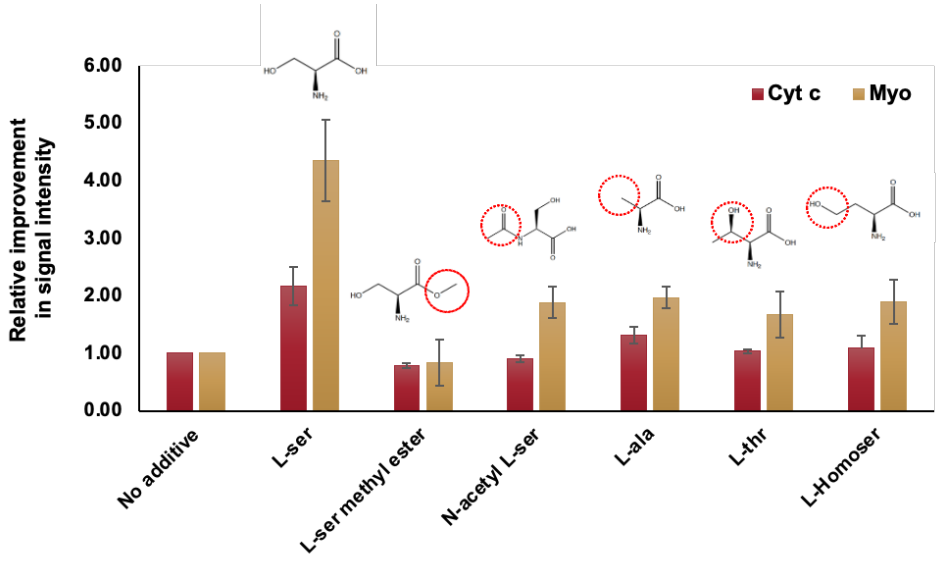

Figure 4.8. L-serine derivatives with systematically altered functional groups as additives and their effect on signal intensities of natively deposited cytochrome *c* and myoglobin with 0.1% formic acid in 50% MeOH. The modifications are highlighted in red circles and include methylation of the hydroxyl group, amidification of the primary amine of serine, a secondary versus primary hydroxyl or amine, and moving the hydroxyl group further away.

Removing the hydroxyl group from L-serine (by using L-alanine) had the least deleterious effect on signal enhancement and still improved the signal intensity, albeit not as effectively as L-serine. The strongest deleterious effect was observed with blocking the carboxylate group, noting the importance of this functional group in the interactions between L-serine and protein. Similarly, FTIR and molecular dynamic simulations have also reported that

the carboxyl group of proline plays a dominant role in direct proline-protein interactions.[42] Earlier, we demonstrated that L-serine is much more effective in improving protein the signal intensity of unfolding protein when the protein has a net positive charge (Table 4.2). One could speculate that the interaction between the negatively charged carboxyl group on the zwitterionic serine and positive charges on the protein contributes to the mechanism of protein dissolution improvement.

The observation that all three functional groups of L-serine are important in the beneficial interaction with protein during dissolution can support one of two hypotheses: Zwitterionic L-serine could potentially have a direct interaction that involves all 3 functional groups interacting with positively charged unfolding proteins; Alternatively, homochiral serine clusters might be at play, as evidenced by lack of efficacy of racemic serine mixtures, and the potential for any structural changes to also affect clustering. To elucidate the exact points of interactions on protein, detailed investigations with complementary techniques such as molecular modeling is needed.

4.4 Conclusion

We demonstrated the application of DESI-MS combined with ESI-MS as a novel approach for probing the mechanism of solubility-enhancing additives such as amino acids by using L-serine as a model additive. The effects of L-serine on signal intensity were investigated by using five different native-state preserving and denaturing solvent systems, changing the protein conformation prior to interaction with the additive, and measuring changes in protein signal during unfolding in the bulk solution before and after addition of L-serine, *versus* unfolding during dissolution. These results were interpreted at the hand of existing models of

amino acid action on protein solubility. Our results indicate that protein-surface interaction interruption is unlikely to contribute to improvements in protein signal enhancement. We hypothesize that L-serine potentially influences protein-protein interactions by acting as a destabilizing neutral crowder and by suppressing aggregation when it is present during unfolding of proteins carrying a net positive charge in solution. Our observations could be explained by a possible direct, noncovalent, chiral, three-pronged interaction between L-serine and the protein. Alternatively, it is possible that serine clusters could be involved in the dissolution-enhancing effect.

DESI-MS studies provide a novel perspective for understanding the mechanisms governing the effects of additives on protein dissolution, solubility, and aggregation. Complementary DESI-MS and direct ESI-MS experiments under controlled conditions allow differentiating between thermodynamic and kinetic effects of additives on solubility and dissolution. Integration of other complementary tools such as ion mobility and delayed desorption with DESI-MS will enable time-resolved analysis of protein dissolution processes and aggregate measurement in the presence of additives. In addition to providing new insights into mechanisms of different additive effects, even at low concentrations, this novel perspective can be a useful tool for the rapid development of additives important for protein chemistry and its applications, such as protein therapeutics and formulation.

4.5 References

1. Zhou, H.-X.; Pang, X., Electrostatic Interactions in Protein Structure, Folding, Binding, and Condensation. *Chemical Reviews* **2018,** *118* (4), 1691-1741.
2. Leader, B.; Baca, Q. J.; Golan, D. E., Protein Therapeutics: A Summary and Pharmacological Classification. *Nature Reviews Drug discovery* **2008,** *7* (1), 21-39.

3. Bye, J. W.; Platts, L.; Falconer, R. J., Biopharmaceutical Liquid Formulation: A Review of the Science of Protein Stability and Solubility in Aqueous Environments. *Biotechnology Letters* **2014,** *36* (5), 869-875.
4. Yancey, P. H.; Clark, M. E.; Hand, S. C.; Bowlus, R. D.; Somero, G. N., Living with Water Stress: Evolution of Osmolyte Systems. *Science* **1982,** *217* (4566), 1214-1222.
5. Ignatova, Z.; Gierasch, L. M., Inhibition of Protein Aggregation in Vitro and in Vivo by a Natural Osmoprotectant. *Proceedings of the National Academy of Sciences* **2006,** *103* (36), 13357-13361.
6. Rabbani, G.; Choi, I., Roles of Osmolytes in Protein Folding and Aggregation in Cells and Their Biotechnological Applications. *International Journal of Biological Macromolecules* **2018,** *109*, 483-491.
7. Wlodarczyk, S. R.; Custódio, D.; Pessoa Jr, A.; Monteiro, G., Influence and Effect of Osmolytes in Biopharmaceutical Formulations. *European Journal of Pharmaceutics and Biopharmaceutics* **2018,** *131*, 92-98.
8. Yancey, P. H.; Clark, M. E.; Hand, S. C.; Bowlus, R. D.; Somero, G. N., Living with Water Stress: Evolution of Osmolyte Systems. *Science* **1982,** *217* (4566), 1214.
9. Ohtake, S.; Kita, Y.; Arakawa, T., Interactions of Formulation Excipients with Proteins in Solution and in the Dried State. *Advanced Drug Delivery Reviews* **2011,** *63* (13), 1053-1073.
10. Kendrick, B. S.; Li, T.; Chang, B. S., Physical Stabilization of Proteins in Aqueous Solution. *Rational Design of Stable Protein Formulations* **2002**, 61-84.
11. Kamerzell, T. J.; Esfandiary, R.; Joshi, S. B.; Middaugh, C. R.; Volkin, D. B., Protein–Excipient Interactions: Mechanisms and Biophysical Characterization Applied to Protein Formulation Development. *Advanced Drug Delivery Reviews* **2011,** *63* (13), 1118-1159.
12. Tsumoto, K.; Umetsu, M.; Kumagai, I.; Ejima, D.; Philo, J. S.; Arakawa, T., Role of Arginine in Protein Refolding, Solubilization, and Purification. *Biotechnology Progress* **2004,** *20* (5), 1301-1308.
13. Lange, C.; Rudolph, R., Suppression of Protein Aggregation by L-Arginine. *Current Pharmaceutical Biotechnology* **2009,** *10* (4), 408-414.
14. Arakawa, T.; Timasheff, S., The Stabilization of Proteins by Osmolytes. *Biophysical Journal* **1985,** *47* (3), 411-414.
15. Bourot, S.; Sire, O.; Trautwetter, A.; Touzé, T.; Wu, L. F.; Blanco, C.; Bernard, T., Glycine Betaine-Assisted Protein Folding in a Lysamutant of Escherichia Coli. *Journal of Biological Chemistry* **2000,** *275* (2), 1050-1056.
16. Kumat, T.; Samuel, D.; Jayaraman, G.; Srimathi, T.; Yu, C., The Role of Proline in the Prevention of Aggregation During Protein Folding in Vitro. *IUBMB Life* **1998,** *46* (3), 509-517.
17. Samuel, D.; Kumar, T. K. S.; Ganesh, G.; Jayaraman, G.; Yang, P.-W.; Chang, M.-M.; Trivedi, V. D.; Wang, S.-L.; Hwang, K.-C.; Chang, D.-K., Proline Inhibits Aggregation During Protein Refolding. *Protein Science* **2000,** *9* (2), 344-352.
18. Xia, Y.; Park, Y.-D.; Mu, H.; Zhou, H.-M.; Wang, X.-Y.; Meng, F.-G., The Protective Effects of Osmolytes on Arginine Kinase Unfolding and Aggregation. *International Journal of Biological Macromolecules* **2007,** *40* (5), 437-443.
19. Meng, F.-G.; Park, Y.-D.; Zhou, H.-M., Role of Proline, Glycerol, and Heparin as Protein Folding Aids During Refolding of Rabbit Muscle Creatine Kinase. *The International Journal of Biochemistry & Cell Biology* **2001,** *33* (7), 701-709.
20. Kim, S.-H.; Yan, Y.-B.; Zhou, H.-M., Role of Osmolytes as Chemical Chaperones During the Refolding of Aminoacylase. *Biochemistry and Cell Biology* **2006,** *84* (1), 30-38.
21. Katayama, D. S.; Nayar, R.; Chou, D. K.; Valente, J. J.; Cooper, J.; Henry, C. S.; Vander Velde, D. G.; Villarete, L.; Liu, C.; Manning, M. C., Effect of Buffer Species on the Thermally Induced Aggregation of Interferon-Tau. *Journal of Pharmaceutical Sciences* **2006,** *95* (6), 1212-1226.
22. Mehta, A. D.; Seidler, N. W., B-Alanine Suppresses Heat Inactivation of Lactate Dehydrogenase. *Journal of Enzyme Inhibition and Medicinal Chemistry* **2005,** *20* (2), 199-203.

23. Shukla, D.; Trout, B. L., Understanding the Synergistic Effect of Arginine and Glutamic Acid Mixtures on Protein Solubility. *The Journal of Physical Chemistry B* **2011,** *115* (41), 11831-11839.
24. Shiraki, K.; Kudou, M.; Aso, Y.; Takagi, M., Dissolution of Protein Aggregation by Small Amine Compounds. *Science and Technology of Advanced Materials* **2003,** *4* (1), 55-59.
25. Shiraki, K.; Tomita, S.; Inoue, N., Small Amine Molecules: Solvent Design toward Facile Improvement of Protein Stability against Aggregation and Inactivation. *Current Pharmaceutical Biotechnology* **2016,** *17* (2), 116-125.
26. Shukla, D.; Schneider, C. P.; Trout, B. L., Molecular Level Insight into Intra-Solvent Interaction Effects on Protein Stability and Aggregation. *Advanced Drug Delivery Reviews* **2011,** *63* (13), 1074-1085.
27. Sharma, G. S.; Krishna, S.; Khan, S.; Dar, T. A.; Khan, K. A.; Singh, L. R., Protecting Thermodynamic Stability of Protein: The Basic Paradigm against Stress and Unfolded Protein Response by Osmolytes. *International Journal of BiologicalMacromolecules* **2021,** *177*, 229-240.
28. Arakawa, T.; Kita, Y.; Ejima, D.; Tsumoto, K.; Fukada, H., Aggregation Suppression of Proteins by Arginine During Thermal Unfolding. *Protein and Peptide Letters* **2006,** *13* (9), 921-927.
29. Shah, D.; Shaikh, A. R.; Peng, X.; Rajagopalan, R., Effects of Arginine on Heat-Induced Aggregation of Concentrated Protein Solutions. *Biotechnology Progress* **2011,** *27* (2), 513-520.
30. Baynes, B. M.; Wang, D. I. C.; Trout, B. L., Role of Arginine in the Stabilization of Proteins against Aggregation. *Biochemistry* **2005,** *44* (12), 4919-4925.
31. Shiraki, K.; Kudou, M.; Fujiwara, S.; Imanaka, T.; Takagi, M., Biophysical Effect of Amino Acids on the Prevention of Protein Aggregation. *The Journal of Biochemistry* **2002,** *132* (4), 591-595.
32. Hamada, H.; Arakawa, T.; Shiraki, K., Effect of Additives on Protein Aggregation. *Current Pharmaceutical Biotechnology* **2009,** *10* (4), 400-407.
33. Arakawa, T.; Ejima, D.; Tsumoto, K.; Obeyama, N.; Tanaka, Y.; Kita, Y.; Timasheff, S. N., Suppression of Protein Interactions by Arginine: A Proposed Mechanism of the Arginine Effects. *Biophysical Chemistry* **2007,** *127* (1), 1-8.
34. Arakawa, T.; Timasheff, S. N., Preferential Interactions of Proteins with Solvent Components in Aqueous Amino Acid Solutions. *Archives of Biochemistry and Biophysics* **1983,** *224* (1), 169-177.
35. Schneider, C. P.; Trout, B. L., Investigation of Cosolute− Protein Preferential Interaction Coefficients: New Insight into the Mechanism by Which Arginine Inhibits Aggregation. *The Journal of Physical Chemistry B* **2009,** *113* (7), 2050-2058.
36. Street, T. O.; Bolen, D. W.; Rose, G. D., A Molecular Mechanism for Osmolyte-Induced Protein Stability. *Proceedings of the National Academy of Sciences* **2006,** *103* (38), 13997-14002.
37. Kim, Y. C.; Mittal, J., Crowding Induced Entropy-Enthalpy Compensation in Protein Association Equilibria. *Physical Review Letters* **2013,** *110* (20), 208102.
38. Munishkina, L. A.; Cooper, E. M.; Uversky, V. N.; Fink, A. L., The Effect of Macromolecular Crowding on Protein Aggregation and Amyloid Fibril Formation. *Journal of Molecular Recognition* **2004,** *17* (5), 456-464.
39. Baynes, B. M.; Trout, B. L., Rational Design of Solution Additives for the Prevention of Protein Aggregation. *Biophysical Journal* **2004,** *87* (3), 1631-1639.
40. Golovanov, A. P.; Hautbergue, G. M.; Wilson, S. A.; Lian, L.-Y., A Simple Method for Improving Protein Solubility and Long-Term Stability. *Journal of the American Chemical Society* **2004,** *126* (29), 8933-8939.
41. Blobel, J.; Brath, U.; Bernadó, P.; Diehl, C.; Ballester, L.; Sornosa, A.; Akke, M.; Pons, M., Protein Loop Compaction and the Origin of the Effect of Arginine and Glutamic Acid Mixtures on Solubility, Stability and Transient Oligomerization of Proteins. *European Biophysics Journal* **2011,** *40* (12), 1327-1338.

42. Bruździak, P.; Adamczak, B.; Kaczkowska, E.; Czub, J.; Stangret, J., Are Stabilizing Osmolytes Preferentially Excluded from the Protein Surface? Ftir and Md Studies. *Physical Chemistry Chemical Physics* **2015,** *17* (35), 23155-23164.
43. Javanshad, R.; Venter, A., Ambient Ionization Mass Spectrometry: Real-Time, Proximal Sample Processing and Ionization. *Analytical Methods* **2017,** *9* (34), 4896-4907.
44. Venter, A.; Sojka, P. E.; Cooks, R. G., Droplet Dynamics and Ionization Mechanisms in Desorption Electrospray Ionization Mass Spectrometry. *Analytical Chemistry* **2006,** *78* (24), 8549-8555.
45. Shin, Y.-S.; Drolet, B.; Mayer, R.; Dolence, K.; Basile, F., Desorption Electrospray Ionization-Mass Spectrometry of Proteins. *Analytical Chemistry* **2007,** *79* (9), 3514-3518.
46. Takats, Z.; Wiseman, J. M.; Cooks, R. G., Ambient Mass Spectrometry Using Desorption Electrospray Ionization (Desi): Instrumentation, Mechanisms and Applications in Forensics, Chemistry, and Biology. *Journal of Mass Spectrometry* **2005,** *40* (10), 1261-1275.
47. Honarvar, E.; Venter, A. R., Comparing the Effects of Additives on Protein Analysis between Desorption Electrospray (Desi) and Electrospray Ionization (Esi). *Journal of The American Society for Mass Spectrometry* **2018,** *29* (12), 2443-2455.
48. Douglass, K. A.; Venter, A. R., Protein Analysis by Desorption Electrospray Ionization Mass Spectrometry and Related Methods. *Journal of Mass Spectrometry* **2013,** *48* (5), 553-560.
49. Garza, K. Y.; Feider, C. L.; Klein, D. R.; Rosenberg, J. A.; Brodbelt, J. S.; Eberlin, L. S., Desorption Electrospray Ionization Mass Spectrometry Imaging of Proteins Directly from Biological Tissue Sections. *Analytical Chemistry* **2018,** *90* (13), 7785-7789.
50. Towers, M. W.; Karancsi, T.; Jones, E. A.; Pringle, S. D.; Claude, E., Optimised Desorption Electrospray Ionisation Mass Spectrometry Imaging (Desi-Msi) for the Analysis of Proteins/Peptides Directly from Tissue Sections on a Travelling Wave Ion Mobility Q-Tof. *Journal of The American Society for Mass Spectrometry* **2018,** *29* (12), 2456-2466.
51. Ambrose, S.; Housden, N. G.; Gupta, K.; Fan, J.; White, P.; Yen, H. Y.; Marcoux, J.; Kleanthous, C.; Hopper, J. T.; Robinson, C. V., Native Desorption Electrospray Ionization Liberates Soluble and Membrane Protein Complexes from Surfaces. *Angewandte Chemie* **2017,** *129* (46), 14655-14660.
52. Maser, T. L.; Honarvar, E.; Venter, A. R., Delayed Desorption Improves Protein Analysis by Desorption Electrospray Ionization Mass Spectrometry. *Journal of The American Society for Mass Spectrometry* **2020,** *31* (4), 803-811.
53. Douglass, K. A.; Jain, S.; Brandt, W. R.; Venter, A. R., Deconstructing Desorption Electrospray Ionization: Independent Optimization of Desorption and Ionization by Spray Desorption Collection. *Journal of The American Society for Mass Spectrometry* **2012,** *23* (11), 1896-1902.
54. Sun, J.; Kitova, E. N.; Sun, N.; Klassen, J. S., Method for Identifying Nonspecific Protein− Protein Interactions in Nanoelectrospray Ionization Mass Spectrometry. *Analytical Chemistry* **2007,** *79* (21), 8301-8311.
55. Hilton, G. R.; Benesch, J. L., Two Decades of Studying Non-Covalent Biomolecular Assemblies by Means of Electrospray Ionization Mass Spectrometry. *Journal of the Royal Society Interface* **2012,** *9* (70), 801-816.
56. Davidson, K. L.; Oberreit, D. R.; Hogan Jr, C. J.; Bush, M. F., Nonspecific Aggregation in Native Electrokinetic Nanoelectrospray Ionization. *International Journal of Mass Spectrometry* **2017,** *420*, 35-42.
57. Costa, A. B.; Cooks, R. G., Simulated Splashes: Elucidating the Mechanism of Desorption Electrospray Ionization Mass Spectrometry. *Chemical Physics Letters* **2008,** *464* (1-3), 1-8.
58. Dokoumetzidis, A.; Macheras, P., A Century of Dissolution Research: From Noyes and Whitney to the Biopharmaceutics Classification System. *International Journal of Pharmaceutics* **2006,** *321* (1-2), 1-11.

59. Badu-Tawiah, A.; Bland, C.; Campbell, D. I.; Cooks, R. G., Non-Aqueous Spray Solvents and Solubility Effects in Desorption Electrospray Ionization. *Journal of The American Society for Mass Spectrometry* **2010,** *21* (4), 572-579.
60. Javanshad, R.; Maser, T. L.; Honarvar, E.; Venter, A. R., The Addition of Polar Organic Solvent Vapors During the Analysis of Proteins by Desi-Ms. *Journal of The American Society for Mass Spectrometry* **2019,** *30* (12), 2571-2575.
61. Honarvar, E.; Venter, A. R., Ammonium Bicarbonate Addition Improves the Detection of Proteins by Desorption Electrospray Ionization Mass Spectrometry. *Journal of The American Society for Mass Spectrometry* **2017,** *28* (6), 1109-1117.
62. Javanshad, R.; Honarvar, E.; Venter, A. R., Addition of Serine Enhances Protein Analysis by Desi-Ms. *Journal of The American Society for Mass Spectrometry* **2019,** *30* (4), 694-703.
63. Zhang, H.; Lu, H.; Chingin, K.; Chen, H., Stabilization of Proteins and Noncovalent Protein Complexes During Electrospray Ionization by Amino Acid Additives. *Analytical Chemistry* **2015,** *87* (14), 7433-7438.
64. Kitova, E. N.; Yao, Y.; Klassen, J. S., Stabilizing Protein-Ligand Complexes in Esi–Ms Using Solution Additives: Comparing the Effects of Amino Acids and Imidazole. *International Journal of Mass Spectrometry* **2017,** *420*, 2-8.
65. Bagal, D.; Kitova, E. N.; Liu, L.; El-Hawiet, A.; Schnier, P. D.; Klassen, J. S., Gas Phase Stabilization of Noncovalent Protein Complexes Formed by Electrospray Ionization. *Analytical Chemistry* **2009,** *81* (18), 7801-7806.
66. Clarke, D. J.; Campopiano, D. J., Desalting Large Protein Complexes During Native Electrospray Mass Spectrometry by Addition of Amino Acids to the Working Solution. *Analyst* **2015,** *140* (8), 2679-2686.
67. Takáts, Z.; Wiseman, J. M.; Gologan, B.; Cooks, R. G., Electrosonic Spray Ionization. A Gentle Technique for Generating Folded Proteins and Protein Complexes in the Gas Phase and for Studying Ion−Molecule Reactions at Atmospheric Pressure. *Analytical Chemistry* **2004,** *76* (14), 4050-4058.
68. Konermann, L.; Douglas, D., Unfolding of Proteins Monitored by Electrospray Ionization Mass Spectrometry: A Comparison of Positive and Negative Ion Modes. *Journal of The American Society for Mass Spectrometry* **1998,** *9* (12), 1248-1254.
69. Zhang, Z.; Marshall, A. G., A Universal Algorithm for Fast and Automated Charge State Deconvolution of Electrospray Mass-to-Charge Ratio Spectra. *Journal of The American Society for Mass Spectrometry* **1998,** *9* (3), 225-233.
70. Young, L. M.; Saunders, J. C.; Mahood, R. A.; Revill, C. H.; Foster, R. J.; Ashcroft, A. E.; Radford, S. E., Esi-Ims–Ms: A Method for Rapid Analysis of Protein Aggregation and Its Inhibition by Small Molecules. *Methods* **2016,** *95*, 62-69.
71. Young, L. M.; Saunders, J. C.; Mahood, R. A.; Revill, C. H.; Foster, R. J.; Tu, L.-H.; Raleigh, D. P.; Radford, S. E.; Ashcroft, A. E., Screening and Classifying Small-Molecule Inhibitors of Amyloid Formation Using Ion Mobility Spectrometry–Mass Spectrometry. *Nature Chemistry* **2015,** *7* (1), 73-81.
72. Hedges, J. B.; Vahidi, S.; Yue, X.; Konermann, L., Effects of Ammonium Bicarbonate on the Electrospray Mass Spectra of Proteins: Evidence for Bubble-Induced Unfolding. *Analytical Chemistry* **2013,** *85* (13), 6469-6476.
73. Sterling, H. J.; Cassou, C. A.; Susa, A. C.; Williams, E. R., Electrothermal Supercharging of Proteins in Native Electrospray Ionization. *Analytical Chemistry* **2012,** *84* (8), 3795-3801.
74. Hemdan, E. S.; Zhao, Y.-J.; Sulkowski, E.; Porath, J., Surface Topography of Histidine Residues: A Facile Probe by Immobilized Metal Ion Affinity Chromatography. *Proceedings of the National Academy of Sciences* **1989,** *86* (6), 1811-1815.
75. Bergers, J. J.; Vingerhoeds, M. H.; van Bloois, L.; Herron, J. N.; Janssen, L. H.; Fischer, M. J.; Crommelin, D. J., The Role of Protein Charge in Protein-Lipid Interactions. Ph-Dependent Changes of

the Electrophoretic Mobility of Liposomes through Adsorption of Water-Soluble, Globular Proteins. *Biochemistry* **1993,** *32* (17), 4641-4649.
76. Collins, K. D., Ions from the Hofmeister Series and Osmolytes: Effects on Proteins in Solution and in the Crystallization Process. *Methods* **2004,** *34* (3), 300-311.
77. Zhang, Y.; Cremer, P. S., Chemistry of Hofmeister Anions and Osmolytes. *Annual Review of Physical Chemistry* **2010,** *61*, 63-83.
78. Siddiqi, M. K.; Alam, P.; Chaturvedi, S. K.; Shahein, Y. E.; Khan, R. H., Mechanisms of Protein Aggregation and Inhibition. *Front Biosci (Elite Ed)* **2017,** *9*, 1-20.
79. Ghosh, R.; Sharma, S.; Chattopadhyay, K., Effect of Arginine on Protein Aggregation Studied by Fluorescence Correlation Spectroscopy and Other Biophysical Methods. *Biochemistry* **2009,** *48* (5), 1135-1143.
80. Tsumoto, K.; Ejima, D.; Kita, Y.; Arakawa, T., Why Is Arginine Effective in Suppressing Aggregation? *Protein and Peptide Letters* **2005,** *12* (7), 613-619.
81. Ito, L.; Shiraki, K.; Makino, M.; Hasegawa, K.; Kumasaka, T., Glycine Amide Shielding on the Aromatic Surfaces of Lysozyme: Implication for Suppression of Protein Aggregation. *FEBS Letters* **2011,** *585* (3), 555-560.
82. Samuel, D.; Ganesh, G.; Yang, P. W.; Chang, M. M.; Wang, S. L.; Hwang, K. C.; Yu, C.; Jayaraman, G.; Kumar, T. K. S.; Trivedi, V. D., Proline Inhibits Aggregation During Protein Refolding. *Protein Science* **2000,** *9* (2), 344-352.
83. Saadati-Eskandari, N.; Navidpour, L.; Yaghmaei, P.; Ebrahim-Habibi, A., Amino Acids as Additives against Amorphous Aggregation: In Vitro and in Silico Study on Human Lysozyme. *Applied Biochemistry and Biotechnology* **2019,** *189* (1), 305-317.
84. Zalar, M.; Svilenov, H. L.; Golovanov, A. P., Binding of Excipients Is a Poor Predictor for Aggregation Kinetics of Biopharmaceutical Proteins. *European Journal of Pharmaceutics and Biopharmaceutics* **2020,** *151*, 127-136.
85. Schneider, C. P.; Trout, B. L., Investigation of Cosolute−Protein Preferential Interaction Coefficients: New Insight into the Mechanism by Which Arginine Inhibits Aggregation. *The Journal of Physical Chemistry B* **2009,** *113* (7), 2050-2058.
86. Timasheff, S. N., Protein-Solvent Preferential Interactions, Protein Hydration, and the Modulation of Biochemical Reactions by Solvent Components. *Proceedings of the National Academy of Sciences* **2002,** *99* (15), 9721-9726.
87. Baynes, B. M.; Wang, D. I.; Trout, B. L., Role of Arginine in the Stabilization of Proteins against Aggregation. *Biochemistry* **2005,** *44* (12), 4919-4925.
88. Katyal, N.; Deep, S., A Computational Approach to Get Insights into Multiple Faces of Additives in Modulation of Protein Aggregation Pathways. *Physical Chemistry Chemical Physics* **2019,** *21* (44), 24269-24285.
89. Hong, J.; Gierasch, Lila M.; Liu, Z., Its Preferential Interactions with Biopolymers Account for Diverse Observed Effects of Trehalose. *Biophysical Journal* **2015,** *109* (1), 144-153.
90. Lu, H.; Guo, Y.; Yang, P., Using Amino Acids for Probing Structural Information of Cytochrome C by Electrospray Ionization Mass Spectrometry. *Journal of The American Society for Mass Spectrometry* **2004,** *15* (11), 1612-1615.
91. Scuderi, D.; Le Barbu-Debus, K.; Zehnacker, A., The Role of Weak Hydrogen Bonds in Chiral Recognition. *Physical Chemistry Chemical Physics* **2011,** *13* (40), 17916-17929.
92. Yang, G.; Xu, Y., Probing Chiral Solute-Water Hydrogen Bonding Networks by Chirality Transfer Effects: A Vibrational Circular Dichroism Study of Glycidol in Water. *The Journal of Chemical Physics* **2009,** *130* (16), 164506.
93. Perets, E. A.; Videla, P. E.; Yan, E. C. Y.; Batista, V. S., Chiral Inversion of Amino Acids in Antiparallel B-Sheets at Interfaces Probed by Vibrational Sum Frequency Generation Spectroscopy. *The Journal of Physical Chemistry B* **2019,** *123* (27), 5769-5781.

94. Das, U.; Hariprasad, G.; Ethayathulla, A. S.; Manral, P.; Das, T. K.; Pasha, S.; Mann, A.; Ganguli, M.; Verma, A. K.; Bhat, R., Inhibition of Protein Aggregation: Supramolecular Assemblies of Arginine Hold the Key. *PloS one* **2007,** *2* (11), e1176.
95. Cooks, R. G.; Zhang, D.; Koch, K. J.; Gozzo, F. C.; Eberlin, M. N., Chiroselective Self-Directed Octamerization of Serine: Implications for Homochirogenesis. *Analytical Chemistry* **2001,** *73* (15), 3646-3655.
96. Nanita, S. C.; Cooks, R. G., Serine Octamers: Cluster Formation, Reactions, and Implications for Biomolecule Homochirality. *Angewandte Chemie International Edition* **2006,** *45* (4), 554-569.
97. Jordan, J. S.; Williams, E. R., Effects of Electrospray Droplet Size on Analyte Aggregation: Evidence for Serine Octamer in Solution. *Analytical Chemistry* **2021,** *93* (3), 1725-1731.
98. Jordan, J. S.; Williams, E. R., Dissociation of Large Gaseous Serine Clusters Produces Abundant Protonated Serine Octamer. *Analyst* **2021,** *146* (8), 2617-2625.

CHAPTER 5

5. THE ADDITION OF POLAR ORGANIC SOLVENT VAPORS DURING THE ANALYSIS OF PROTEINS BY DESI-MS

Reprinted with permission from

R. Javanshad, T. L. Maser, E. Honarvar and A. R. Venter

J. Am. Soc. Mass Spectrom. **2019**, 30, 12, 2571–2575

5.1 Introduction

Implementations of desorption electrospray ionization mass spectrometry (DESI-MS) has been disproportionately in favor of direct/ambient analysis of smaller molecules such as metabolites and lipids since the analysis of larger molecules such as proteins by DESI-MS has proven to be challenging.[1-2] However, with the continuous efforts toward improving DESI-MS of proteins, this technique is rapidly becoming a powerful tool for direct analysis of large proteins (>25 kDa) from complex mixtures.

Solvent additives such as ammonium bicarbonate[3] and serine,[4] or delayed-desorption-DESI[266] and combinations of these approaches have aimed to address supposed problems with the slow kinetics of protein dissolution during the analysis of proteins by DESI. Another very powerful approach entails the coupling of DESI-MS to ion mobility which now allows for imaging of small proteins and peptides directly from tissue samples.[6-7]

The addition of polar organic vapors into the spray chamber or curtain gas during ESI analysis was shown to enhance the electrospray ionization of proteins and peptides. Under such conditions, a reduction of alkali metal adduction was observed together with changes in proteins charge states, typically to lower charge values.[8-10] The addition of polar organic vapors such as acetonitrile, acetone, ethyl acetate, water, and small alcohols helped remove metal adducts, presumably via ion evaporation. It was suggested that the effectiveness of these vapors in the removal of the metal species comes from their ability to lower the activation energy required for metal ion evaporation. Vapors that have a greater impact in lowering the activation energy of ion evaporation of the metal will be more beneficial in terms of removing adducts from protein complexes.[8] Additionally, an enclosed commercial ionization source was shown to increase the charge states of tryptic peptides when ionized in an atmosphere enriched in acetonitrile vapors.[11]

Given the similarities between ESI and DESI, it is likely that the same treatment could positively affect DESI-MS analysis of proteins. Despite the differences in the initial sample phase, after dissolution and desorption, DESI follows similar ionization mechanisms as ESI.[12] Therefore, successful approaches to improving protein analysis by ESI have often been applicable to DESI as well. The application of vapor additives in DESI requires enclosure of the DESI desorbing and ionizing plume to contain the vapors. An enclosed DESI source was previously described.[13] Here, we introduce polar organic vapors of acetone, acetonitrile, ethyl acetate, methanol, and water to the gas phase through a semi-enclosed DESI system.

5.2 Experimental

5.2.1 Materials

Equine cytochrome *c* (Cyt *c*, 12.3 kDa), bovine erythrocyte carbonic anhydrase isozyme II (CAII, 30.0 kDa) and bovine serum albumin (BSA, 66 kDa) were purchased from Sigma-Aldrich (St. Louis, MO). Bovine myoglobin (Myo, 16.9 kDa) was purchased from Protea (Morgantown, WV). HPLC-MS grade methanol, acetone, and acetonitrile were purchased from Sigma-Aldrich (St. Louis, MO). Extra dry (water<50ppm) ethyl acetate was purchased from ACROS Organics (Geel, Belgium). LC-MS grade formic acid was purchased from Fluka Analytical (Morris Plains, NJ). Ultrapure water was supplied from Thermo-Barnstead Water Polisher. Porous-polyethylene surfaces (PE) with an average pore size of 15-45 μm (POREX-4900) were purchased from Interstate Specialty Products (Sutton, MA).

5.2.2 Sample preparation

Each protein standard was prepared and analyzed independently. Lyophilized proteins were first dissolved in milliQ water to prepare stock solutions. Protein samples were made from the stock solutions by further dilution with milliQ water to reach a final concentration of 80 μM. The protein solutions were spray-deposited onto a PE surface to yield sample lines with an estimated surface concentration of 20 - 25 pmol/mm^2. For each experiment, at least 3 sample lines were scanned. Error bars represent ± standard deviation.

5.2.3 Instrumentation

DESI-MS analysis was performed with a linear ion trap mass spectrometer (LTQ, Thermo Scientific, Waltham, MA, USA) combined with a 3-dimensional translational stage

(Purdue University, West Lafayette, IN, USA). A house-built electrosonic spray ionization source (ESSI) was used for generating pneumatically assisted electrospray using two co-axial fused silica capillaries inside a T-piece. An 80% methanol solution containing 0.1% formic acid was delivered through the inner silica capillary (I.D. 50 μm, O.D. 220 μm) with the flow rate of 5 μL/min and nebulizing nitrogen gas was delivered through the outer silica capillary (I.D. 320 μm, O.D. 450 μm, length 1.5 cm) at 100 psi. For generating charged solvent droplets, 4.0 kV was applied to the syringe delivering the DESI spray solvent. The MS inlet temperature was set at 250°C. LTQ ion optics voltages were optimized for each protein individually. Tube lens voltage and ion transfer capillary voltage were optimized between 110-130 V and 20-45 V, respectively.

5.2.4 DESI parameters and enclosure

The sprayer to MS inlet distance and sprayer to surface distances were set at 4 mm and 1 mm respectively, and the incident spray angle was adjusted to 54° - 55°. The plastic enclosure was cut from a 1 mL plastic pipette tip which fitted tightly around the front ring of the 1/16" Swagelok nut that secures the gas nebulizing capillary of the ESSI sprayer assembly, as shown in Figure 5.1.

The enclosure was specifically cut for the desorption sprayer so that attaching the enclosure would make minimum change in the desorption spray geometry. To fit the extended MS inlet inside the enclosure, a small opening was cut in the front rim of the plastic enclosure. Vapors were delivered to the enclosure cavity by 1/8" PTFE tubing that was connected to a Schott ® bottle half-filled with solvent. The N_2 inlet tube protruded into the bottle to a position close to the solvent surface and below that of the vapor exit tube. The vapor exit tube entered the

enclosure through a small hole positioned behind the DESI sprayer drilled into the back of the plastic tip.

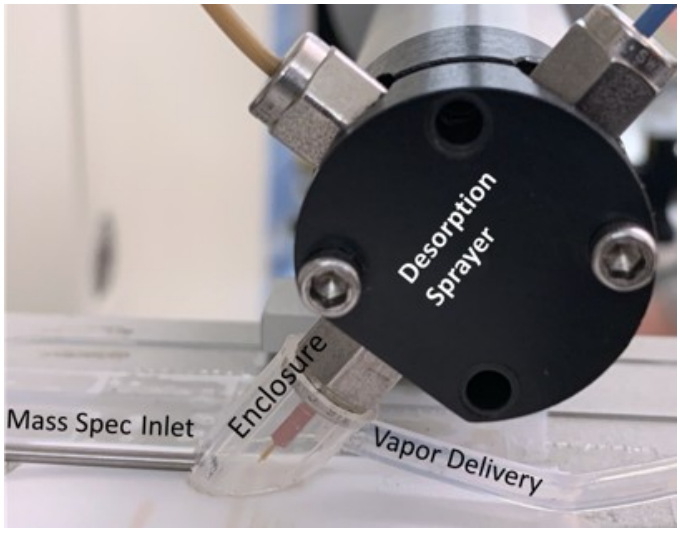

Figure 5.1. Photo of enclosed DESI sprayer and vapor addition setup.

The nitrogen flow rate was controlled with a needle valve and optimized at 1 L/min or 50 mL/min for less or more confining enclosures, respectively, as discussed below. Reagent vapors investigated were acetone, acetonitrile, ethyl acetate, methanol, and water.

5.3 Results and discussion

5.3.1 Enclosure considerations

The effects resulting from vapor addition during DESI analysis are the consequence of two facets: physical effects and chemical effects. Physically attaching the enclosure to the DESI sprayer can affect the performance of the DESI source, most notably through subtle changes in DESI sprayer geometry, which influences droplet dynamics. Moreover, the enclosure's physical parameters such as the shape, position of vapor delivery inlet and whether the surface and DESI

sprayer are completely confined within the enclosure cavity can affect the gas flow dynamics. For example, a less confining enclosure with space between the surface and the enclosure optimizes to higher vapor flow rates (1 L/min), whereas in a tightly confined enclosure cavity the flow dynamics are completely disturbed with such high vapor flow rates, and as a result, signal deteriorates. In the following experiments, the enclosure was made to maintain the optimized non-enclosed DESI spray geometry as much as possible. The back of the enclosure was also raised slightly above the surface to provide a less restricted cavity which allows using higher vapor flow rates.

Aside from the physical effects, the chemical effects of each solvent vapor on the primary electrospray droplets leaving the ion source, on the sample on the surface, or on the secondary droplets after desorption are related to the properties of the solvent molecules such as polarity, gas-phase proton affinity, dipole moment, etc. Optimal conditions, therefore, will depend on an intricate balance between the shape of the enclosure, DESI sprayer parameters, vapor flow rate, and possibly also the chemical identity of the vapor.

5.3.2 Effect of different solvent vapors on different proteins

To survey the effects of different vapors on protein signal, initially, two model proteins (myoglobin and bovine serum albumin) were analyzed by DESI using an array of vapor additives as summarized in Figure 5.2.

Nitrogen gas by itself as control, or doped with methanol, acetone, acetonitrile, water, and ethyl acetate vapors were each separately introduced to the semi-enclosed DESI at a flow rate of 1 L/min. The effect of the vapor additives on protein signal was analyzed in positive ion

mode. The signal intensities of the *highest intensity charge states* (HICS) and the total protein intensities for myoglobin and the HICS for bovine serum albumin were analyzed under nitrogen gas enriched with the different vapors. When ethyl acetate vapor was supplied under these conditions, the HICS signal intensity of both proteins increased approximately four times as shown in Figures 5.2, 5.3 (a), and 5.3 (b).

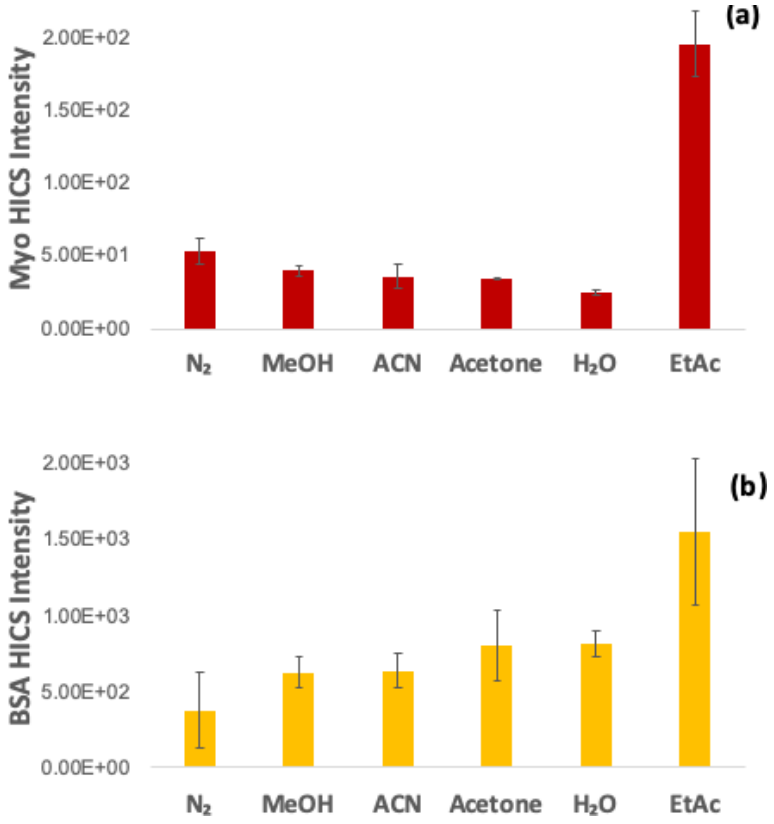

Figure 5.2. Effect of different vapors on signal intensity of natively deposited proteins when analyzed by DESI-MS using 80% methanol containing 0.1% formic acid as the solvent. (a) myoglobin and (b) bovine serum albumin.

However, other vapor additives only mildly affected the HICS intensities and caused the signal to decrease or remain relatively unchanged. The effects of the various vapors on the total protein signal for myoglobin shown in Figure 5.3 mirrors the observations in Figure 5.2 (a).

Unfortunately, the total protein signal intensity for BSA was difficult to obtain due to heavy adduction and the low mass resolution of the mass spectrometer used. These observations were also similar in magnitude to the results previously published when vapors were introduced into the curtain gas during ESI-MS of holo-myoglobin.[268]

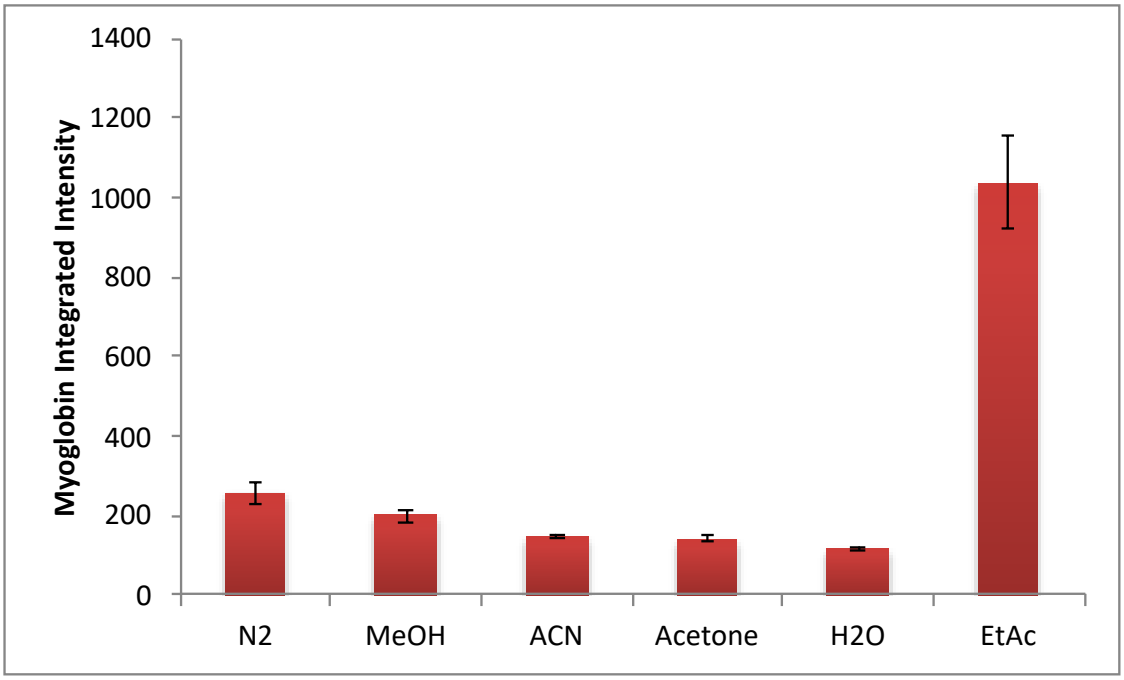

Figure 5.3. Effect of different vapors on deconvoluted protein signal intensity of natively deposited myoglobin when analyzed by DESI-MS using 80% methanol containing 0.1% formic acid as the solvent.

The addition of ethyl acetate as a fraction directly into the desorption spray solvent reduced the signal intensity dramatically. Figure 5.4 shows data for CAII analyzed with and without ethyl acetate mixed as a fraction into the desorption spray solvent. Ethyl acetate is miscible in water up to 10% and totally miscible in 50%MeOH solutions. When 10% ethyl acetate was added as a fraction into the desorption spray solvent, the signal intensity was reduced by over an order of magnitude. When the fraction of ethyl acetate was further increased to 20% it

was hard to detect any protein peaks. Considering the 5 µL/min desorption spray flow rate, even at 20% the total moles of ethyl acetate delivered per unit time was still significantly lower than when ethyl acetate vapors were supplied as dopant into the auxiliary gas, where the ethyl acetate consumption was measured at the supply bottle was approximately 500 µL/min.

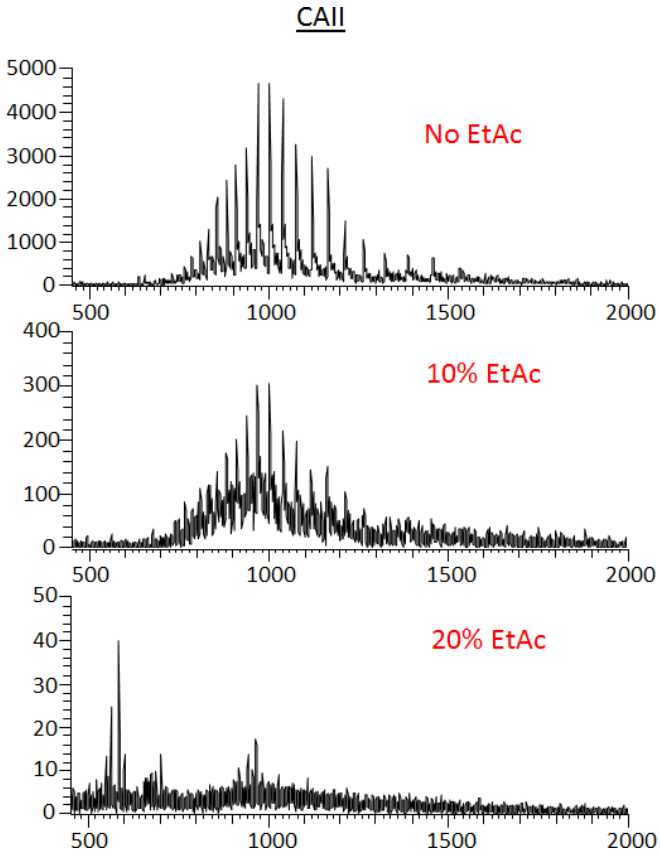

Figure 5.4. The addition of ethyl acetate as a fraction directly into the desorption spray solvent reduces the signal intensity. Demonstrated is 40 pmol/mm^2 carbonic anhydrase II analyzed with 50% MeOH, 0.1% formic acid, and with and without ethyl acetate as indicated.

The remarkable effect of ethyl acetate vapors on signal intensity was also observed with other proteins such as cytochrome *c* (Figure 5.5 (c)) and carbonic anhydrase II (Figure 5.5 (d)). Figure 3 shows the effect of ethyl acetate vapor on signal intensities and mass spectra for four

different proteins compared to nitrogen. Here, when envelopes were deconvoluted, the summed signal intensities for each protein increased by factors of 6, 5 and 3 times each for myo, cyt *c* and CAII, respectively. (The unresolved envelope of BSA could not be deconvoluted).

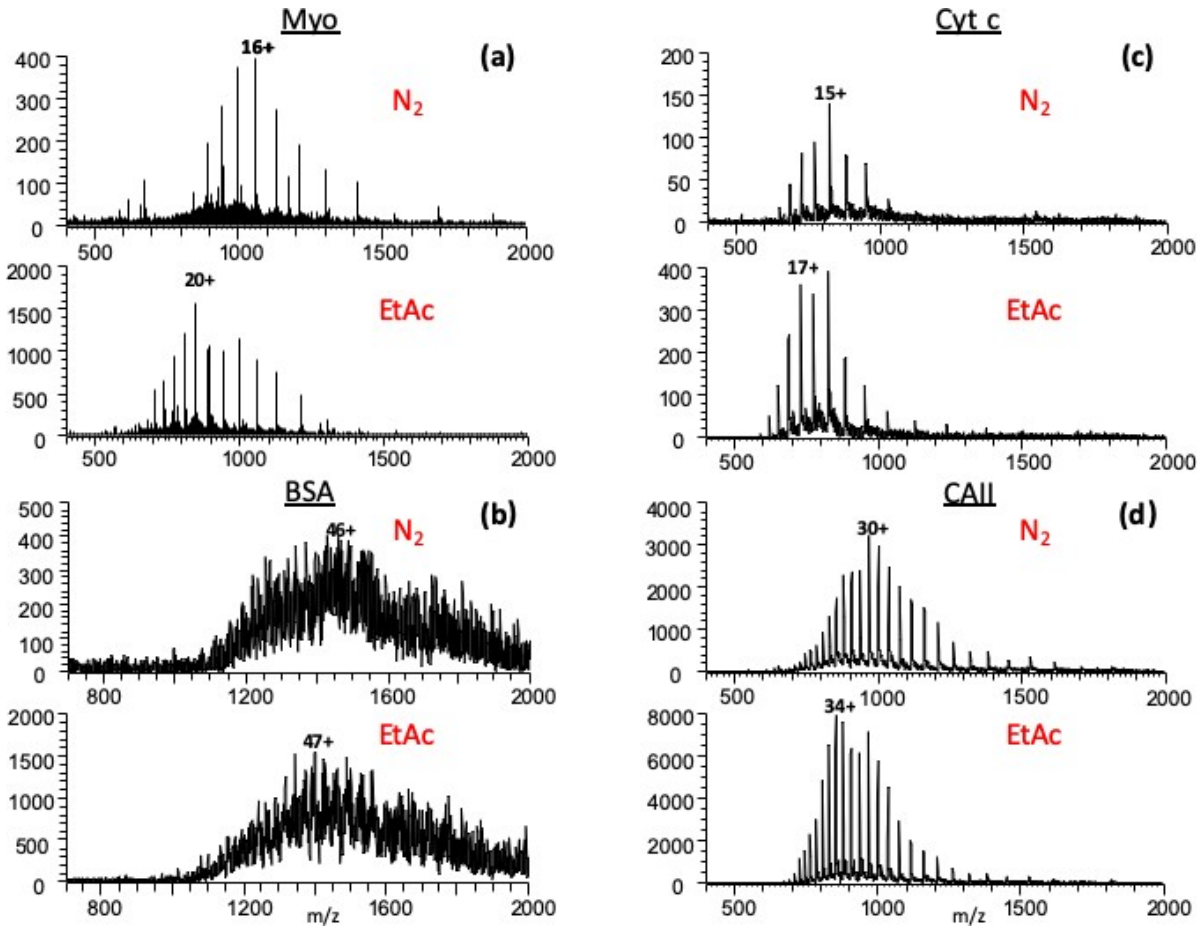

Figure 5.5. Comparison of spectra and signal intensity for different proteins when exposed to N2 vapor (top spectra) and when exposed to ethyl acetate vapor (bottom spectra) Comparison of spectra and signal intensity for different proteins (a) myoglobin, (b) bovine serum albumin, (c) cytochrome *c*, and (d) carbonic anhydrase II when exposed to N2 vapor (top spectra) and when exposed to ethyl acetate vapor (bottom spectra). Vapor flow rate was set at 1 L/min.

In an attempt to further optimize the conditions, the desorption sprayer and surface were more tightly enclosed, i.e., the plastic tip completely touched the sample surface and enclosed the DESI sprayer. This setup was not tolerant of the 1 L/min vapor flow rate, and the vapor doped nitrogen auxiliary gas flow rate optimized at 50 mL/min. With the more confining setup, ethyl acetate vapors increased the signal of cytochrome *c* (Figure 5.6 (a)) and carbonic anhydrase II (Figure 5.6 (b)) even more, to approximately six times when compared to nitrogen vapor.

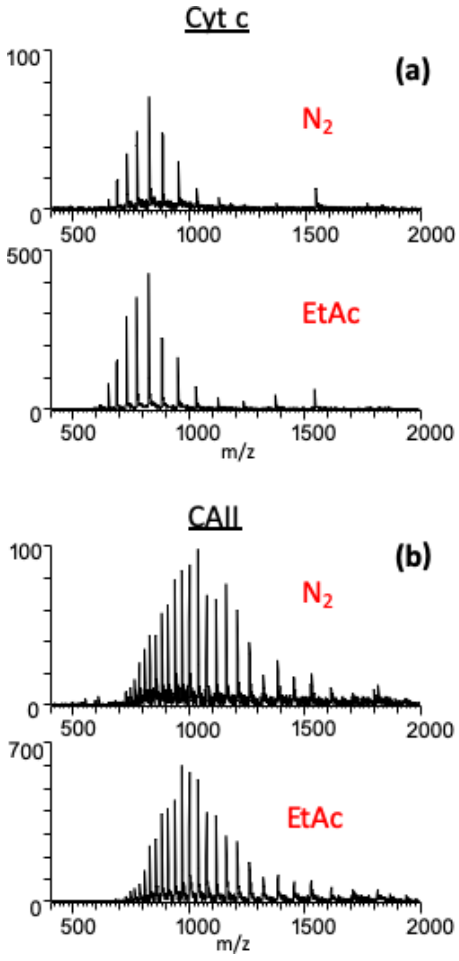

Figure 5.6. Comparison of spectra and signal intensity for cytochrome *c*, and carbonic anhydrase II when enclosure area was more restricted. Vapor flow rate was set at 50 mL/min.

This illustrates that further improvements to signal intensity will be possible with a carefully designed and optimized enclosure geometry and operating conditions. The chemical effect of ethyl acetate on signal intensity can be observed regardless of the physical complications of the addition of an enclosure and the introduction of auxiliary N_2 gas, both of which affect the droplet dynamics of the DESI processes.

A noteworthy observation from comparing the spectra for all proteins exposed to ethyl acetate vapors was an overall shift towards higher charge states. For example, the addition of ethyl acetate vapors to CAII caused a shift in the HICS to slightly higher charge states (z = +33) compared to nitrogen controls (z = +30). The HICS of cyt *c* increased by two when comparing nitrogen vapor to ethyl acetate. The *highest observed charge state* (HOCS) for cyt *c* exposed to nitrogen was z = +19 and this increased to z = +21 when exposed to ethyl acetate vapor. The addition of ethyl acetate leads to a complicated envelope, as if bimodal ion populations are created. Interestingly, organic vapors in ESI and nano-ESI showed an overall charge reduction for native proteins when vapors were introduced through the curtain gas.[8,10] The opposite effect can be seen here with all proteins showing an overall increase to higher charge states after ethyl acetate vapor interaction. This is possibly a consequence of the denaturing solvent used in the DESI desorbing spray, even as the proteins were deposited in a native state. Previously, it was shown that peptides and proteins analyzed in ESI under denaturing conditions responded differently to vapors in the gas phase compared to when analyzed under native-state preserving conditions.[11,14] This observation can be explained through the possibility of a different ionization mechanism recently proposed for denatured proteins, known as the chain ejection mechanism (CEM).[15]

5.4 Conclusion

In conclusion, exposure of the DESI spray plume to organic vapors demonstrated the ability to change the charge state distributions, and in the case of ethyl acetate, also to increase signal intensities obtained for proteins. This effect appears to be independent of protein characteristics, such as size or isoelectric point values. The magnitude of this effect is, however, dependent on the enclosure setup and vapor flow rate. The physical parameters are also interdependent, and in addition to geometrical complexities, determines the amount of vapor that can be delivered to the spray plume. Therefore, detailed optimization of enclosure parameters and vapor flow rates are necessary. The promising observation was that regardless of the physical parameters of the process, the improvement in signal intensity was observed for multiple proteins, including proteins larger than 25 kDa, which are challenging to analyze by DESI-MS.

5.5 References

1. Shin, Y. S.; Drolet, B.; Mayer, R.; Dolence, K.; Basile, F., Desorption electrospray ionization-mass spectrometry of proteins. *Analytical Chemistry* **2007,** *79* (9), 3514-3518.
2. Douglass, K. A.; Venter, A. R., Protein analysis by desorption electrospray ionization mass spectrometry and related methods. *Journal of Mass Spectrometry* **2013,** *48* (5), 553-560.
3. Honarvar, E.; Venter, A. R., Ammonium Bicarbonate Addition Improves the Detection of Proteins by Desorption Electrospray Ionization Mass Spectrometry. *Journal of the American Society for Mass Spectrometry* **2017,** *28* (6), 1109-1117.
4. Javanshad, R.; Honarvar, E.; Venter, A. R., Addition of Serine Enhances Protein Analysis by DESI-MS. *Journal of The American Society of Mass Spectrometry* **2019,** *30* (4), 694-703.
5. Maser, T.; Honarvar, E.; Venter, A. R. In *Delayed Desorption Improves Protein Analysis by Desorption Electrospray Ionization Mass Spectrometry*, Proceedings of the 65th ASMS Conference on Mass Spectrometry and Allied Topics, Indianpolis, Indiana, Indianpolis, Indiana, 2017; p 290061.
6. Garza, K. Y.; Feider, C. L.; Klein, D. R.; Rosenberg, J. A.; Brodbelt, J. S.; Eberlin, L. S., Desorption Electrospray Ionization Mass Spectrometry Imaging of Proteins Directly from Biological Tissue Sections. *Analytical Chemistry* **2018,** *90* (13), 7785-7789.
7. Towers, M. W.; Karancsi, T.; Jones, E. A.; Pringle, S. D.; Claude, E., Optimised Desorption Electrospray Ionisation Mass Spectrometry Imaging (DESI-MSI) for the Analysis of Proteins/Peptides Directly from Tissue Sections on a Travelling Wave Ion Mobility Q-ToF. *Journal of The American Society for Mass Spectrometry* **2018,** *29* (12), 2456-2466.

8. DeMuth, J. C.; Bu, J.; McLuckey, S. A., Electrospray droplet exposure to polar vapors: delayed desolvation of protein complexes. *Rapid Communication in Mass Spectrometry* **2015,** *29* (10), 973-81.
9. DeMuth, J. C.; McLuckey, S. A., Electrospray droplet exposure to organic vapors: metal ion removal from proteins and protein complexes. *Analytical Chemistry* **2015,** *87* (2), 1210-8.
10. Hopper, J. T.; Sokratous, K.; Oldham, N. J., Charge state and adduct reduction in electrospray ionization-mass spectrometry using solvent vapor exposure. *Analytical Biochemistry* **2012,** *421* (2), 788-90.
11. Kaspar, S.; Ledertheil, T.; Hartmer, R.; Hagedorn, T.; Baessmann, C.; Nugent, K., TN-44: Increasing Peptide Identification Rates for Proteomics Samples by Controlling Peptide Charge States Using CaptiveSpray nanoBooster. In *Increasing Peptide Identification Rates for Proteomics Samples by Controlling Peptide Charge States Using CaptiveSpray nanoBooster*, Bruker Daltonics: Bremen, Germany, 2013; Vol. TN-44.
12. Cooks, R. G.; Ouyang, Z.; Takats, Z.; Wiseman, J. M., Detection Technologies. Ambient mass spectrometry. *Science* **2006,** *311* (5767), 1566-70.
13. Venter, A.; Cooks, R. G., Desorption electrospray ionization in a small pressure-tight enclosure. *Analytical Chemistry* **2007,** *79* (16), 6398-403.
14. Venter, A. R.; Cole, R. B. In *Electrospray droplet exposure to polar organic vapors provides evidence for different mechanisms for native versus denatured protein ionization*, Proceedings of the 66th ASMS Conference on Mass Spectrometry and Allied Topics, San Diego, California, San Diego, California, 2018; p 294109.
15. Metwally, H.; Duez, Q.; Konermann, L., Chain Ejection Model for Electrospray Ionization of Unfolded Proteins: Evidence from Atomistic Simulations and Ion Mobility Spectrometry. *Analytical Chemistry* **2018,** *90* (16), 10069-10077.

CHAPTER 6

6. EVALUATING THE APPLICATION OF DESI-MS AND DIRECT ESI-MS IN RAPID ANALYSIS OF HIS-TAGGED PROTEIN FROM IMAC SURFACES

6.1 Introduction

The recombinant DNA technology not only revolutionized molecular biology, but also marked the birth of modern biotechnology. Since its introduction in the 1970s,[1] the recombinant DNA technology has found widespread multidisciplinary applications in various fields, including agriculture, biomedical sciences and medicine.[2] Recombinant protein production is one of the most prominent applications of recombinant DNA technology.[3-5] Simply put, a recombinant protein is a target protein encoded by recombinant DNA. Recombinant protein production is comprised of four major stages: gene cloning, protein expression, protein purification, and characterization by different techniques, such as mass spectrometry, as illustrated in Figure 6.1.[6] The recombinant DNA code of the target protein is first cloned in an expression vector designed to transfer and express the recombinant DNA in a host cell.[7] The target protein gene is usually under the control of an inducible promoter, which allows controlled overexpression of the target protein in the host cell upon the addition of the chemical inducer.[8-9] This process is also known as heterologous expression since the host expresses a protein that it does not naturally make.[10] After the recombinant protein expression has reached satisfactory levels, the host cells, now containing the target protein, are harvested through centrifugation and lysed by chemical or physical methods (or a combination of both). The protein of interest is then separated from the host cell components and indigenous proteins through protein purification.[11-15] Although

the purification of recombinant proteins is time-consuming and labor-intensive, it is currently a prerequisite for most types of analyses, including characterization, functional or structural studies.

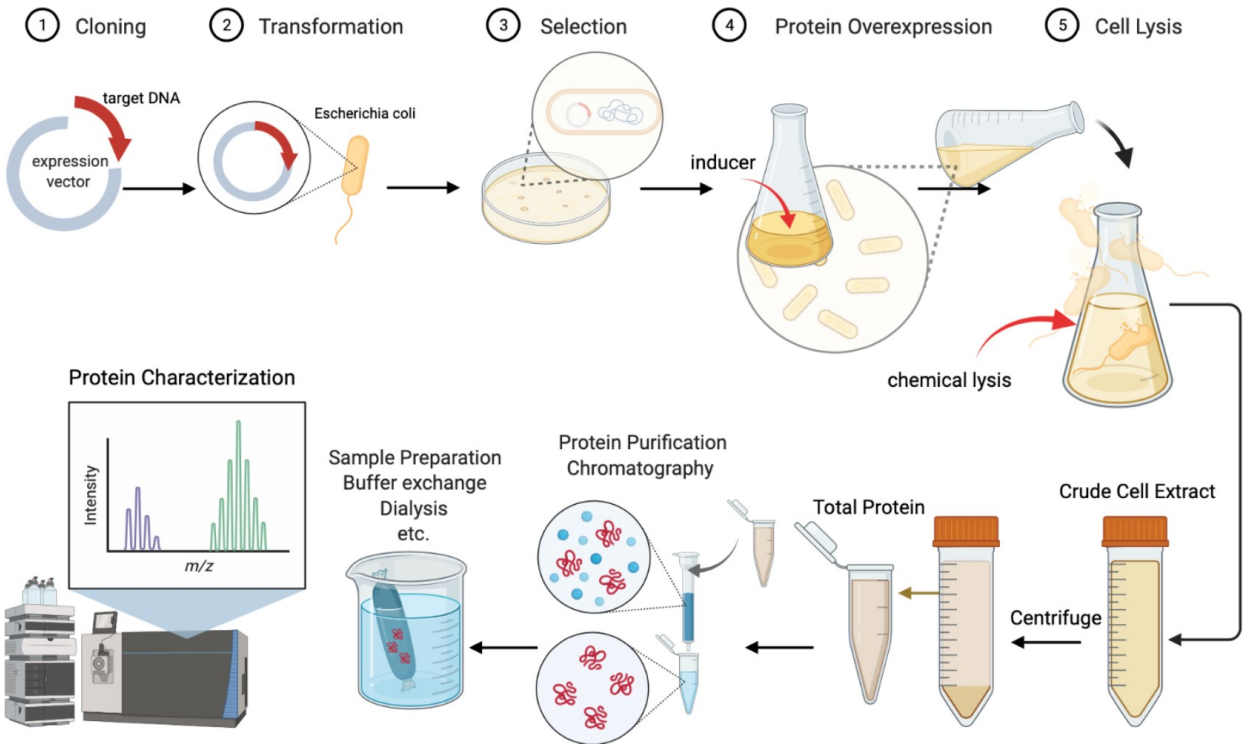

Figure 6.1. A typical workflow of recombinant protein expression and characterization by mass spectrometry. Created with BioRender.com

One of the most widely used protein purification methods is expressing the target protein with an affinity fusion tag and purifying it through immobilized metal affinity chromatography (IMAC).[16-17] A DNA sequence specifying a string of amino acids, which make the fusion tag, is frequently used in vectors to produce recombinant proteins. Polyhistidine tag (His-tag®) is one of the most popular affinity tags for recombinant protein purification. His-tag is a series of six

histidines that are fused to the protein N- or C- terminus. The optimal position of the tag is protein-dependent, although N-terminus His-tag is more common in bacterial expression systems.[18] The short length of the 6xHis reduces the likelihood of altering the conformation of the protein, and maintains its function. His-tagged protein purification generally uses an affinity resin, a resin such as agarose functionalized with a chelator that is loaded with divalent transition metal ions. The histidine side chain, imidazole, has a high binding affinity to the divalent metal ions.[19] When the cell lysate is incubated on the affinity resin, the His-tagged recombinant protein is immobilized on the resin through the interaction of histidine with the metal ions and is consequently separated from the rest of the cell lysate components.

The first reports of IMAC purification used iminodiacetic acid (IDA) as the chelator for binding the transition metals through three coordination sites, leaving three coordination sites open for binding to the His-tag.[17] IDA, however, only weakly secures the metal ion, leading to metal leaching from the matrix into the purified protein sample. Nitrilotriacetic acid (NTA)[20] and carboxymethyl aspartate (CM-Asp)[21] were introduced afterward as superior, tetradentate chelators, specifically suitable for binding transition metal ions with a coordination number of six, leaving two valences open for reversible binding to two histidines. Ni-NTA is arguably the most commonly used IMAC system for purifying His-tagged proteins since it offers good binding efficiency and minimal metal ion leaching. However, Ni-NTA tends to bind nonspecifically to non-tagged proteins that contain histidine clusters, resulting in moderate specificity. A common strategy to reduce non-specific binding is to add low millimolar concentrations of additives such as imidazole to the equilibrium buffer. Cobalt exhibits a more specific interaction with His-tag, resulting in lower binding but higher specificity. For this

reason, cobalt is the preferred metal for purifying His-tagged proteins when high purity is a primary concern, or milder elution conditions are required. Copper binds His-tag more strongly than cobalt or nickel, providing the highest possible binding capacity but also the poorest specificity. The use of copper is mainly limited to high-capacity binding of already purified His-tagged proteins for applications such as ELISA assays. A variety of IMAC matrices and form factors are available for His-tag protein purification, each with specific advantages and issues.[22] The "metal loaded" resin can be immobilized in columns, onto planar form factors such as a microscope glass slides, or in 96-well plates. Amongst the variety of IMAC systems, the best choice ultimately depends on the type of study and the requirements while taking into consideration the cost in terms of time and labor.

In the post-genomic era, analysis at the level of proteomes and metabolomes is becoming increasingly crucial for understanding the link between genomic information and phenotype. Although gigabytes of DNA sequences continue to be generated daily,[23] only a substantially small percentage of the related proteins are experimentally characterized.[24] The significant gap between the number of sequences and what we experimentally know about them indicates a lack of rapid, inexpensive, and efficient methodologies for characterization of recombinant proteins. Mass spectrometry can be used for rapid methodologies to generate information-rich spectra and perform fundamental characterization of proteins at the structural and functional levels.[25-27] With the significant developments in instrumentation, the number of rapid mass spectrometry-based assays for analysis of intact proteins from complex matrices, without any purification or with online purification steps, has been growing.[28-30]

Direct ESI methods have become increasingly more powerful as a new approach for the rapid analysis of intact, recombinant proteins from crude samples without purification.[31] Recently, the characterization of overexpressed recombinant proteins from crude bacterial cell lysate without prior purification was demonstrated by direct ESI using modified Qstar Elite and Orbitrap platforms.[32] A similar direct ESI approach for the analysis of overexpressed recombinant proteins in eukaryotic expression systems has also been reported.[33] These novel methodologies take advantage of the well-known drawback of mass spectrometry, its limited dynamic range. This limitation leads to the "masking" of low-abundance indigenous proteins by higher-abundance recombinant protein overexpressed in the host. This inherent signal suppression enables overcoming the need for prior protein purification, provided that the MS has high sensitivity and resolution to detect the protein peaks unambiguously.[28] However, these methodologies still rely on optimized expression conditions that yield high levels of recombinant protein in the host cell, which is not always easily feasible.

In most cases, accurate recombinant protein characterization relies on protein purification to some extent prior to analysis, which can be a laborious and time-consuming step depending on how rigorous the purification step needs to be. Rapid online buffer exchange (OBE) of recombinant protein in cell lysate has been combined with native direct ESI-MS to overcome this issue and accelerate the workflow.[34] Recently, online buffer exchange (OBE) chromatography has been coupled with online immobilized metal affinity chromatography (IMAC) and size exclusion chromatography (SEC) for a streamlined native ESI-MS analysis of tagged recombinant proteins from bacterial cell lysate.[35] DESI-MS of tagged recombinant proteins immobilized on agarose slides have been shown to provide rapid online purification and has

been used successfully to screen small molecule binding and monitor the enzymatic reactions,[36] however, characterization of the immobilized tagged recombinant proteins has remained elusive.

In this chapter, detection of immobilized His-tagged recombinant proteins by direct ESI-MS analysis or DESI-MS was investigated. The His-tagged recombinant protein was immobilized on two commercially available IMAC purification form factors and two different chelating metal ions: Ni-NTA or Cu-NTA coated glass slides (MicroSurfaces,Inc), and Ni-NTA or Cu-NTA coated 96-well plates (Thermo Fischer Scientific). The immobilized protein was released from the surface using formic acid as the eluent reagent in the ESI working solution or DESI desorption spray.

6.2 Experimental

6.2.1 Materials and reagents

Cu-NTA and Ni-NTA coated glass slides were purchased from Microsurfaces, Inc. Pierce™ Ni-NTA and Cu-NTA coated 96-well plates were purchased from Thermo Fisher Scientific (Waltham, MA). BioUltra grade ammonium bicarbonate, ammonium acetate, HPLC-MS grade methanol (MeOH), LC-MS grade formic acid, BioUltra grade L-serine, lyophilized chicken egg lysozyme (>98%) were purchased from Sigma-Aldrich (St. Louis, MO). Milli Q water was obtained from a Thermo-Barnstead Water Polisher.

6.2.2 Protein standards and samples

Lyophilized bovine ubiquitin (Ubq, 8.6 kDa) at 95% purity was purchased from Sigma-Aldrich (St. Louis, MO). Recombinant human ubiquitin with N-terminus His-tag (His-Ubq,

predicted molecular weight 9.6 kDa) was purchased from R&D systems (Minneapolis, MN). The recombinant protein was at ³95% purity by SDS-PAGE under reducing conditions and visualized by Colloidal Coomassie® Blue stain and was carrier free (no BSA was added as carrier protein). The His-tagged recombinant human ubiquitin stock was 2.4 mg/ml (250 µM) in 10 mM HEPES pH 7.5 and prior to mass spectrometry analysis, the stock solution was buffer exchanged into 100 mM ammonium acetate solution pH=7.0 with no additive using Zeba spin desalting spin columns with a molecular weight cut off of 7 kDa (Thermo Fisher Scientific) following the manufacturer's instruction. The buffer exchanged protein was filtered with a 0.2-micron filter.

6.2.3 Heterologous protein expression

His-tagged methyltransferases were expressed at Dr. Todd Barkman's research lab at the Department of Biological Sciences, Western Michigan University. The recombinant protein gene sequence was cloned into pET15b expression vector (Novagen) for overexpression in *E. coli* BL-21 (DE3) cells. The host bacterial cells were grown on agar plate and transferred to 5 ml of lysogeny broth or Luria broth (LB) with 100 µg/ml ampicillin. The culture was incubated overnight on a shaker at 30ºC. After 12-13 hours, 2.5 ml of culture was transferred to a flask and 47.5 ml of LB was added. The culture was put on shaker for 3 hours in 32ºC. Optical density of the culture was measured using Biophotometer (Eppendorf, Germany) at 600 nm. After reaching the desired optical density (0.6-0.8), induction of His-tagged protein expression was innitiated with the addition of isopropyl β-D-1-thiogalactopyranoside (IPTG) to the culture at final concentration of 1 mM. The culture was further incubated on a shaker at room temperature for 6 hours. After overexpression, the culture was centrifuged for 15 min at 4000 rpm and 8ºC. The supernatant was thrown out and the pellet was stored at -80ºC for future use.

6.2.4 Total protein extraction and His-tag purification

For extraction of total protein, the *E.coli* pellet was thawed on ice. The lysis buffer was 50 mM sodium phosphate buffer (pH 8.0), 10 mM imidazole, 12% glycerol, 300 mM NaCl and 0.75 mg/ml lysozyme. The pellet was resuspended in 3.6 ml of lysis buffer. The mixture was incubated on ice on a shaker for 30 min followed by repeated sonication for 20 seconds, with 10 seconds pause in between each of four repeats. The mixture was then centrifuged for 20 min, 1000Xg at 4ºC. The supernatant (total protein) was stored at -80ºC for future use.

Purification of His-tagged TcCS2 was performed with a Ni-NTA TALON® spin column from Clontech (Takara Bio Company, CA, USA) following the manufacturer's instruction. The elution buffer contained 150mM imidazole in 50 mM sodium phosphate (pH 8.0), 300 mM NaCl, and 12% glycerol.

6.2.5 IMAC sample preparation

For IMAC 96-well plates, 100 µl of protein sample was added to each well and incubated on a shaker for 1 hour at room temperature. For spot analysis on IMAC glass slides, 1 µl droplets of sample were carefully pipetted on the slides and dried under vacuum at room temperature for approximately 15 minutes.

6.2.6 Instrumentation

Experiments were performed on a LTQ linear ion trap and a LTQ Orbitrap XL mass spectrometers (Thermo Scientific, Waltham, MA, USA). Direct ESI experiments on the Orbitrap was performed using a commercial IonMax source. Direct ESI and DESI experiments on the LTQ were by the electrospray emitter made from a Swagelok T-piece and two pieces of coaxial

fused silica capillary tubing for DESI analysis, similar to that described in previous chapters.[37] DESI solvent flow rate was 3 µl/min, with N_2 as nebulizing gas at 100 psi. Speed of the stage was 150 µm/s for DESI analysis. Capillary temperature and voltage were 250°C and 3-4 kV, respectively for all experiments. DESI geometry was similar to previously described. The sprayer incident angle was 54°, the distance between the desorption sprayer and heated extended capillary was 4 mm and the height of the desorption spray from the surface was 1 mm.

6.3 Results and Discussion

For this study, Ni-NTA and Cu-NTA were chosen as the model IMAC systems for coupling to direct mass spectrometry analysis, as leaching metal ions would be a serious concern for mass spectrometry analysis. Ni^{2+} provides a good binding capacity and is reportedly more applicable for His-tagged protein purification from crude bacterial cell lysate. Cu^{2+} provides maximum binding capacity and highest protein yield,[38-39] theoretically resulting in higher protein signal intensity. Two different form factors for both metals were evaluated for direct, mass spectrometry-based analysis by direct ESI and DESI-MS: Ni-NTA and Cu-NTA coated 96-well plates (Thermo Fischer Scientific), designed for ELISA assays, and Ni-NTA and Cu-NTA coated microscope glass slides (Microsurfaces Inc.), designed for protein microarray assays.

Forces that maintain the complex of His-tag and bound divalent metals (Ni^{2+} and Cu^{2+}) include electrostatic interactions, hydrophobic interactions, and hydrogen bonding. Any agent that disrupts these interactions can be used as an elution technique.[40] Commonly used methods for elution of soluble His-tagged proteins are: competitive binding agents such as imidazole or free histidine, chelating agents, such as EDTA, or lowering the pH below 5. Among these methods, elution with the help of an acid is the most mass-spectrometry friendly option. The pH

of 0.2% (v/v %) formic acid solution is approximately 2.7, well below the pK_a of histidine's side chain, imidazole, but not too low to damage the IMAC form factors or the mass spectrometer. Additionally, volatile acid additives such as formic acid dramatically improve ionization of proteins in positive mode ESI, therefore, increasing sensitivity for protein detection and identification. Increasing the charges on the proteins have been reported to improve detection of proteins by increasing sensitivity and efficiency of protein fragmentation,[41] all of which are valuable for top-down sequencing or characterization of intact proteins.[42-43] Therefore, the acidic solvent system containing 0.2% formic acid in 50% MeOH was evaluated as the first choice for elution of His-tagged protein from IMAC surfaces.

6.3.1 Purification of His-tag ubiquitin from protein mixture using IMAC 96-well plates and detection by direct ESI-MS

In Figure 6.2 (a), the extended charge state distributions (CSD) for both His-Ubq and Ubq indicates the presence of proteins in unfolded state, with highest intensity charge state (HICS) of His-Ubq at m/z 676.8, corresponding to charge state 14+, and HICS of Ubq at m/z 716.1 corresponding to charge state 12+. The integrated signal intensities of His-Ubq and Ubq in Figure 6.2 (a) are 1.99E6 and 1.40E6, respectively. In Figure 6.2 (b), 100 µl of a 100 mM ammonium acetate solution containing 1 µM of both His-Ubq and Ubq was added to a well in Ni-NTA 96-well plate and incubated on a shaker at room temperature for an hour (following manufacturer's instruction). After the incubation period, the protein solution was pipetted out of the well and 100 µl of 50% MeOH+0.2% formic acid was added to the well. This solution was immediately analyzed by ESI-MS. Both His-Ubq and Ubq charge states are clearly visible in the spectra.

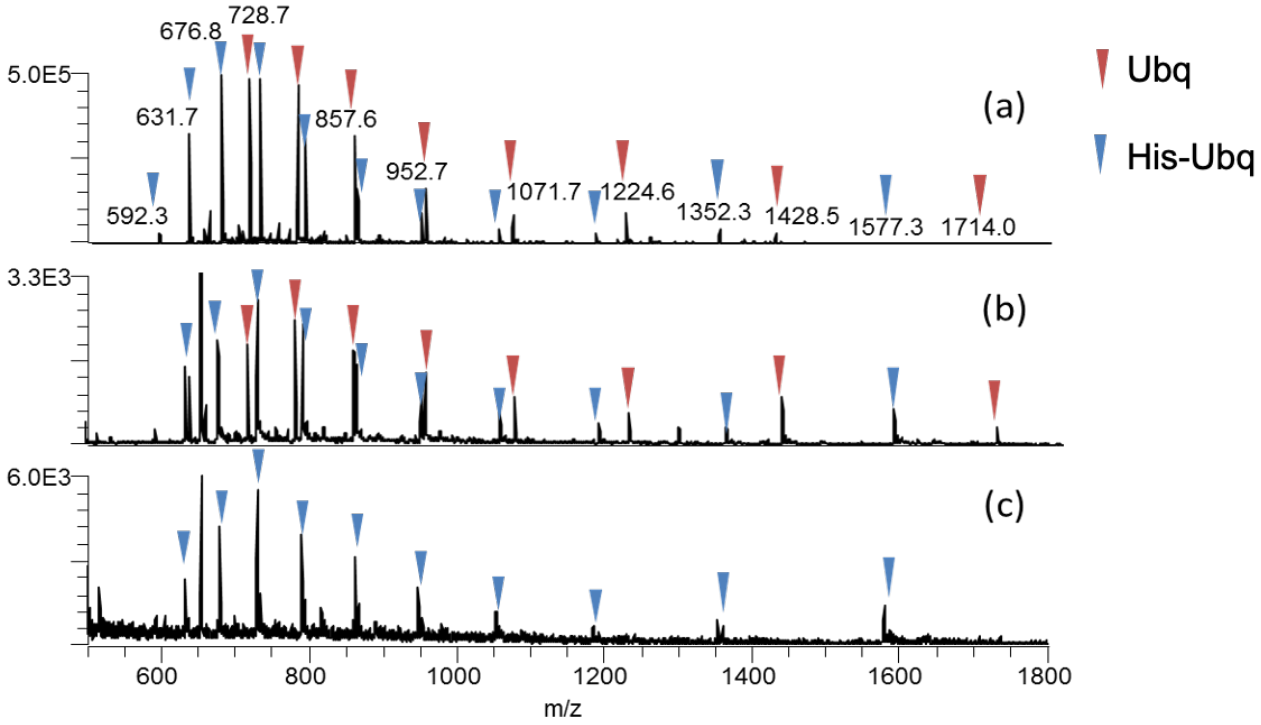

Figure 6.2. ESI-MS spectra of an equimolar mixture of ubiquitin (Ubq) (red mark) and His-tagged ubiquitin (His-Ubq) (blue mark) from Ni-NTA 96-well plates. Spectra obtained by (a) direct infusion in 50% MeOH+0.2% formic acid; (b) direct infusion after incubation on a Ni-NTA 96-well plate in 100 mM ammonium acetate, and subsequently eluted with 50% MeOH+0.2% formic acid; (c) direct infusion after incubation on a Ni-NTA 96-well plate in 100 mM ammonium acetate on a Ni-NTA 96-well plate, **rinsed 10X** with 100 mM ammonium acetate, and eluted with 50% MeOH+0.2% formic acid.

In Figure 6.2 (c), similar to Figure 6.2 (b), a 100 mM ammonium acetate solution containing 1 µM of both His-Ubq and Ubq was added to a well in Ni-NTA 96-well plate and incubated on a shaker at room temperature for an hour. After the incubation period, the protein solution was pipetted out of the well. However, for this experiment the well was rigorously rinsed 10X with 300 µl aliquots of 100 mM ammonium acetate (pH=7.0) by pipetting the solution up and down at least 5 times during each rinse. After rinsing the well, 100 µl of 50% MeOH+0.2% formic acid was added to the well and the solution was immediately analyzed by

direct ESI. In Figure 6.2 (c), only His-Ubq peaks are detectable, indicating Ubq has been washed out of the Ni-NTA well while His-Ubq was captured in the well until released with the formic acid solution.

Similarly, Figure 6.3 shows His-Ubq detection from the protein mixture on Cu-NTA 96-well plate where again only the His-Ubq was observed with direct infusion after repeated washing with ammonium acetate solution and release using 50% MeOH+0.2% formic acid.

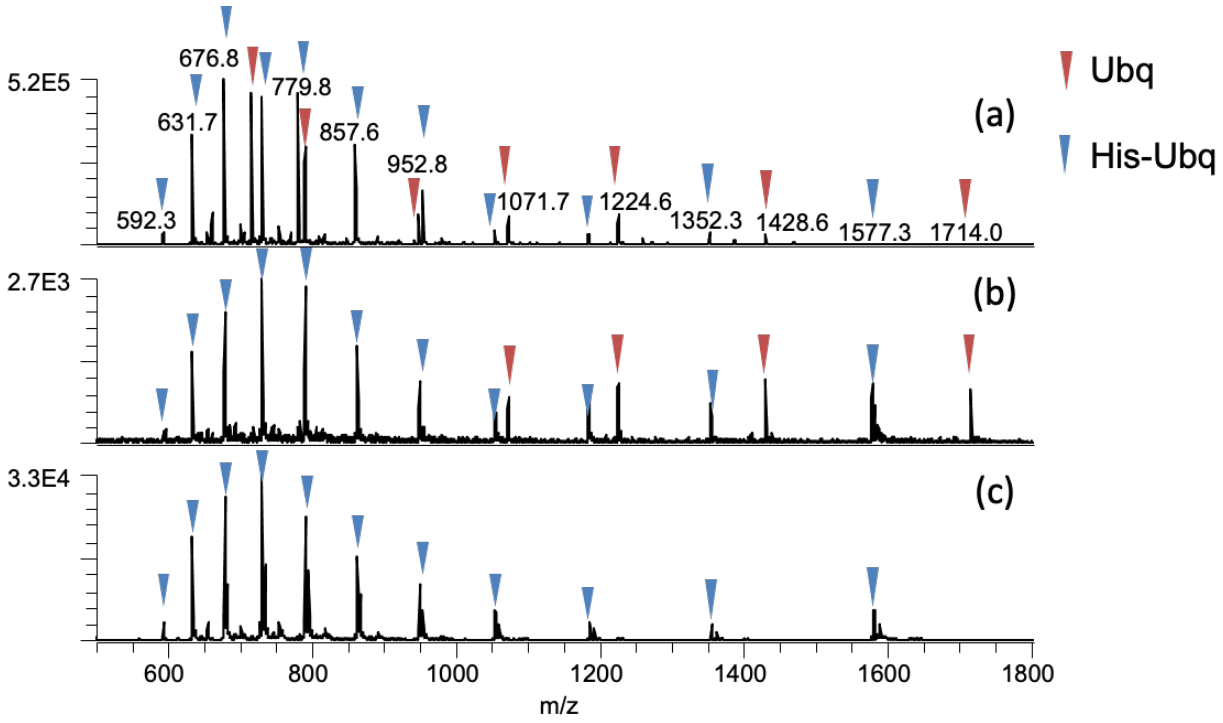

Figure 6.3. ESI-MS spectra of an equimolar mixture of ubiquitin (Ubq) (red mark) and His-tagged ubiquitin (His-Ubq) (blue mark) from Cu-NTA 96-well plates. Spectra were obtained by (a) direct infusion in 50% MeOH+0.2% formic acid; (b) direct infusion after incubation on a **Cu-NTA** 96-well plate in 100 mM ammonium acetate, and subsequently eluted with 50% MeOH+0.2% formic acid; (c) direct infusion after incubation on a **Cu-NTA** 96-well plate in 100 mM ammonium acetate on a **Cu-NTA** 96-well plate, rinsed 10X with 100 mM ammonium acetate, and eluted with 50% MeOH+0.2% formic acid.

The signal intensity of released His-Ubq in Cu-NTA was approximately 5 times higher than Ni-NTA plates after repeated washing of the protein mixture and elution with 50% MeOH+0.2% formic acid as can be seen by comparing Figure 6.2 (c) to Figure 6.3 (c). According to the manufacturer (Thermo Scientific), The Pierce^{TM} copper coated high binding capacity plates use a proprietary coating process to increase the amount of His-tagged protein that will bind to the plate surface, increasing the binding capacity four-fold compared to nickel coated plate, as established by fluorescence.[44] Based on this data, the high-capacity binding Cu-NTA plates can bind up to 36.5 pmol of protein per well, whereas Ni-NTA plates bind 8.9 pmol under similar experimental conditions. This difference in binding capacity correlates with the increased signal intensity of purified His-Ubq from the Cu-NTA plate relative to the Ni-NTA plate.

An interesting observation from the ESI spectra of proteins incubated on these plates is the differences in CSD of Ubq from Cu-NTA versus Ni-NTA. When incubated on Ni-NTA, the unlabled Ubq CSD expands from charge state +6 to +13, whereas in Cu-NTA the CSD is from +6 to +9. As discussed in Chapter 2, higher charge states and wider CSD usually indicate presence of unfolded proteins, although parameters other than conformation can also influence shifting the protein CSD. Surprisingly, such differences in CSD were not observed for His-Ubq. For both Ni-NTA and Cu-NTA, CSD of His-Ubq expanded from 6+ to 16+. To unambiguously assign whether this difference is due to conformation or other factors, ion mobility experiments need to be coupled to the direct ESI experiments.

Another noteworthy observation is the deterioration of protonated peaks and apparent mass shifts on His-Ubq peaks analyzed from both Cu-NTA or Ni-NTA coated IMAC wells,

whereas in the direct infusion spectra, barely any mass shift from protonated His-Ubq peaks are detected. Figure 6.4 shows a closeup of two charge states of His-Ubq and Ubq, at m/z 1052.0 and m/z 1071.6, respectively, corresponding to charge states 9+ and 8+. The peak adjacent to His-Ubq charge state 9+ at m/z 1053 in panels (b), (c), (d), and (e) of Figure 6.4 corresponds to a mass difference of +16 Da in the deconvoluted spectrum, matching an oxidation product.

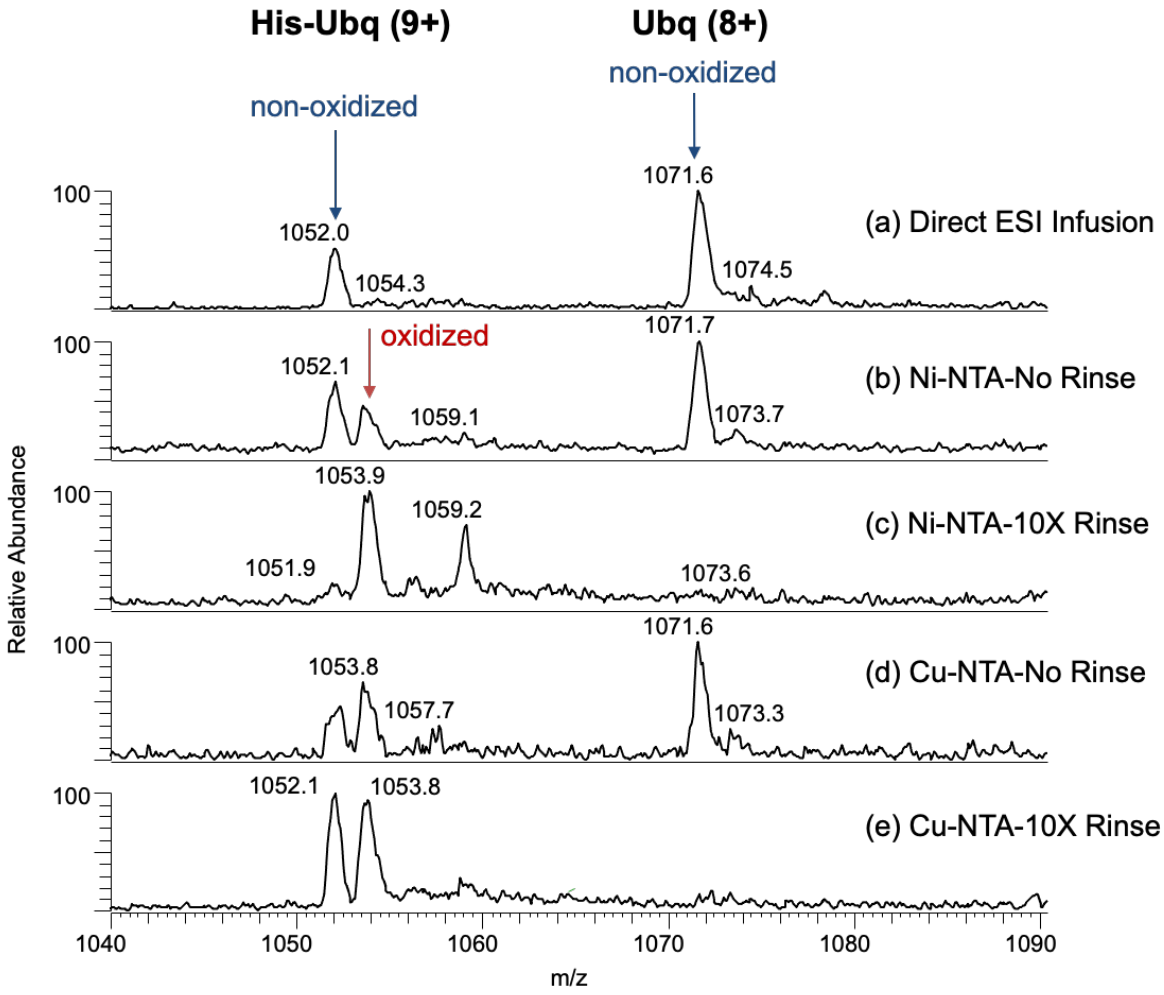

Figure 6.4. ESI-MS of an equimolar mixture of His-Ubq and Ubq showing charge states 9+ and 8+. (a) direct infusion of the mixture, (b) IMAC incubated but unrinsed protein mixture on Ni-NTA, (c) after repeated washing on Ni-NTA and release by aqueous formic acid, (d) unrinsed protein mixture in Cu-NTA and (e) after repeated washing in Cu-NTA and release by FA. All samples are in 50% MeOH+0.2% formic acid as ESI solution.

The relative intensity of the oxidation product is most severe in the case of rinsed His-Ubq in Ni-NTA well, where the oxidized protein dominates. It is interesting that very little oxidation was observed for Ubq in the IMAC control spectra in Figure 6.4 (b) and (d), and oxidation on Ni-NTA is considerably more severe than Cu-NTA.

To further verify that the mass shifted additional peaks observed are oxidation products, high resolution mass spectra of His-Ubq in 50% MeOH+0.2% formic acid was compared to spectra of His-Ubq incubated in Cu-NTA 96-well plate, rinsed with 100 mM ammonium acetate (pH=7.0), and eluted with 50% MeOH+0.2% formic acid (Figure 6.5).

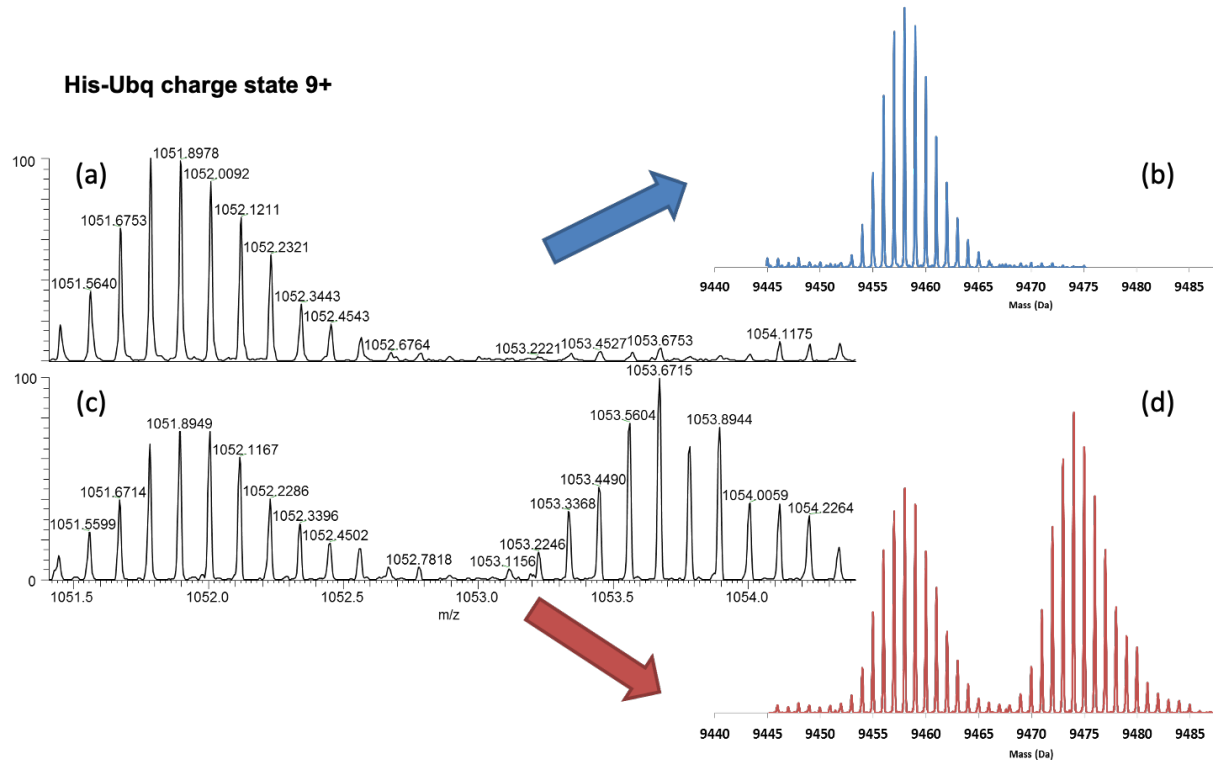

Figure 6.5. High-resolution FT-MS spectra of His-Ubq charge states 9+. Resolution = 100,000. (a) Direct infusion of His-Ubq in 50% MeOH+0.2% formic acid, and (b) deconvoluted mass spectrum of directly infused His-Ubq, (c) His-Ubq released from a **Cu-NTA** 96-well plate, rinsed 10X with 100 mM ammonium acetate, and eluted with 50% MeOH+0.2% formic acid, (d) The deconvoluted mass spectrum for the His-Ubq analyzed after release from Cu-NTA showing the oxidized His-Ubq at M+16 Da.

As can be seen in Figure 6.5, the mass shift on charge state 9+ corresponds to a mass shift of +16 on the protein with mass accuracy of 1 ppm. The deconvoluted protein spectra of His-Ubq in direct ESI infusion and His-Ubq after IMAC purification are shown in Figure 6.5, which clearly shows the oxidized protein in IMAC purified His-Ubq spectra.

Protein oxidation during production and purification is a common concern[18, 45] and in IMAC purification systems has been at least partially attributed to the catalyst effect of the divalent transition metals.[46] However, protein oxidation is often prevented by addition of a reducing agent such as β-mercaptoethanol to maintain an adequate reducing environment. Unfortunately, most reducing agents are not ESI friendly and can cause severe ion suppression even at low concentrations. A small amount of these reagents may be enough to substantially reduce oxidation during IMAC purification, but the tolerated concentration limit and the adverse effect on protein detection by ESI-MS will have to be experimentally verified. Alternatively, for types of analysis that are dramatically affected by protein oxidation, such as structural analysis studies, a high concentration of a reducing agent is required, which then would need to be removed by a second purification step after IMAC purification.

6.3.2 Direct ESI-MS analysis of His-tagged proteins from *E.coli* cell lysate using IMAC 96-well plates

After optimizing the washing and release protocol using a simple protein mixture, we embarked on testing the one-step purification of recombinant protein out of the complex matrix of a bacterial cell lysate. The bacterial cell lysate of *E.coli* BL-21 with a N-terminus His-tagged xanthine alkaloid methyltransferase from yerba mate (IPCS3, predicted molecular weight 42.8 kDa) was used for this experiment. The cell lysate was in 50 mM Na_2HPO_4 buffer (pH 8.0) with

300 mM NaCl, 10 mM imidazole and 12% (v/v%) glycerol with 0.75 mg/ml lysozyme. IPCS3 expression and total protein extraction are described in Section 6.2.3 and 6.2.4.

For positive control, 1 µM His-Ubq was spiked into the IPCS3 total protein solution in the IMAC wells prior to incubation. Similar to the procedure in Section 6.3.1, 100 µl of sample was added to Ni-NTA and Cu-NTA wells and then incubated on a shaker at room temperature for 1 hour. After incubation, the samples were pipetted out and the wells were rinsed 10X with 300 µl of 100 mM ammonium acetate (pH=7.0). After the washing step, 100 µl of 50% MeOH+0.2% formic acid (elution solvent) was added to each well to the release the protein. This solution was recovered and immediately and analyzed by direct ESI. The resulting spectrum obtained from each sample is shown in Figure 6.6.

Based on a manual method for predicting highest intensity charge state (HICS) of unfolded proteins proposed by Douglass *et al*.[47] and the His-tagged IPCS3 amino acid sequence (see Appendix B, Figure 1B), the predicted HICS based on the grouping of the basic amino acids would be charge state 38+, and would be observed at m/z 1160. According to Douglass *et al*., the predicted HICS by this method typically falls short of the experimental HICS for large proteins (>30 kDa) when those proteins have disulfide bonds preventing complete unfolding. However, this can be addressed by reducing disulfide bonds using DTT forcing more complete unfolding. On the other hand, in the study by Douglass a similar His-tagged xanthine alkaloid methyltransferase with mass of 42.8 kDa and a predicted HICS of 38+ had an experimental HICS of 47+.[47] The reason for the positive deviation from the predicted HICS was not discussed.

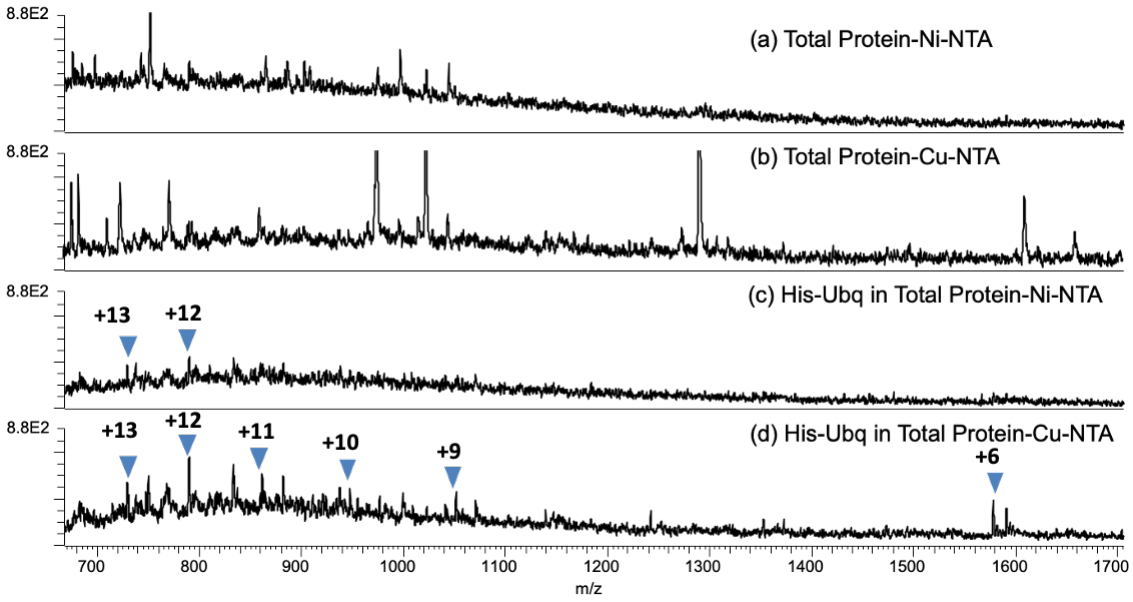

Figure 6.6. Direct ESI-MS spectra of the elution solution (50% MeOH+0.2% formic acid) of crude *E.coli* cell lysate (total protein) from expression of His-tagged IPCS3. (a) eluted from Ni-NTA well, (b) eluted from Cu-NTA well, (c) incubated with 1 µM His-Ubq and eluted from Ni-NTA (d) incubated with 1 µM His-Ubq and eluted from Cu-NTA.

As can be seen in Figure 6.6, no expected charge states of IPCS3 could be detected with S/N>3. However, in positive control spectra in Figure 6.6 panels (c) and (d), His-Ubq HICS peaks were detected at S/N = 3 from Ni-NTA and at S/N = 7 from Cu-NTA for a 1uM spike concentration. The signal intensity and S/N of His-Ubq HICS detected from Cu-NTA was almost double Ni-NTA, which can be expected based on the higher binding capacity of the Cu-NTA plate compared to Ni-NTA.[44] Accordingly, Cu-NTA 96-well plates seem to be the superior IMAC system for coupling to ESI-MS in terms of providing higher signal intensity and signal to noise ratio. The common concern regarding non-specific binding of indigenous cell lysate proteins due to the low specificity of Cu-NTA is consequential for immunological assays such as ELISA, but with mass spectrometry such false positives can be detected based on the molecular

weight of the protein. Therefore, in ESI-MS analysis, the main concern with non-specific binding solely remains the low signal intensity of the His-tagged protein, especially with large target proteins.

The detection of His-Ubq peaks in the positive control experiments in Figure 6.6 suggests that 1) the concentration of IPCS3 in the elution solvent was too low, either due to low expression level or low concentration in the total protein fraction, and/or 2) more rigorous purification might be required for larger proteins to remove adducts and reduce chemical noise and peak congestion in order to increase S/N. Based on the results shown in Figure 6.6 obtained for His-Ubq, a small and easily ionizable protein, concentrations higher than 1 μM would be needed in cell lysate to detect larger protein peaks at S/N>3.

To evaluate whether further purification would improve protein detection for larger proteins, a His-tagged xanthine alkaloid methyltransferase from Theobroma cacao (TcCS2, UniProt accession number A0A061E330) was purified using a Ni-NTA agarose resin spin column. The results for protein detection by direct ESI-MS from the Cu-NTA plate was compared for samples with and without pre-purification using the Ni-NTA column, as shown in Figure 6.7. The amino acid sequence of His-tagged TcCS2 and the predicted charge states can be found in Appendix B, Figure B1 and Table B1. Figure 6.7 shows the m/z range of predicted TcCS2 HICS in direct ESI-MS spectra of purified TcCS2 (panel A) and TcCS2 in total protein (panel B).

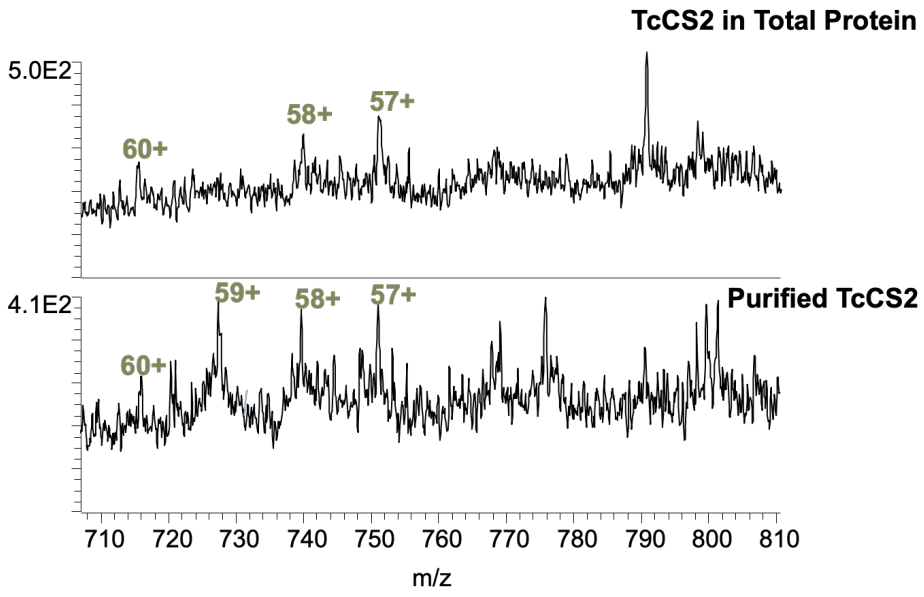

Figure 6.7. Direct ESI-MS spectra of the elution (50% MeOH+0.2% formic acid) for His-tagged TcCS2. Direct ESI-MS spectra of the elution solution (50% MeOH+0.2% formic acid) for (a) His-tagged TcCS2 pre-purified with a Ni-NTA column and subsequently incubated and washed on a Cu-NTA 96-well plate, (b) crude *E.coli* cell lysate (total protein) from expression of His-tagged TcCS2 without prior purification.

The S/N ratios for expected protein peaks increased with additional purification and subsequent incubation on the Cu-NTA plate. Without additional purification, a few expected charge states were observed, but with S/N below 3. After additional Ni-NTA column purification, at least 3 consecutive charge states were detected at S/N>3. This confirms that additional purification could be beneficial to improve protein detection by IMAC 96-well plates by enriching the target protein in the sample solution. There is however more room for improvements, for example by implementing strategies developed in earlier chapters to reduce adduction.

6.3.3 Detection of His-tag ubiquitin from IMAC glass slides by DESI-MS

Methods for high throughput protein expression and functional protein analysis have increasingly become popular in the post-genomic era, leading to the design of multiple platforms capable of such assays. Protein microarrays represent one of the most powerful and commonly used methods for such assays.[48-49] Protein microarrays are typically designed for high throughput analysis of purified proteins, therefore in situ protein purification systems using IMAC surfaces have been developed for streamlining the workflow.[38] Here, we evaluated such surfaces for integration with DESI-MS, as recent advances has demonstrated the potential of DESI-MS for high throughput mass spectrometry-based assays.[50-52]

Polyethylene glycol (PEG) covered microscope glass slides functionalized with Ni-NTA and Cu-NTA (Microsurface Inc.) were used as the DESI surface. 1 µl droplets of equimolar 1 µM His-Ubq and Ubq in 100 mM ammonium acetate were deposited on Cu-NTA and Ni-NTA slides and the spots were dried under vacuum for approximately 15 minutes. In Figure 6.8 (a) (c), the unwashed dried protein mixture spots were desorbed with 50% MeOH+0.2% formic acid and both the tagged and untagged proteins were detected. After washing the slides 3 times using 1 ml of 100 mM ammonium acetate and desorbing with MeOH+0.2% formic acid no peaks corresponding to untagged Ubq were detected. Figure 6.8 (b) and (e) demonstrates that even a considerably short incubation time of 15 min is enough for binding of the His-tagged protein to the IMAC slides. Moreover, this experiment demonstrates that using 50% MeOH+0.2% formic acid as the desorption solvent is an effective releasing agent of the His-tagged protein from the IMAC slide in the short timescale of DESI.

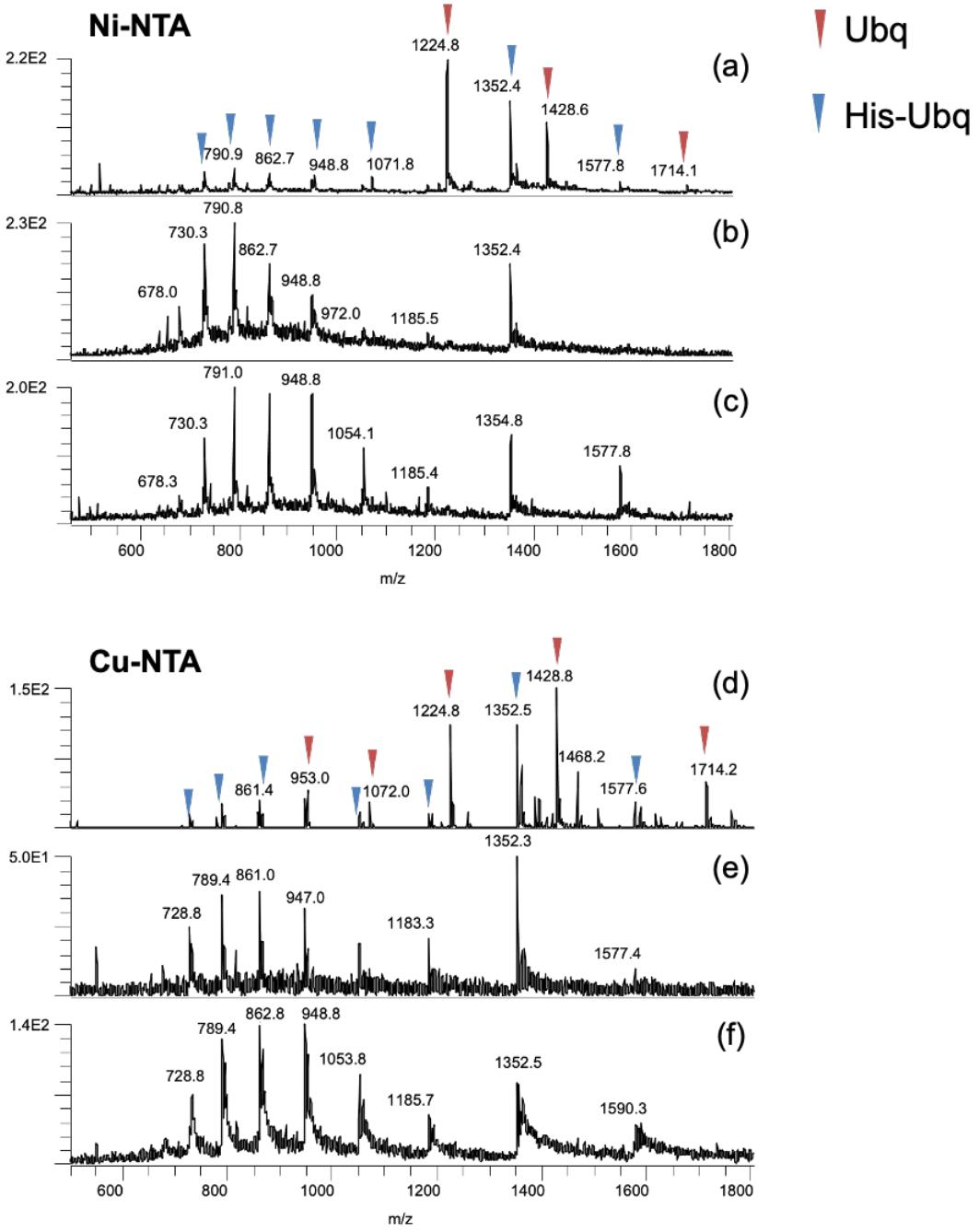

Figure 6.8. DESI-MS spectra of an equimolar mixture of His-Ubq and Ubq in 100 mM ammonium acetate deposited on microscope slides covered in Ni-NTA (a-c) or Cu-NTA (d-f). (a), (c) spectra of unwashed spots desorbed with 50% MeOH+0.2% formic acid showing the presence of both tagged and untagged Ubq. (b), (e) Spectra after rinsing with ammonium acetate solution, analyzed with 50% MeOH+0.2% formic acid, showing the presence of only the His-tagged Ubq. (c), (f) Spectra after rinsing and analyzed with 50% MeOH+0.2% formic acid with the addition of 100 µM L-serine.

The detection of released His-tagged protein in DESI can be further improved through solution-phase additives. Similar to the work presented in Chapter 3, the effect of L-serine as desorption solvent additive on improving His-tagged protein signal intensity was also investigated, 100 μM L-serine was added to the elution solvent as desorption spray and the results are presented in Figure 6.8 (c) and (f).

After the rinsing step, when 100 μM L-serine was added to the 50% MeOH+0.2% formic acid desorption solvent, the integrated signal intensity of His-Ubq in the analyzed spots increased by 3.2±0.9 times for Cu-NTA. For Ni-NTA the relatively minor improvement of 1.2±0.4 X was not statistically significant (p-value>0.1). Surprisingly, Cu-NTA gave a much lower His-Ubq signal intensity compared to Ni-NTA, even though the binding capacity of Cu-NTA is higher than Ni-NTA according to the manufacturer and previous studies[53] (Cu-NTA slides bind approximately 10^{13}-10^{14} proteins/cm^2, which corresponds to a nearly close-packed monolayer of protein molecules,[53] whereas Ni-NTA binds 10^{9}-10^{11} proteins/cm^2). One possible explanation of this observation is that since Cu^{2+} has higher affinity for His-tag, the release and desorption of His-tagged protein from Cu-NTA could be less efficient than Ni-NTA in DESI. Another potential reason for the lower protein signal from Cu-NTA surface compared to Ni-NTA in DESI can be the original problem of protein analysis by DESI: inefficient protein dissolution. The immobilized proteins might be more likely to aggregate upon release by formic acid solvent during DESI on Cu-NTA because they are highly packed and likely have higher concentration in the micro-localized solvent layer. This hypothesis is supported by the positive influence that L-serine had on the signal intensity of immobilized protein detected from Cu-NTA but not Ni-NTA. This improvement could be a result of reduced aggregation on the highly packed Cu-NTA

surface in the presence of serine during the dissolution, as discussed in Chapter 4. Study of immobilized proteins is indeed an interesting method for investigating protein dissolution and desorption by DESI-MS, and strategies to improve protein dissolution in DESI can also benefit analysis of immobilized proteins by DESI-MS.

6.4 Conclusion

The immobilization and release of His-tagged protein using IMAC surfaces for ESI-MS and DESI-MS analysis were successfully demonstrated in this chapter. Two different IMAC systems, Ni-NTA and Cu-NTA, were compared in two form factors, 96-well plates, and microscope glass slides. 96-well plates provide a 3-dimensional system with more surface area that allows for longer incubation periods in solution. The sample can be either extracted with the elution solvent (50% MeOH+0.2% formic acid) and directly sprayed in ESI, or alternatively analyzed by DESI-MS using an enclosure modified for sampling from 9-well plates.[54] Ni-NTA and Cu-NTA microscope glass slides are more suitable for regular 2-dimensional DESI-MS analysis and require much smaller sample volumes, shorter incubation time, and less vigorous rinsing. These features would be advantageous for high throughput assay development.

The proof-of-concept experiments will need to be optimized for direct analysis of His-tagged proteins from crude samples to facilitate functional studies without a need for lengthy purification processes, enabling in-depth analysis of recombinant proteins by shorter workflows. Detection of large proteins by mass spectrometry from the IMAC systems proved to be challenging. Spectral complexity increases with protein size, as large proteins have more complex isotopic distributions and adduct formation patterns, leading to peak broadening and low S/N. Strategies for improved detection of proteins that have been discussed in the earlier

chapters can be beneficial for both ESI-MS and DESI-MS, specifically strategies that increase S/N. A potential strategy can be using L-serine in the elution buffer to remove sodium adducts, as discussed in Chapter 3.

Another strategy to improve S/N of large proteins is introducing organic vapors to proteins post-ionization. Organic vapors have been reported to remove alkali metal adducts in ESI,[55] which can increase S/N and improve protein detection from complex samples such as bacterial cell lysate. An additional benefit of some organic vapors is that they shift the protein charge state envelope to higher m/z ranges and lower charge states where the spectrum usually is less congested, a practice referred to as "sub-charging." Sub-charging of proteins by organic vapors, especially methanol vapor, in post-ionization has been previously reported for ESI-MS.[55-57] Sub-charging is particularly useful for large proteins as it can help narrow the complex charge state distribution of large proteins and concentrate the signal into fewer peaks.[41] The enclosure discussed in Chapter 5 can be easily used on planar IMAC surfaces to sub-charge large His-tagged proteins, increasing protein signal intensity and removing alkali metal adducts in DESI-MS.

Issues that remain to be resolved are inhibiting protein oxidation on IMAC surfaces by using reducing agents and enriching His-tagged proteins in sample to increase their S/N. Ultimately, a two-step purification system integrated into the workflow might be necessary for the rapid analysis of large His-tagged proteins from crude cell lysate by DESI-MS.

6.5 References

1. Morrow, J. F.; Cohen, S. N.; Chang, A. C.; Boyer, H. W.; Goodman, H. M.; Helling, R. B., Replication and Transcription of Eukaryotic DNA in Esherichia Coli. *Proceedings of the National Academy of Sciences* **1974,** *71* (5), 1743-1747.
2. Khan, S.; Ullah, M. W.; Siddique, R.; Nabi, G.; Manan, S.; Yousaf, M.; Hou, H., Role of Recombinant DNA Technology to Improve Life. *International Journal of Genomics* **2016,** *2016*, 2405954.
3. Hayat, S. M.; Farahani, N.; Golichenari, B.; Sahebkar, A., Recombinant Protein Expression in Escherichia Coli (E. Coli): What We Need to Know. *Current Pharmaceutical Design* **2018,** *24* (6), 718-725.
4. Demain, A. L.; Vaishnav, P., Production of Recombinant Proteins by Microbes and Higher Organisms. *Biotechnology Advances* **2009,** *27* (3), 297-306.
5. Rosano, G. L.; Ceccarelli, E. A., Recombinant Protein Expression in Escherichia Coli: Advances and Challenges. *Frontiers in Microbiology* **2014,** *5*.
6. Terpe, K., Overview of Bacterial Expression Systems for Heterologous Protein Production: From Molecular and Biochemical Fundamentals to Commercial Systems. *Applied Microbiology and Biotechnology* **2006,** *72* (2), 211-222.
7. Jonasson, P.; Liljeqvist, S.; Nygren, P. A. k.; Ståhl, S., Genetic Design for Facilitated Production and Recovery of Recombinant Proteins in Escherichia Coli. *Biotechnology and Applied Biochemistry* **2002,** *35* (2), 91-105.
8. Marbach, A.; Bettenbrock, K., Lac Operon Induction in Escherichia Coli: Systematic Comparison of Iptg and Tmg Induction and Influence of the Transacetylase Laca. *Journal of Biotechnology* **2012,** *157* (1), 82-88.
9. Marschall, L.; Sagmeister, P.; Herwig, C., Tunable Recombinant Protein Expression in E. Coli: Promoter Systems and Genetic Constraints. *Applied Microbiology and Biotechnology* **2017,** *101* (2), 501-512.
10. Tabor, S.; Richardson, C. C., A Bacteriophage T7 Rna Polymerase/Promoter System for Controlled Exclusive Expression of Specific Genes. *Proceedings of the National Academy of Sciences* **1985,** *82* (4), 1074-1078.
11. Mahmoodi, S.; Pourhassan-Moghaddam, M.; Wood, D. W.; Majdi, H.; Zarghami, N., Current Affinity Approaches for Purification of Recombinant Proteins. *Cogent Biology* **2019,** *5* (1).
12. Mishra, V., Affinity Tags for Protein Purification. *Current Protein & Peptide Science* **2020,** *21* (8), 821-830.
13. Gomari, M. M.; Saraygord-Afshari, N.; Farsimadan, M.; Rostami, N.; Aghamiri, S.; Farajollahi, M. M., Opportunities and Challenges of the Tag-Assisted Protein Purification Techniques: Applications in the Pharmaceutical Industry. *Biotechnology Advances* **2020,** *45*.
14. McCue, J. T., Theory and Use of Hydrophobic Interaction Chromatography in Protein Purification Applications. *Methods in Enzymology* **2009,** *463*, 405-414.
15. Jungbauer, A.; Hahn, R., Ion-Exchange Chromatography. *Methods in Enzymology* **2009,** *463*, 349-371.
16. Block, H.; Maertens, B.; Spriestersbach, A.; Brinker, N.; Kubicek, J.; Fabis, R.; Labahn, J.; Schäfer, F., Immobilized-Metal Affinity Chromatography (Imac): A Review. *Methods in Enzymology* **2009,** *463*, 439-473.
17. Porath, J.; Carlsson, J.; Olsson, I.; Belfrage, G., Metal Chelate Affinity Chromatography, a New Approach to Protein Fractionation. *Nature* **1975,** *258* (5536), 598-599.
18. Gräslund, S.; Nordlund, P.; Weigelt, J.; Hallberg, B. M.; Bray, J.; Gileadi, O.; Knapp, S.; Oppermann, U.; Arrowsmith, C.; Hui, R., Protein Production and Purification. *Nature Methods* **2008,** *5* (2), 135-146.

19. Crowe, J.; Dobeli, H.; Gentz, R.; Hochuli, E.; Stiiber, D.; Henco, K., 6xffis-Ni-Nta Chromatography as a Superior Technique in Recombinant Protein Expression/Purification. In *Protocols for Gene Analysis*, Springer: 1994; pp 371-387.
20. Hochuli, E.; Döbeli, H.; Schacher, A., New Metal Chelate Adsorbent Selective for Proteins and Peptides Containing Neighbouring Histidine Residues. *Journal of Chromatography A* **1987,** *411*, 177-184.
21. Chaga, G.; Hopp, J.; Nelson, P., Immobilized Metal Ion Affinity Chromatography on Co2+-Carboxymethylaspartate–Agarose Superflow, as Demonstrated by One-Step Purification of Lactate Dehydrogenase from Chicken Breast Muscle. *Biotechnology and Applied Biochemistry* **1999,** *29* (1), 19-24.
22. Gaberc-Porekar, V.; Menart, V., Perspectives of Immobilized-Metal Affinity Chromatography. *Journal of Biochemical and Biophysical Methods* **2001,** *49* (1-3), 335-360.
23. Levitt, M., Nature of the Protein Universe. *Proceedings of the National Academy of Sciences* **2009,** *106* (27), 11079-11084.
24. Furnham, N.; de Beer, T. A.; Thornton, J. M., Current Challenges in Genome Annotation through Structural Biology and Bioinformatics. *Current Opinion in Structural Biology* **2012,** *22* (5), 594-601.
25. Rogawski, R.; Sharon, M., Characterizing Endogenous Protein Complexes with Biological Mass Spectrometry. *Chemical Reviews* **2021**.
26. Domon, B.; Aebersold, R., Mass Spectrometry and Protein Analysis. *Science* **2006,** *312* (5771), 212-217.
27. Benesch, J. L.; Ruotolo, B. T.; Simmons, D. A.; Robinson, C. V., Protein Complexes in the Gas Phase: Technology for Structural Genomics and Proteomics. *Chemical Reviews* **2007,** *107* (8), 3544-3567.
28. Vimer, S.; Ben-Nissan, G.; Sharon, M., Mass Spectrometry Analysis of Intact Proteins from Crude Samples. *Analytical Chemistry* **2020,** *92* (19), 12741-12749.
29. Takano, K.; Arai, S.; Sakamoto, S.; Ushijima, H.; Ikegami, T.; Saikusa, K.; Konuma, T.; Hamachi, I.; Akashi, S., Screening of Protein-Ligand Interactions under Crude Conditions by Native Mass Spectrometry. *Analytical and Bioanalytical Chemistry* **2020,** *412* (17), 4037-4043.
30. Tousi, F.; Jiang, Y.; Sivendran, S.; Song, Y.; Elliott, S.; Paiva, A.; Lund, A.; Albee, K.; Lee, K., Intact Protein Mass Spectrometry of Cell Culture Harvest Guides Cell Line Development for Trispecific Antibodies. *Analytical Chemistry* **2020,** *92* (3), 2764-2769.
31. Vimer, S.; Ben-Nissan, G.; Sharon, M., Direct Characterization of Overproduced Proteins by Native Mass Spectrometry. *Nature Protocols* **2020,** *15* (2), 236-265.
32. Gan, J.; Ben-Nissan, G.; Arkind, G.; Tarnavsky, M.; Trudeau, D.; Noda Garcia, L.; Tawfik, D. S.; Sharon, M., Native Mass Spectrometry of Recombinant Proteins from Crude Cell Lysates. *Analytical Chemistry* **2017,** *89* (8), 4398-4404.
33. Ben-Nissan, G.; Vimer, S.; Warszawski, S.; Katz, A.; Yona, M.; Unger, T.; Peleg, Y.; Morgenstern, D.; Cohen-Dvashi, H.; Diskin, R.; Fleishman, S. J.; Sharon, M., Rapid Characterization of Secreted Recombinant Proteins by Native Mass Spectrometry. *Communications Biology* **2018,** *1* (1), 213.
34. VanAernum, Z. L.; Busch, F.; Jones, B. J.; Jia, M.; Chen, Z.; Boyken, S. E.; Sahasrabuddhe, A.; Baker, D.; Wysocki, V. H., Rapid Online Buffer Exchange for Screening of Proteins, Protein Complexes and Cell Lysates by Native Mass Spectrometry. *Nature Protocols* **2020,** *15* (3), 1132-1157.
35. Busch, F.; VanAernum, Z. L.; Lai, S. M.; Gopalan, V.; Wysocki, V. H., Analysis of Tagged Proteins Using Tandem Affinity-Buffer Exchange Chromatography Online with Native Mass Spectrometry. *Biochemistry* **2021,** *60* (24), 1876-1884.
36. Yao, C.; Wang, T.; Zhang, B.; He, D.; Na, N.; Ouyang, J., Screening of the Binding of Small Molecules to Proteins by Desorption Electrospray Ionization Mass Spectrometry Combined with Protein Microarray. *Journal of the American Society for Mass Spectrometry* **2015,** *26* (11), 1950-1958.

37. Takáts, Z.; Wiseman, J. M.; Gologan, B.; Cooks, R. G., Electrosonic Spray Ionization. A Gentle Technique for Generating Folded Proteins and Protein Complexes in the Gas Phase and for Studying Ion−Molecule Reactions at Atmospheric Pressure. *Analytical Chemistry* **2004,** *76* (14), 4050-4058.
38. Kwon, K.; Grose, C.; Pieper, R.; Pandya, G. A.; Fleischmann, R. D.; Peterson, S. N., High Quality Protein Microarray Using in Situprotein Purification. *BMC Biotechnology* **2009,** *9* (1), 72.
39. Ueda, E.; Gout, P.; Morganti, L., Current and Prospective Applications of Metal Ion–Protein Binding. *Journal of Chromatography A* **2003,** *988* (1), 1-23.
40. Bornhorst, J. A.; Falke, J. J., Purification of Proteins Using Polyhistidine Affinity Tags. *Methods in Enzymology* **2000,** *326*, 245-254.
41. Tillner, J.; Wu, V.; Jones, E. A.; Pringle, S. D.; Karancsi, T.; Dannhorn, A.; Veselkov, K.; McKenzie, J. S.; Takats, Z., Faster, More Reproducible Desi-Ms for Biological Tissue Imaging. *Journal of The American Society for Mass Spectrometry* **2017,** *28* (10), 2090-2098.
42. Zhang, J.; Loo, R. R. O.; Loo, J. A., Increasing Fragmentation of Disulfide-Bonded Proteins for Top–Down Mass Spectrometry by Supercharging. *International Journal of Mass Spectrometry* **2015,** *377*, 546-556.
43. Cassou, C. A.; Sterling, H. J.; Susa, A. C.; Williams, E. R., Electrothermal Supercharging in Mass Spectrometry and Tandem Mass Spectrometry of Native Proteins. *Analytical Chemistry* **2013,** *85* (1), 138-146.
44. Scientific™, T. Pierce™ Copper Coated High Capacity Plates, Clear, 96-Well. https://www.thermofisher.com/order/catalog/product/15143#/15143 (accessed 04/01/2021).
45. Grassi, L.; Cabrele, C., Susceptibility of Protein Therapeutics to Spontaneous Chemical Modifications by Oxidation, Cyclization, and Elimination Reactions. *Amino Acids* **2019,** *51* (10), 1409-1431.
46. Tan, Y.-F.; O'Toole, N.; Taylor, N. L.; Millar, A. H., Divalent Metal Ions in Plant Mitochondria and Their Role in Interactions with Proteins and Oxidative Stress-Induced Damage to Respiratory Function. *Plant Physiology* **2010,** *152* (2), 747-761.
47. Douglass, K. A.; Venter, A. R., Predicting the Highest Intensity Ion in Multiple Charging Envelopes Observed for Denatured Proteins During Electrospray Ionization Mass Spectrometry by Inspection of the Amino Acid Sequence. *Analytical Chemistry* **2013,** *85* (17), 8212-8218.
48. Kwon, K.; Grose, C.; Pieper, R.; Pandya, G. A.; Fleischmann, R. D.; Peterson, S. N., High Quality Protein Microarray Using in Situ Protein Purification. *BMC Biotechnology* **2009,** *9* (1), 1-10.
49. Lee, Y.; Lee, E. K.; Cho, Y. W.; Matsui, T.; Kang, I. C.; Kim, T. S.; Han, M. H., Proteochip: A Highly Sensitive Protein Microarray Prepared by a Novel Method of Protein Immobilization for Application of Protein-Protein Interaction Studies. *Proteomics* **2003,** *3* (12), 2289-2304.
50. Wleklinski, M.; Loren, B. P.; Ferreira, C. R.; Jaman, Z.; Avramova, L.; Sobreira, T. J.; Thompson, D. H.; Cooks, R. G., High Throughput Reaction Screening Using Desorption Electrospray Ionization Mass Spectrometry. *Chemical Science* **2018,** *9* (6), 1647-1653.
51. Morato, N. M.; Holden, D. T.; Cooks, R. G., High-Throughput Label-Free Enzymatic Assays Using Desorption Electrospray-Ionization Mass Spectrometry. *Angewandte Chemie International Edition* **2020,** *59* (46), 20459-20464.
52. Sawicki, J. W.; Bogdan, A. R.; Searle, P. A.; Talaty, N.; Djuric, S. W., Rapid Analytical Characterization of High-Throughput Chemistry Screens Utilizing Desorption Electrospray Ionization Mass Spectrometry. *Reaction Chemistry & Engineering* **2019,** *4* (9), 1589-1594.
53. Cha, T.; Guo, A.; Zhu, X. Y., Enzymatic Activity on a Chip: The Critical Role of Protein Orientation. *Proteomics* **2005,** *5* (2), 416-419.
54. Venter, A.; Cooks, R. G., Desorption Electrospray Ionization in a Small Pressure-Tight Enclosure. *Analytical Chemistry* **2007,** *79* (16), 6398-6403.
55. DeMuth, J. C.; McLuckey, S. A., Electrospray Droplet Exposure to Organic Vapors: Metal Ion Removal from Proteins and Protein Complexes. *Analytical Chemistry* **2015,** *87* (2), 1210-1218.

56. Lee, J. W.; Kim, H. I., Solvent-Induced Structural Transitions of Lysozyme in an Electrospray Ionization Source. *Analyst* **2015,** *140* (10), 3573-3580.
57. DeMuth, J. C.; Bu, J.; McLuckey, S. A., Electrospray Droplet Exposure to Polar Vapors: Delayed Desolvation of Protein Complexes. *Rapid Communications in Mass Spectrometry* **2015,** *29* (10), 973-981.

CHAPTER 7

7. CONCLUSIONS AND PERSPECTIVES

DESI-MS was introduced almost two decades ago and initially, it was envisioned to eventually supersede conventional ESI-MS in popularity on account of its relative ease of use, versatility in sampling/ionization under ambient conditions. However, besides several applications in which DESI shows great superiority compared to ESI-MS (most notably imaging), it has failed to reach the popularity of ESI-MS, especially for intact protein analyses. It is not surprising that the majority of studies by DESI-MS focus on small molecule analysis and its applications in different fields such as forensic studies,[1] clinical applications,[2] and of course, imaging.[3-5] Recent advances in instrumentation, such as coupling ion-mobility to DESI-MS,[6-9] have been demonstrated for improved signal detection for protein analysis. However, in the absence of such expensive instrumentations, additives, whether ESI-MS-friendly solution-phase or post-ionization gas-phase additives, can be a convenient approach for improving protein analysis in DESI-MS and mitigating some of the shortcomings. Improving DESI-MS analysis of proteins through simple, convenient methods can hopefully broaden the applications of DESI-MS and lead to more diverse types of studies using this technique.

7.1 Towards improved DESI-MS analysis of proteins and novel applications

In present work, I have described my efforts to improve DESI-MS analysis of proteins by simple techniques and explore the application of DESI-MS in investigating fundamental

questions regarding protein behaviors. As DESI-MS and ESI-MS share many similarities, especially in the ionization process, using DESI-MS followed by direct ESI-MS experiments for complementary analyses can reveal valuable information about protein dissolution and ionization. Understanding protein behavior during dissolution and ionization can lead to better insight into improving protein analysis by DESI-MS.

In Chapter 3, the effectiveness of different solution-phase additives and their combination, including formic acid, ammonium bicarbonate,[10] and L-serine,[11] for increasing protein signal intensity in DESI-MS was studied. The desalting effect of L-serine for native proteins in DESI-MS, which was similar to results previously reported in ESI-MS,[12] is particularly important for native protein analysis from complex mixtures with high salt concentrations such as most biological samples prior to purification. The study also revealed an intriguing effect of L-serine on unfolded protein signal intensity during DESI-MS, increasing the absolute signal intensity of the unfolded protein. Since such improvement was not observed in direct ESI-MS of unfolded proteins, it was proposed that L-serine positively affects protein extraction/dissolution processes during DESI-MS.

Following up on the positive observations regarding serine addition for protein analysis by DESI-MS, Chapter 4 explored the effects of amino acid additives, in particular L-serine, on protein solubility and dissolution processes. Through careful design of experiments using DESI-MS and direct ESI-MS, it was demonstrated that important mechanistic conclusions can be drawn about solubility-enhancing additives and their general mechanism of action. This approach provided mechanistic insights on protein dissolution while using significantly lower concentrations of additives and very small amounts of protein compared to classic biophysical

methods. We demonstrated that the limitation of DESI-MS in protein analysis can actually be used to provide a novel perspective for understanding the mechanisms governing the effects of amino acids, and by extension, other additives, on proteins solubility, dissolution, and aggregation. These assays have the potential to be powerful tools for the rapid development of additives important for pharmaceutical applications and formulation.

Chapter 5 explored a different approach for improving protein detection by DESI-MS. When introducing organic solvent vapors into an enclosed DESI-MS environment, substantial improvements in protein signal could be achieved. This study was motivated by the reported effects of organic solvent vapors addition to the analysis of proteins by ESI-MS, which was shown to impact charge states distribution,[13-14] alkali metal adduction,[15-16] denaturation,[17] protein-substrate complex stability,[18] and signal intensity.[19-20] Since DESI and ESI share similar ionization mechanisms, the implementation of organic vapors was anticipated to improve the analysis of proteins in DESI-MS as well. A simple plastic enclosure was designed and built for this study, allowing exposure of the DESI-MS sampling area to gas-phase additives. This effect was independent of protein characteristics, such as size or isoelectric point values. The vapors of acetone, acetonitrile, ethyl acetate, methanol, and water were investigated. Vapors of acetone and especially ethyl acetate showed promising results in terms of increasing protein signal intensity in DESI-MS, regardless of protein size and isoelectric point.

Chapter 6 described evaluation and proof-of-concept experiments for development of a simple direct assay for rapid analysis of immobilized His-tagged proteins from IMAC surfaces, in particular Ni-NTA and Cu-NTA. The ultimate goal of this study is to couple purification of His-tagged recombinant proteins from the bacterial cell lysate for developing fast and simple

high throughput assays that provide more information in a shorter time frame compared to conventional methods. Issues that need to be addressed for achieving this goal are reducing protein oxidation during IMAC purification without suppressing protein signal and increasing His-tagged protein S/N by increasing the concentration of the His-tagged protein in the cell lysate. This will be especially important for the analysis of larger proteins that typically suffer from lower sensitivity in ESI-MS and DESI-MS. Several approaches were discussed in Chapter 6 to address these issues, including incorporating an additional purification step after introducing reducing reagents to the incubation step, and using organic solvent vapors to sub-charge large proteins and concentrate the signal into fewer peaks. Ultimately, this project is an ambitious attempt to enable an on-line study of both the protein and the protein enzymatic reaction by DESI-MS, which could be highly impactful for protein engineering, and when studying enzyme evolution, where functional analysis of thousands of candidates is necessary.

7.2 Final remarks

Despite the remarkable versatility of DESI-MS in the analysis of different samples and recent advances in instrumentation, DESI lacks behind other developments in the field for protein studies. Investigating the mechanisms involved in protein detection enables developing strategies for improving protein analysis by DESI-MS that are simple and easy to incorporate. These strategies should target key factors involved in protein extraction, desorption, or ionization. Ultimately, by improving protein detection in DESI-MS, applications of DESI-MS can be extended beyond what is currently possible, including developing a high throughput tool for functional analysis of immobilized recombinant proteins.

7.3 References

1. Wójtowicz, A.; Wietecha-Posłuszny, R., Desi-Ms Analysis of Human Fluids and Tissues for Forensic Applications. *Applied Physics A* **2019,** *125* (5), 1-9.
2. Abbassi-Ghadi, N.; Jones, E. A.; Veselkov, K. A.; Huang, J.; Kumar, S.; Strittmatter, N.; Golf, O.; Kudo, H.; Goldin, R. D.; Hanna, G. B., Repeatability and Reproducibility of Desorption Electrospray Ionization-Mass Spectrometry (Desi-Ms) for the Imaging Analysis of Human Cancer Tissue: A Gateway for Clinical Applications. *Analytical Methods* **2015,** *7* (1), 71-80.
3. Sugiura, Y.; Sugiyama, E.; Suematsu, M., Desi-Based Imaging Mass Spectrometry in Forensic Science and Clinical Diagnosis. In *Ambient Ionization Mass Spectrometry in Life Sciences*, Elsevier: 2020; pp 107-118.
4. Parrot, D.; Papazian, S.; Foil, D.; Tasdemir, D., Imaging the Unimaginable: Desorption Electrospray Ionization–Imaging Mass Spectrometry (Desi-Ims) in Natural Product Research. *Planta medica* **2018,** *84* (09/10), 584-593.
5. Liu, C.; Qi, K.; Yao, L.; Xiong, Y.; Zhang, X.; Zang, J.; Tian, C.; Xu, M.; Yang, J.; Lin, Z., Imaging of Polar and Nonpolar Species Using Compact Desorption Electrospray Ionization/Postphotoionization Mass Spectrometry. *Analytical chemistry* **2019,** *91* (10), 6616-6623.
6. Garza, K. Y.; Feider, C. L.; Klein, D. R.; Rosenberg, J. A.; Brodbelt, J. S.; Eberlin, L. S., Desorption Electrospray Ionization Mass Spectrometry Imaging of Proteins Directly from Biological Tissue Sections. *Analytical chemistry* **2018,** *90* (13), 7785-7789.
7. Towers, M. W.; Karancsi, T.; Jones, E. A.; Pringle, S. D.; Claude, E., Optimised Desorption Electrospray Ionisation Mass Spectrometry Imaging (Desi-Msi) for the Analysis of Proteins/Peptides Directly from Tissue Sections on a Travelling Wave Ion Mobility Q-Tof. *Journal of The American Society for Mass Spectrometry* **2018,** *29* (12), 2456-2466.
8. Yan, B.; Bunch, J., Probing Folded Proteins and Intact Protein Complexes by Desorption Electrospray Ionization Mass Spectrometry. *Journal of The American Society for Mass Spectrometry* **2021,** *32* (3), 690-699.
9. Sans, M.; Feider, C. L.; Eberlin, L. S., Advances in Mass Spectrometry Imaging Coupled to Ion Mobility Spectrometry for Enhanced Imaging of Biological Tissues. *Current opinion in chemical biology* **2018,** *42*, 138-146.
10. Honarvar, E.; Venter, A. R., Ammonium Bicarbonate Addition Improves the Detection of Proteins by Desorption Electrospray Ionization Mass Spectrometry. *Journal of The American Society for Mass Spectrometry* **2017,** *28* (6), 1109-1117.
11. Javanshad, R.; Honarvar, E.; Venter, A. R., Addition of Serine Enhances Protein Analysis by Desi-Ms. *Journal of The American Society for Mass Spectrometry* **2019,** *30* (4), 694-703.
12. Clarke, D. J.; Campopiano, D. J., Desalting Large Protein Complexes During Native Electrospray Mass Spectrometry by Addition of Amino Acids to the Working Solution. *Analyst* **2015,** *140* (8), 2679-2686.
13. Jonasson, P.; Liljeqvist, S.; Nygren, P. A. k.; Ståhl, S., Genetic Design for Facilitated Production and Recovery of Recombinant Proteins in Escherichia Coli. *BIOTECHNOLOGY AND APPLIED BIOCHEMISTRY* **2002,** *35* (2), 91-105.
14. Girod, M.; Antoine, R.; Dugourd, P.; Love, C.; Mordehai, A.; Stafford, G., Basic Vapor Exposure for Tuning the Charge State Distribution of Proteins in Negative Electrospray Ionization: Elucidation of Mechanisms by Fluorescence Spectroscopy. *Journal of The American Society for Mass Spectrometry* **2012,** *23* (7), 1221-1231.
15. DeMuth, J. C.; McLuckey, S. A., Electrospray Droplet Exposure to Organic Vapors: Metal Ion Removal from Proteins and Protein Complexes. *Analytical Chemistry* **2015,** *87* (2), 1210-1218.

16. Hopper, J. T.; Sokratous, K.; Oldham, N. J., Charge State and Adduct Reduction in Electrospray Ionization–Mass Spectrometry Using Solvent Vapor Exposure. *Analytical biochemistry* **2012,** *421* (2), 788-790.
17. Kharlamova, A.; DeMuth, J. C.; McLuckey, S. A., Vapor Treatment of Electrospray Droplets: Evidence for the Folding of Initially Denatured Proteins on the Sub-Millisecond Time-Scale. *Journal of the American Society for Mass Spectrometry* **2012,** *23* (1), 88-101.
18. DeMuth, J. C.; Bu, J. X.; McLuckey, S. A., Electrospray Droplet Exposure to Polar Vapors: Delayed Desolvation of Protein Complexes. *Rapid Communications in Mass Spectrometry* **2015,** *29* (10), 973-981.
19. Chen, J.; Wang, F.; Liu, Z.; Liu, J.; Zhu, Y.; Zhang, Y.; Zou, H., Electrospray Ionization in Concentrated Acetonitrile Vapor Improves the Performance of Mass Spectrometry for Proteomic Analyses. *Journal of Chromatography A* **2017,** *1483*, 101-109.
20. Li, Z.; Li, L., Chemical-Vapor-Assisted Electrospray Ionization for Increasing Analyte Signals in Electrospray Ionization Mass Spectrometry. *Analytical chemistry* **2014,** *86* (1), 331-335.

APPENDICES

A. Review of Ambient Methods

Reproduced with permission from

R. Javanshad, and A. R. Venter

Anal. Methods, 2017, **9**, 4896

Analytical Methods

MINIREVIEW

View Article Online
View Journal | View Issue

Check for updates

Cite this: *Anal. Methods*, 2017, **9**, 4896

Ambient ionization mass spectrometry: real-time, proximal sample processing and ionization

R. Javanshad and A. R. Venter *

Received 11th April 2017
Accepted 15th May 2017

DOI: 10.1039/c7ay00948h

rsc.li/methods

The definition of ambient ionization is updated from "no sample preparation" to sample preparation proximal and in real time with the ionization and analysis step. We differentiate between ambient ionization methods and the direct and hyphenated techniques. Ambient ionization has been reviewed many times and we summarise some of the approaches that reviews have taken to categorize the many ambient ionization methods. Due to the large number of permutations, frequent redundancy and complexity of the 80+ techniques developed so far, none of the review classifications is successful in classifying all the ambient ionization methods based on the chosen scheme. Likewise our classification based on major sample preparation method also fails at finding a good category for every method, but it does highlight the central role that real-time, proximal sample preparation plays in ambient analysis.

Introduction

What ambient ionization is, and what it isn't

Ambient ionization methods have been revolutionary in sample analysis by mass spectrometry. It is a form of ionization in which ions are formed in an ion source outside the vacuum system of the mass spectrometer. While it is often said that ambient ionization methods do not require sample preparation,[1–4] our view is that it is more accurate to say these methods frequently require no sample preparation, other than the sample processing that takes place during the analysis. In other words *ambient ionization is a form of ionization where sample preparation takes place in real-time and proximal to the ionization and during the analysis of analytes*.

A purely ambient method is one where the sample is available for mass spectrometry analysis without any *prior* sample preparation or, in the ultimate case the mass spectrometer is taken to the sample for analysis without disturbing the sample from its environment. Sample processing, introduction and ionization then all take place in a concerted, simultaneous manner during a single analysis step near the point of ion introduction into the vacuum system of the mass spectrometer. It is the immediacy of sample preparation that differentiates the

Department of Chemistry, Western Michigan University, Kalamazoo, Michigan, 49008-5413, USA. E-mail: andre.venter@wmich.edu

Roshan Javanshad studied chemistry at University of Tehran (Tehran, Iran), where she received her Bachelor of Science in Chemistry in 2015. Roshan is enrolled in the Ph.D. program at the Department of Chemistry at Western Michigan University (Kalamazoo, MI). Her field of interest is bioanalytical chemistry and proteomics. Her current research activities involve improving ambient ionization mass spectrometry for protein detection and developing novel methods for the analysis and quantification of proteins.

Andre Venter is an associate professor at Western Michigan University. His research group studies spray ionization mechanisms and ambient surface analysis mass spectrometry for protein analysis. Prior to coming to WMU in 2008 he worked with Prof. Graham Cooks at Purdue University. During this post-doc he investigated fundamentals of desorption electrospray ionization mass spectrometry and other ionization methods. He obtained his tertiary education from the University of Pretoria in South Africa and a Ph.D. in 2003 with Prof. Egmont Rohwer, where he developed a comprehensive multidimensional supercritical fluid and gas chromatography (SFCxGC) method for petrochemical and natural product analyses.

	Hyphenated/ Online Separation	Direct Analysis	Pure Ambient
	Processing Step(s)		
Defining Step	Offline + Online	Offline	Real-Time
Degree of "Ambience"			
Example Methods	GC-MS LC-MS	Nano-ESI Infusions Loop Injections Paper Spray	DESI DART LAESI LMJ-SSP Nano-DESI Substrate Spray

Fig. 1 Hyphenated methods on the left frequently require offline sample preparation and online separation. Direct methods rely solely on offline sample preparation, while analysis relies on the mass spectrometer alone for separation. The ambient methods typically do the bulk of sample processing during the analysis step, and like direct methods, rely on the mass spectrometer for separation and detection.

ambient analysis methods from direct mass spectrometry analysis.

To better differentiate between ambient, direct and hyphenated techniques we provide Fig. 1. Direct analysis methods imply the use of offline sample preparation but without an inline sample separation step. Hyphenated chromatography-mass spectrometry techniques usually include both offline and online sample preparation prior to MS detection and analysis. Direct methods rely solely on offline sample preparation, while analysis relies on the mass spectrometer alone for separation. The ambient methods typically do the bulk of sample processing during the analysis step, and like direct methods, rely on the mass spectrometer for separation and detection.

Reviews of reviews of ambient ionization

Ambient ionization has been reviewed frequently over the past 10 years. A number of excellent review articles are available on the topic of ambient ionization, and the reader is kindly referred to those for more inclusive information on both the methods and their common applications.[5] Without aiming for inclusivity we first attempt to show the diversity, complexity and possible redundancies of ambient ionization by highlighting the major schemes by which various reviewers have classified the more than 80 ambient ionization techniques.[6]

An obvious approach is for methods to be arranged primarily by either desorption method or ionization method, although it is common to first separate by one aspect and then a second.

Primary categorization by ionization is frequently used as the basis for categorization.[2] An example is shown in Fig. 2a, which divides techniques based on electrospray ionization (ESI) and atmospheric-pressure chemical ionization (APCI) mechanisms. Table 1 similarly separates on ionization first and then further differentiates the methods in terms of the approach used for sampling. A similar approach was followed by Huang *et al.*[7]

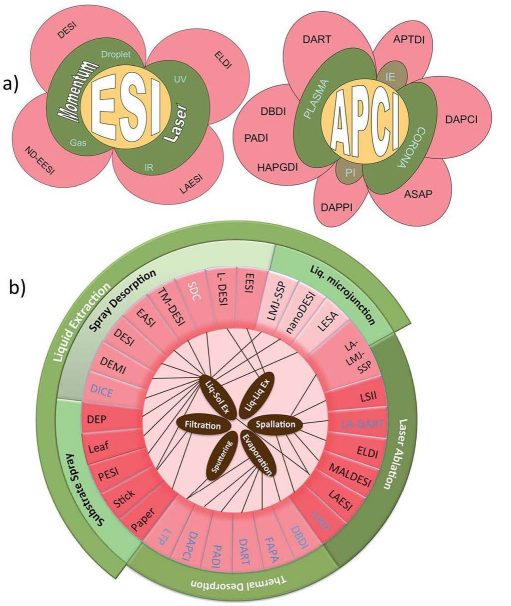

Fig. 2 (a) Flowergrams depicting classification of ambient ionization methods based on ionization mechanism (Reprinted from TrAC, 27 Venter, Nefliu, Cooks, 284–290, Copyright (2008) with permission from Elsevier). (b) Summary of the major classes of ambient ionization methods based on traditional groupings (green), examples of methods (shades of pink), and the various sample processing methods (black). The mechanism of ionization is indicated by the font color for each listed example. Black indicates ESI, blue APCI, and white ambient sample processing without ionization. (Reprinted with permission from Venter, Douglass *et al.* Anal. Chem., 86, 233–249. Copyright (2014) American Chemical Society).

In some instances ionization and desorption occur in a concerted fashion or no desorption step is required, while others use distinct desorption and ionization processes. This aspect of ambient ionization was captured by Huang *et al.* in yet another classification scheme, based on basic principles of ionization: direct ionization methods, direct ionization/desorption methods, and methods based on a two-step ionization process.[7]

Alternatively the methods have been arranged by the desorption mechanism, or as shown in Fig. 2b, by the major processing steps of liquid extraction, spallation/laser ablation or thermal desorption.[8] A "technique-centric" organization for the material has also been published based on both the extraction/desorption technique and ionization mechanism.[3]

Ambient methods are also frequently classified based on one of the three major techniques: spray, plasma and laser ionization methods.[8,9]

There are also many reviews that focus only on a particular subcategory of ambient ionization. For example the plasma methods were reviewed recently,[10,11] and so were electrospray

Table 1 Ambient ionization methods arranged first by ionization method then desorption agent and indicating sample processing method

Ionization agent	Desorption agent	Sample processing method	Acronym	Method name	Reference
None	Spray desorption/ momentum transfer	Liq–Sol Ex.	SDC	Spray desorption collection	65
ESI		Liq–Sol Ex.	DESI[a]	Desorption electrospray ionization	1
		Liq–Liq Ex.	L-DESI	Liquid desorption electrospray ionization	27
		Liq–Sol Ex.	TM-DESI	Transmission mode DESI	60
		Liq–Sol Ex.	EASI	Easy ambient sonic-spray ionization	61
		Liq–Sol Ex.	DEMI	Desorption electrospray/metastable-induced plasma	62
		Liq–Sol Ex.	DICE	Desorption ionization by charge exchange	63
		Liq–Liq Ex.	EESI	Extractive electrospray ionization	28
	None	Dissolution	DEP	Direct electrospray probe	79
		Filtration	PS	Paper spray	29
		Liq–Sol Ex.	—	Leaf spray	82
		Dissolution	PESI	Probe electrospray ionization	80
		Liq–Sol Ex.	LMJ-SSP	Liquid microjunction surface sampling probe	57
		Liq–Sol Ex.	Nano-DESI	Nanospray desorption electrospray ionization	24
		Liq–Sol Ex.	LESA[a]	Liquid extraction surface analysis	71
	Laser ablation	Spallation	LA-LMJ-SSP	Laser ablation liquid microjunction surface sampling probe	70
		Spallation	LSII	Laserspray inlet ionization	133
		Spallation	ELDI	Electrospray-assisted laser desorption/ ionization	120
		Spallation	MALDESI	Matrix-assisted laser desorption electrospray ionization	33
		Spallation Liq–Sol Ex.	LAESI[a]	Laser ablation electrospray ionization	32
		Spallation	LA-DART	Laser-assisted direct analysis in real time	101
		Spallation	LIAD	Laser induced acoustic desorption	144
APCI	Thermal desorption	Evaporation	ASAP[a]	Atmospheric solids analysis probe	31
		Evaporation	DART[a]	Direct analysis in real time	30
		Evaporation	DAPCI	Desorption atmospheric-pressure chemical ionization	96
		Evaporation	DBDI	Dielectric barrier discharge ionization	95
		Evaporation	FAPA	Flowing atmospheric-pressure afterglow	93
		Evaporation	PADI	Plasma-assisted desorption/ionization	107
		Evaporation sputtering	LTP	Low temperature plasma	94

Table 1 (*Contd.*)

Ionization agent	Desorption agent	Sample processing method	Acronym	Method name	Reference
Joule heating	Thermal evaporation	Rapid evaporation	REIMS[a]	Rapid evaporative ionization mass spectrometry	101

[a] Commercially available techniques.

based methods.[12] Ambient laser-based mass spectral analysis using femtosecond (fs) and nanosecond (ns) duration laser desorption electrospray ionization were also reviewed.[13] Other subcategory reviews are focused on the chemical aspects of extractive methods of ambient ionization mass spectrometry[14] or the accompanying chemical processes in DESI and other ambient methods.[15]

Classifications of ambient methods by major processing method

As seen above, it is possible to categorize ambient methods in various ways, but in this short review, as in another recent review by our group,[8] we categorize the different methods based on their primary means of sample processing to highlight the importance of real-time, proximal sample preparation that occurs during ambient analysis. In each major class we also discuss methods of ionization that have been implemented for each class.

All of the ambient analysis methods are similar in the way that they produce ions outside of the ion source at atmospheric pressure, or in the intermediate pressure region of the ion inlet during sampling and ion transport into the mass spectrometer.[16] Ions are usually produced by well-known atmospheric pressure ionization methods such as ion–molecule reactions, photochemical ionization, or from charged droplets or clusters by ESI mechanisms.[3,4,14,17–23]

Sample processing steps are related to classical methods of preparation, but implemented on a micro scale and localized, often retaining spatial distributions, and typically proximal to the immediate location of ionization. Sample processing steps such as dilution, preconcentration, liquid–solid extraction (DESI,[1] nano-DESI,[24] LMJ[25,26]), liquid–liquid extraction (liquid-DESI,[27] EESI[28]), filtration (Paper Spray[29]), thermal desorption (DART,[30] ASAP[31]), spallation by energy sudden desorption, (LAESI,[32] MALDESI,[33] LA-FAPA,[34] Laserspray[35]), and others have all been used during ambient sample introduction.

Over the past 15 years, more than 80 distinct ambient ionization methods have been introduced which combine and implement various combinations of these sample-processing steps with well-known but novel implementations of ionization methods.[6] Acronyms for many of these methods can be found in Table 1.

In the first domain of methods, sample processing is achieved mostly through substrate–liquid extraction. This class is further divided into: (1) spray desorption methods where solvent extraction is followed by momentum transfer, (2) the liquid junction techniques, where extraction occurs inline with an electrospray emitter, and (3) substrate spray, which has no desorption step prior to ionization. Illustrated in Fig. 2b these divisions are collected under separate lighter green arcs with black lettering under the liquid extraction arc.

The second major class of sample processing is comprised of methods that use thermal desorption as a means to produce molecules from surfaces. Since mostly small molecules are able to thermally desorb from surfaces, this form of processing is highly suited for combination with the chemical ionization methods.

Finally in the third class, laser ablation methods are described, where spallation of larger particles are entrained in an electrospray plume and a second processing step of liquid–solid extraction leads to the production of ions by ESI methods.

Extraction methods

There are three major extraction-based methods for sample processing in ambient ionization: spray desorption, liquid microjuntion and substrate spray. They involve liquid–solid or sometimes liquid–liquid extraction as their principal step. These methods are organized based on the process by which the analyte is directed towards ionization step. In spray desorption techniques, charged droplets of solvent form a thin solvent layer on the sample, where the analyte is rapidly extracted from the surface through transfer process. In liquid microjunction techniques, a continuous-flow liquid stream forms a microjunction on the surface and extraction occurs inline. In techniques known as substrate spray, the sample is directly used for extraction and the sample substrate itself works as both the introduction and ionization device.

Spray desorption methods. In most spray desorption techniques solvent in a pneumatically assisted electrospray removes analyte from an intact sample surface and directs the analytes towards subsequent ionization and introduction to the mass spectrometer. The sample analysis occurs through five steps: (1) formation of a spray plume (primary droplets) directed at the intact sample,[36,37] (2) formation of a micro-localized liquid layer on the sample surface,[38–41] (3) dissolution/extraction of the analyte into the liquid layer,[36,42,43] (4) release of analyte containing droplets (secondary droplets) from the liquid layer by pneumatically accelerated primary droplets[37,39–41,44] and finally, (5) analyte ion generation from charged secondary droplets. The main technique that falls into the spray desorption category is DESI which was first introduced by Cooks and colleagues in 2004.[1] DESI and its variations or other spray desorption techniques share many similarities in their mechanism, so

mechanistic studies for an individual technique can be applicable to others as well. Spray desorption methods are commonly used in analysis of a continuous solid surfaces such as sample deposited on glass or PTFE,[45–48] a pharmaceutical tablet,[38,49] tissue samples,[50,51] plant material[52–56] and a chromatography plate after separation,[57,58] *etc.* For analysis of liquid samples, the sample can be continuously driven through a silica capillary (liquid-DESI).[27,59] Samples can also be deposited on a mesh substrate and analyzed in transmission geometry, without burdensome optimization of spray distances or angles and without the preparation time essential to solvent evaporation (transmission mode DESI, TM-DESI).[60] Another method is the dual sprayer arrangement, where the charged solvent spray interacts with the sample spray (extractive electrospray ionization, EESI).[28]

Extraction is greatly affected by solubility. In general, increasing solubility improves the response. However, samples with high solubility erode over time[36] which can lead to sample degradation and loss of signal.[38] It is important to note that in spray desorption methods where analysis of sample on solid surface is desired (*e.g.* DESI, EASI,[61] DEMI,[62] DICE[63]), the solvent spray plume droplets form a liquid layer on the surface. In methods where the sample is already in liquid state (such as liquid-DESI and EESI), dissolution is not part of the mechanism. Instead, mixing of the two liquid phases occur. For some types of analyte which does not readily dissolve on the time scale of the solid surface methods, such as proteins,[23] these liquid-sampling methods have been found to be much more sensitive than the other spray desorption ambient methods.[64] The characteristics of the thin liquid layer formed in the impact zone depend on (1) solvent composition and gas flows, (2) solvent physicochemical properties, and (3) the physicochemical properties of the surface.[38] The optimum combination, or range of combinations, of solvent and flow rate produces a spray that effectively wets the surface and is energetic enough to produce secondary droplets, yet dry enough and not so energetic as to cause sheeting of the solvent along the surface.[45]

Studies of spray desorption for DESI separated from the ionization process, termed spray desorption collection (SDC),[65] have shown that desorption is not dependent on the spray voltage. Geometric source parameters such as the distance of the spray from the surface and the sheath gas velocity can affect desorption,[45] so the use of a sealed geometry-independent source design can reduce the influence of these factors.[66] However, the range of DESI parameters compiled from a considerable number of literature sources show wide scale flexibility in the parameter space available for successful analysis by DESI and likely also the other spray methods.[45]

Ionization during and after the solvent extraction methods. The mechanism of ionization for extraction spray methods is often similar. Generation of charged secondary droplets during desorption leads to an electrospray-like charging process. During this process small molecules become charged by ion evaporation[67] while larger molecules such as proteins become charged by charge residue.[68] Charged secondary droplets which undergo evaporation as well as ions formed in the region in front of MS inlet which has atmospheric pressure, are sucked into the MS inlet. Needless to say, the desorption process can affect the ionization signal.[42,44]

Similar to DESI, DICE works with a charged primary spray. However, instead of protonated solvent molecules, the charge carriers are odd-electron molecular ions of toluene, which were formed by electrochemical oxidation and corona discharge at the spray capillary.[63] Charge transfer happens between molecular ions of toluene and analyte molecules, which lead to formation of molecular ions of analyte.[63] During DEMI, analyte molecules are first desorbed by charged solvent spray and then are intercepted by a plume of metastable species directed towards MS inlet. In the positive ionization mode, highly polar molecules are ionized by sodiation and/or protonation while neutral molecules are protonated by reacting with protonated water clusters formed from interaction of the metastable plume with atmospheric gases.[62]

Not every desorption spray method use a high voltage for generation of charged primary droplets in the desorption spray. During EASI, no voltage is applied to the primary solvent spray, yet significant analyte ion signal can be observed.[38,61] It has been suggested that charged droplets are produced by minuscule fluctuations in the ion concentrations of the bulk solution occurring immediately prior to nebulization and due to interactions with the material of the spray nozzle.[61,69] Another speculation is that atmospheric-pressure chemical ionization might also occur involving charged intermediates formed during droplet collision with the surface.[38]

Liquid microjunction. In the ambient liquid microjunction methods, surface analysis is possible *via* liquid extraction techniques. The solvent is extruded from a capillary or pipet tip to form a continuous solvent bridge, or microjunction, with the sample. Analyte is extracted as it distributes between sample and liquid phase, and is then carried to the ionization source (most commonly ESI). Three techniques which have been reported that use a liquid microjunction for extraction followed by online ionization are liquid microjunction surface sampling probe (LMJ-SSP),[25,70] nano-DESI,[24] and liquid extraction surface analysis (LESA).[71] The primary difference between these techniques is the way solvent is delivered for extraction and then removed from the surface and the implementation of electrospray ionization – whether it is nanospray[24,71] or pneumatically assisted.[26,72] The LMJ-SSP method uses a pair of concentric capillary tubes[26,72] above the sample surface as the probe.[73] During nano-DESI a liquid-microjunction is created between two capillaries. A primary capillary delivers solvent to the foot of a second nanospray capillary held vertically or angled 105° above the surface, to conduct solvent away from the surface by feeding into an electrospray.[25] Liquid extraction surface analysis (LESA) uses discreet droplets hanging from a pipet tip held at a short distance above the sample surface. After a designated amount of extraction time, the solvent is retracted and the pipet tip is repositioned behind an ESI-chip to initialize an electrospray.[68]

Substrate spray. In this method, when a high potential difference is present between a sharp tip and a mass spectrometer inlet, and solvent is applied, an electrospray is generated directly from the sample substrate. A corona discharge mechanism has also been observed under solvent-starved conditions.[74] The most well-known example of this

approach is paper spray ionization,[75] which is typically used as a method for direct ionization.

With direct ionization liquid solutions of samples are applied to a substrate of suitable dimensions for analysis. Substrates such as paper triangles or wooden sticks[76–78] are examples. Direct analysis is also possible with prepared liquid samples spotted on small metal rings (direct electrospray probe, DEP)[79] or needles (probe electrospray ionization, PESI).[80,81]

Ambient analysis applications of substrate spray include plant material such as leaves, fruit, and roots[82–84] scorpion stingers,[85] and biological tissue.[76,86] In theory, as long as the substrate has a sharp tip or can be formed into a sharp angle it is a candidate for ambient analysis by substrate spray.

With substrate spray, processing occurs mainly by extraction, while filtration and selective absorption and/or adsorption can also lead to purification. Small sample consumption, efficient ionization from small sample volumes and minimal carryover make these methods especially suitable for analysis of complex biological samples.[82,87]

With paper spray chromatographic separations has been observed for sample components with large differences in distribution coefficients.[88] Alternatively, different compound classes can selectively be extracted when appropriate solvents are selected.[82,89] There is a wide range of applicable solvents for paper spray as both polar and nonpolar solvents can be used as the spray solvent[90] and additives and buffers can be introduced into the solvent system to promote online derivatization and increase the analyte signal, a method referred to as reactive paper spray ionization.[75,77,91]

Thermal/chemical desorption (plasma) methods

Plasma ambient analysis methods rely on various modes of electrical discharge such as corona discharge techniques, glow discharge techniques and dielectric barrier discharge (DBD) technique for sample processing (*i.e.*, desorption) and/or ionization.[30] Plasma-based methods provide simplicity of design and operation and they are also amenable to portable, *in situ* analyses.[92] The simplest plasma-based sources require only a power source, conductive electrodes, an insulating discharge cell, and an inert discharge gas.[93–95]

Thermal or thermally assisted desorption. The general belief is that for the plasma methods molecules are thermally volatilized into the headspace above the sample and it is these gas-phase species that are ionized. Temperatures of samples analyzed with indirect plasma sources, such as DART or DAPCI,[96] are related to the temperature of the external gas heater and are not appreciably impacted by the discharge conditions.[97] With direct analysis in real time (DART)[30] many small organic molecules and components in complex mixtures[98] can be detected and separated from surfaces directly, but it was noted that the range of detectable species increases when the discharge gas is externally heated.

Transport of ions, electrons or excited species to the sample surface during direct and quasi-direct methods are important to consider. Likewise, with indirect methods, transport of neutral analyte molecules to the reactive plasma needs to be optimized. In all methods after ionization collection of analyte ions from the sample surface by the mass spectrometer also has a significant impact on the detection and quantification of analytes. Mass and ion transport is often difficult to study with plasma ionization methods, due to the transparent and inert plasma gasses often used.[97,99] Even so, Schlieren imaging, using differences in refractive index, has allowed visualization of helium flows in FAPA.[99,100]

Rapid evaporative ionization mass spectrometry (REIMS)[101,102] is a technique that uses thermal energy to generate charged species. When high frequency electric current is applied to surgical blades, tissues in contact ablate,

Table 2 Some major plasma-assisted ambient ionization techniques

Plasma source type	Plasma source	Example methods	Power supply	Basic principle
Indirect plasma	DC corona discharge/glow discharge	DART	DC	Sample surface exposed to the plasma stream
	DC corona discharge	DAPCI	DC	Sample surface is exposed to gaseous reagent species
Direct plasma	Dielectric barrier discharge	DBDI	AC	Sample is desorbed/ionized with ion bombardment through the plasma sheath produced with DBD
	RF glow discharge	PADI	RF	Sample surface is in direct contact with nonthermal plasma
Quasi-direct plasma	DC glow discharge	FAPA	DC	Sample is introduced into the flowing afterglow outside the discharge chamber
	Dielectric barrier discharge	LTP	AC	Plasma plume ejecting from DBD-constructed chamber reacts directly with the sample

producing aerosols and the heat dissipated during the process produces charged species. In the typical REIMS setup, PTFE tubing transport the aerosol containing gaseous ions from the surgical site and the transmission of the ions to the distant mass spectrometer. This method couples rapid evaporation of biological materials with MS analysis to perform *in vivo*, *in situ* mass spectrometric tissue analysis in real time.

Chemical sputtering. Thermally assisted desorption is the most commonly discussed route for analyte desorption, but other mechanisms, especially those related to high-energy species created in the discharge, also exist. The techniques that use chemical sputtering are somewhat related to both plasma and spray-based approaches and include desorption atmospheric pressure chemical ionization (DAPCI) and desorption corona beam ionization (DCBI).[103] Early DART and DESI papers proposed the possibility of sputtering, whereby excited species bombard a sample and liberate analytes through a transfer of chemical energy.[30] However, no direct evidence was shown for that type of process taking place and was theorized due to the ability to detect compounds with relatively low vapor pressure. Therefore an endeavour to discover and understand alternative processes can help in extending the abilities of the plasma-based methods. As discussed by Shelley *et al.* in another review paper,[8] it was demonstrated that LTP mass spectra could be generated from covalently surface-bound monolayers and for compounds with low or no vapor pressure such as salts and ionic liquids.[104] While molecular cation signals were not observed, a protonated fragment of the molecular cation was detected. From these and additional findings, Wiley *et al.* have proposed a mechanism whereby electron transfer from gas-phase reagent species results in reductive bond cleavage, where after neutral fragments are ionized by APCI-like mechanisms.[8,105]

Direct *versus* indirect plasma sources. While in this review we set out to differentiate methods primarily based on sample processing method, the physical design of the plasma source and degree of direct interaction between the plasma and sample are the parameters that can best help in understanding and categorizing real-time sample processing and ionization mechanisms in this group of methods.

In general, the plasma-based methods can use indirect, quasi-direct, or direct plasma interaction as summarized in Table 2.

Indirect plasma sources. In an indirect plasma source, the electrical discharge occurs physically and electrically separated from the sample introduction region. Examples include DART, DAPCI and ASAP.

The direct analysis in real time (DART) source is a prime example. Here a DC corona-to-glow discharge[106] is separated from the sample by one or two chambers, which can be used to electrically filter ions or electrons from the effluent as well as externally heat the discharge gas. Another example is desorption atmospheric-pressure chemical ionization (DAPCI)[96] where a DC corona discharge creates reagent species in a heated chamber and flowing gas transfers the reagent ions and thermal energy to the sample. Atmospheric solids analysis probe (ASAP)[31] is a direct analysis method that can use a commercial electrospray (ESI) but typically an atmospheric pressure chemical ionization (APCI) source with the simple modification of the installation of a port for inserting the sample into a hot gas stream within the ion source region to provide a rapid analysis of volatile and semi-volatile compounds. The method acts as a fast solids/liquid probe introduction as well as an alternative to the DART and desorption electrospray ionization (DESI) methods for many compound types.

Quasi-direct plasma sources. A quasi-direct plasma source physically and/or electrically isolates the primary discharge from the sample introduction region. However, the plasma gas transfers ions, electrons, and excited species into the open air maintaining macroscopic neutrality, which creates afterglow plasma. This afterglow plasma interacts with atmospheric gases and the sample to create reagent and analyte ions, respectively. The flowing atmospheric-pressure afterglow (FAPA)[93] source which consists of a DC and atmospheric-pressure glow discharge between two electrodes in a sealed discharge cell is a prime example of quasi-direct plasma source. Another technique is the low temperature plasma probe (LTP)[94] which is based on a dielectric barrier discharge (DBD) between a grounded pin electrode and an AC- or RF-powered ring electrode separated by a dielectric tube with the discharge gas flowing through the tube. An afterglow in the ambient air is caused by rapid formation of the micro discharges leading to a propagating ionization wave, also called a plasma bullet.[94] It is these plasma bullets and associated atmospheric reagent species that interact with the sample.

Direct plasma sources. When using direct plasma-based methods such as dielectric-barrier discharge ionization (DBDI)[95] and plasma-assisted desorption/ionization (PADI)[107] the sample is in direct contact with the main source of excited species and reagent ions, which should increase desorption and ionization efficiency. However, source instability, memory effects, and analyte fragmentation are among the disadvantages. In DBDI, the sample is located on a dielectric layer between two electrodes where an AC potential is applied in the presence of an inert discharge gas, whereas in PADI, an RF glow discharge is set at the end of a powered pin electrode, which comes in direct contact with the sample. The RF energy will find the easiest path to ground, often through the sample when it is conductive enough.

Ionization mechanisms by plasma sources. Ionization sources for molecular mass spectrometry in plasma-based methods suggest quite similar mechanisms.[108,109] Five major ionization pathways have been observed with plasma-based ambient ionization sources.[30,93,110] These ionization mechanisms are proton transfer, charge transfer, electron capture, ion attachment, and hydride abstraction. Direct penning ionization with excited plasma species such as helium metastable atoms has also been suggested as another possible pathway. Different classes of analytes will ionize through different mechanisms. For instance, many polar analytes will produce spectra consisting of strictly protonated molecular ions, MH^+, indicating they undergo proton-transfer ionization, whereas nonpolar species yield odd-electron molecular ions, $M^{+\bullet}$. Sufficiently electronegative molecules, including halogenated or nitrated compounds, preferentially form negative ions through the

mechanisms. In general, the observed reagent ions and ionization pathways have been demonstrated to be similar to APCI and atmospheric-pressure photoionization.[111,112]

These ionization processes rely on the formation of reagent species (water clusters ($[H_2O]_nH^+$) and N_2^+ created from the interaction of helium plasma species with atmospheric gases). Differences in ionization with different plasmas can be extrapolated from background reagent-ion spectra. The DART source is an indirect plasma source which also filters any electrons and ions from the stream resulting in mostly lower energy reagent ions such as protonated water clusters, $(H_2O)_nH^+$, and negative oxygen ions, O_2^-.[30] In comparison, the quasi-direct plasma sources yield an abundance of higher-energy charge-transfer species, such as N_2^+ and O_2^+.[93,94] The direct plasma methods can provide even higher energy reagent species, to the point where EI-like fragmentation spectra can be observed[113]

Examination of the reagent-ion formation pathways is essential to understanding and expanding the ionization capabilities of plasma-based sources. It was theorized that, because filter electrodes were presumably removing all charged species from the DART stream, only neutral, excited helium species, particularly metastable He^M were responsible for creation of the reagent species.[30] It has been shown that atmospheric gases, namely, nitrogen and water, could undergo penning ionization with He^M to produce primary reagent ions. These primary reagent ions would then undergo a series of reactions known from corona discharge APCI to produce protonated water clusters.[114,115] Studies have been done to measure relative abundance of He^M and other helium species,[116] and the findings have suggested formation of an alternate proton transfer species, such as H_3^+ or HeH^+.[117]

While helium metastable atoms certainly play an important role in the reagent-ion formation with the DART source, quasi-direct and direct plasma methods can have different pathways. Mechanisms of primary reagent-ion formation, which involve charged species, likely play an important role and has been investigated.[118,119]

The distance between plasma and the sample has a major influence on the type of plasma species that interact with the sample and a categorization of the plasma methods could be achieved based on this approach. Accordingly there are methods such as ASAP and DAPPI where desorption occurs prior to and *independently* from interactions with plasma species. DART, DAPCI, and FAPA can be categorized as *distant* techniques where low-energy plasma products (ionization reagents) come in contact with the sample. DBDI and PADI, are examples of *proximal* methods with direct plasma interaction between high-energy plasma species (for example high-energy electrons) and the sample. DART can also be operated in conditions where helium metastable atoms interact with the sample and may sometimes be used as a direct plasma method.

Laser desorption: ablation, spallation and acoustic desorption

Laser-assisted ambient ionization encompasses the techniques in which short bursts (1–100 ns) of spatially well-defined high energy is used to desorb or ablate analyte from a small sample, matrix or substrate area through creation of a shockwave. Either a UV laser (ELDI,[120] and MALDESI[34]) or IR (LAESI,[32] and LADESI[121]) laser pulse generates a plume from the sample. This sample plume is intercepted by an electrospray ion plume[32,33,120] or in the case of AP-LD/CI[122] with a reactive plasma beam for post-ionization. With these so-called "hybrid" or "two-step" techniques[5,7] the desorption and ionization processes are separated in space and time and can be studied separately.

Major advantages of this sub-family of methods include production of highly charged ions that are similar to those observed in direct electrospray, which allows analyses of complex biological targets.[33,123,124] Due to the smaller size of the laser spot, these methods have higher spatial resolution and use minute amounts of sample for analysis.

One of the first laser-assisted techniques was electrospray-assisted laser desorption ionization (ELDI).[120] Here a conventional ELDI MS used a UV laser operating at 337 nm with pulse durations of ±5 ns and energies in the range from 150 to 300 mJ.

LAESI, a popular and commercialized laser desorption ambient technique uses mid-IR that couples directly with absorption bands of water, and is therefore highly suited for the analysis of biological samples.[32,33] Other techniques that use mid-IR lasers are AP-LD/CI,[122] and LA-DESI.[121]

During a typical atmospheric-pressure UV ablation, the ion-to-neutral ratio is between 10^{-5} to 10^{-3}, and in IR is likely to produce even lower ion yields due to the lower photon energies and lower absorption coefficients.[125,126] Thus, other nonthermal processes of photochemical or photomechanical nature are believed to play a minor role in the ions observed by the two- or three-step ambient ionization methods such as ELDI and LAESI, and most observed ions are produced by interaction of the plume of molecules released from the surface with the post-ionization source.[32,33] Some differences do exist between ambient IR and UV ablation, and these differences are reflected in the analytical figures of merit for ELDI, MALDESI, and LAESI.[32,127]

In addition to the desorption of single molecules or (mono) layers from a target surface into the gas phase,[128] the experimental conditions during atmospheric and ambient laser ablation methods such as ELDI, LAESI, and others are generally energetic enough to cause a variety of transfer processes from solid to gas-phase including the production of clusters, particles, or chunks of the bulk sample, to evaporation, liquid boiling, and phase explosion.[125]

Desorption by spallation. Evaporation and spallation occur during laser ablation when the material in the laser focus is heated. Molten material is ejected by boiling as well as by the recoil pressure of the internal shock wave on the back of the molten liquid.[32] This shock wave originates from the laser pulse, which leads to the ionization of the medium and the production of free electrons, a process which gains energy from the laser electric field, causing further ionization. The ionization of the medium results in plasma formation that expands with supersonic velocities producing strong shockwaves in the medium.[129] Recoil pressure in the sample surface which happens when the plume collapses results in the ejection of large sample particles which can travel far distances[32] due to convection, airflows, and particle diffusion.[127] These particles

remain in the ambient air for extended periods of time and are intercepted by the ionizing droplets for post-ionization.

Post-ionization. Because of the inherently poor ion production by laser ablation both in vacuum and at atmospheric pressure, post-ionization has been of interest in mass spectrometry for a long time. Post-ionization by electrospray ionization, for instance, allows the analysis of large biopolymers on high-performance mass spectrometers with limited mass range[33,130] delivers improved detection, and more informative fragmentation which is useful for top-down proteomics.[131] During spray desorption of the ablated spalls, interaction with solvent droplets leads to additional sample processing through solid-liquid extraction and the ability to introduce selectivity through appropriate solvent selection.

Desorption by acoustic ejection

Acoustic wave techniques. There are methods that combine acoustic wave desorption with one of the main categories mentioned so far.

One such method, reminiscent of the ESI charge retention model,[132] is the family of techniques that includes LSII,[133] MAII,[16,134,135] and the related vacuum methods.[136] These do not require the high potential necessary for ESI,[137] nor the nebulizing gas needed for SSI,[61,138] and no chemical or photochemical reactions to produce ions.[18,35,139] Instead, LSII and MAII produces ions from charged airborne spalls produced by laser ablation (LSII)[133,140] or physical means such as the use of an air gun replacing the laser and shooting pellets into a metal plate which has matrix/analyte applied to the opposite side and near the ion entrance inlet to the mass spectrometer (MAII). Ionization requires only that the analyte be mixed with suitable matrixes such as 2,5-dihydroxybenzoic acid, 3-nitrobenzonitrile, or others, as long as a suitable protonation source, such as water, is available during sample preparation and heat to the inlet is provided.[141]

Laser-induced acoustic desorption (LIAD)[142–144] is another example. This technique utilizes nonresonant laser-based matrix-free desorption approach, in which the sample is deposited onto a thin metal foil[145] (*e.g.*, titanium or aluminum), which is irradiated from the backside with a series of high-energy laser pulses.[146] The acoustic waves created by the laser cause desorption of nonvolatile and thermally labile compounds on the other side of the foil.[142]

Surface acoustic wave nebulization (SAWN)[142,147] is a laser-free method that generates ions of low internal energy from a piezoelectric surface. This method uses a radiofrequency signal in a pulsed or continuous mode to a transducer patterned onto a piezoelectric surface. The acoustic wave propagates along the surface and is refracted into a sample drop (~3 μL) deposited on the chip. The acoustic wave causes small droplets to be ejected from the sample, where the droplets and eventually the ions are charged due to statistical distributions of charges.[70]

Conclusions

The real-time sample processing of the ambient ionization methods provide many important advantages including: (1) the sample processing usually follows a simple, easy workflow so it does not require extensive training in analytical chemistry. (2) These processing steps are frequently localized, enabling the spatial distribution of analytes to be determined for chemical microscopy through imaging mass spectrometry. (3) The potential for interface contamination and sample carryover is greatly reduced, since samples often remain outside of the analytical system right up to the point of concurrent processing and ionization.

Ambient ionization also faces many challenges. It is sometimes easier to invent a new method, than to find useful applications for it. Like all new tools one could also be tempted to use it injudiciously, even for situations where the same problem can be solved much easier using more conventional approaches. For example it is sometimes easier to spray a liquid sample, than to analyse it by an ambient desorption method after spotting on a substrate.

The early bloom of ambient ionization as illustrated by the flowergrams in Fig. 2a has since matured and it is clear from Fig. 2b that ambient ionization has been a fruitful endeavour for those researchers pursuing its many challenges. Some of the classical methods that seeded the real-time proximal sample preparation processes taking place during ambient ionization have also sprouted new methods of sample preparation separate from ionization *viz.*; methods such as SDC and LA-SSP show that the micro-localization of sample collection can be used to apply these familiar sample preparation techniques in new and unique ways.

Acknowledgements

This material was supported by the National Science Foundation under grant no. CHE 1506626.

References

1 Z. Takats, J. M. Wiseman, B. Gologan and R. G. Cooks, *Science*, 2004, **306**, 471–473.
2 A. Venter, M. Nefliu and R. Graham Cooks, *TrAC, Trends Anal. Chem.*, 2008, **27**, 284–290.
3 G. A. Harris, A. S. Galhena and F. M. Fernandez, *Anal. Chem.*, 2011, **83**, 4508–4538.
4 M.-Z. Huang, S.-C. Cheng, Y.-T. Cho and J. Shiea, *Anal. Chim. Acta*, 2011, **702**, 1–15.
5 M. E. Monge, G. A. Harris, P. Dwivedi and F. M. Fernández, *Chem. Rev.*, 2013, **113**, 2269–2308.
6 Wikipedia, Ambient Ionization, https://en.wikipedia.org/wiki/Ambient_ionization, accessed 20 March 2017.
7 M.-Z. Huang, C.-H. Yuan, S.-C. Cheng, Y.-T. Cho and J. Shiea, *Annu. Rev. Anal. Chem.*, 2010, **3**, 43–65.
8 A. R. Venter, K. A. Douglass, J. T. Shelley, G. Hasman and E. Honarvar, *Anal. Chem.*, 2014, **86**, 233–249.
9 A. B. T. Lebedev, *Russ. Chem. Rev.*, 2015, **84**, 665.
10 M. Smoluch, P. Mielczarek and J. Silberring, *Mass Spectrom. Rev.*, 2016, **35**, 22–34.
11 A. Albert, J. T. Shelley and C. Engelhard, *Anal. Bioanal. Chem.*, 2014, **406**, 6111–6127.

12 A. K. Meher and Y.-C. Chen, *Mass Spectrometry*, 2017, **6**, S0057.
13 P. Flanigan and R. Levis, in *Annual Review of Analytical Chemistry*, ed. R. G. Cooks and J. E. Pemberton, Annual Reviews, Palo Alto, 2014, vol. 7, pp. 229–256.
14 A. K. Badu-Tawiah, L. S. Eberlin, Z. Ouyang and R. G. Cooks, *Annu. Rev. Phys. Chem.*, 2013, **64**, 481–505.
15 D. R. Ifa, C. Wu, Z. Ouyang and R. G. Cooks, *Analyst*, 2010, **135**, 669–681.
16 C. N. McEwen, V. S. Pagnotti, E. D. Inutan and S. Trimpin, *Anal. Chem.*, 2010, **82**, 9164–9168.
17 R. B. Cole, *Electrospray and MALDI mass spectrometry: fundamentals, instrumentation, practicalities, and biological applications*, John Wiley & Sons, 2011.
18 S. Trimpin, B. Wang, C. B. Lietz, D. D. Marshall, A. L. Richards and E. D. Inutan, *Crit. Rev. Biochem. Mol. Biol.*, 2013, **48**, 409–429.
19 L. Konermann, E. Ahadi, A. D. Rodriguez and S. Vahidi, *Unraveling the Mechanism of Electrospray Ionization*, ACS Publications, 2012.
20 C. J. Hogan Jr, J. A. Carroll, H. W. Rohrs, P. Biswas and M. L. Gross, *Anal. Chem.*, 2009, **81**, 369.
21 C. D. Daub and N. M. Cann, *Anal. Chem.*, 2011, **83**, 8372–8376.
22 J. K. Chung and S. Consta, *J. Phys. Chem. B*, 2012, **116**, 5777–5785.
23 K. A. Douglass and A. R. Venter, *Anal. Chem.*, 2013, **85**, 8212–8218.
24 P. J. Roach, J. Laskin and A. Laskin, *Analyst*, 2010, **135**, 2233–2236.
25 G. J. Van Berkel, A. D. Sanchez and J. M. E. Quirke, *Anal. Chem.*, 2002, **74**, 6216–6223.
26 T. Wachs and J. Henion, *Anal. Chem.*, 2001, **73**, 632–638.
27 Z. Miao and H. Chen, *J. Am. Soc. Mass Spectrom.*, 2009, **20**, 10–19.
28 H. Chen, A. Venter and R. G. Cooks, *Chem. Commun.*, 2006, 2042–2044.
29 H. Wang, N. E. Manicke, Q. Yang, L. Zheng, R. Shi, R. G. Cooks and Z. Ouyang, *Anal. Chem.*, 2011, **83**, 1197.
30 R. B. Cody, J. A. Laramée and H. D. Durst, *Anal. Chem.*, 2005, **77**, 2297–2302.
31 C. N. McEwen, R. G. McKay and B. S. Larsen, *Anal. Chem.*, 2005, **77**, 7826–7831.
32 P. Nemes and A. Vertes, *Anal. Chem.*, 2007, **79**, 8098–8106.
33 J. S. Sampson, A. M. Hawkridge and D. C. Muddiman, *J. Am. Soc. Mass Spectrom.*, 2006, **17**, 1712–1716.
34 J. T. Shelley, S. J. Ray and G. M. Hieftje, *Anal. Chem.*, 2008, **80**, 8308–8313.
35 S. Trimpin, E. D. Inutan, T. N. Herath and C. N. McEwen, *Mol. Cell. Proteomics*, 2010, **9**, 362–367.
36 F. Green, T. Salter, I. Gilmore, P. Stokes and G. O'Connor, *Analyst*, 2010, **135**, 731–737.
37 Z. Olumee, J. H. Callahan and A. Vertes, *J. Phys. Chem. A*, 1998, **102**, 9154–9160.
38 F. Zivolic, F. Zancanaro, D. Favretto, S. D. Ferrara, R. Seraglia and P. Traldi, *J. Mass Spectrom.*, 2010, **45**, 411–420.
39 A. Venter, P. E. Sojka and R. G. Cooks, *Anal. Chem.*, 2006, **78**, 8549–8555.
40 A. B. Costa and R. G. Cooks, *Chem. Commun.*, 2007, 3915–3917.
41 A. B. Costa and R. G. Cooks, *Chem. Phys. Lett.*, 2008, **464**, 1–8.
42 K. A. Douglass and A. R. Venter, *J. Mass Spectrom.*, 2013, **48**, 553–560.
43 A. Badu-Tawiah, C. Bland, D. I. Campbell and R. G. Cooks, *J. Am. Soc. Mass Spectrom.*, 2010, **21**, 572–579.
44 Z. Takats, J. M. Wiseman and R. G. Cooks, *J. Mass Spectrom.*, 2005, **40**, 1261–1275.
45 K. A. Douglass, S. Jain, W. R. Brandt and A. R. Venter, *J. Am. Soc. Mass Spectrom.*, 2012, **23**, 1896–1902.
46 F. Green, P. Stokes, C. Hopley, M. Seah, I. Gilmore and G. O'Connor, *Anal. Chem.*, 2009, **81**, 2286–2293.
47 I. Cotte-Rodríguez, Z. Takáts, N. Talaty, H. Chen and R. G. Cooks, *Anal. Chem.*, 2005, **77**, 6755–6764.
48 T. J. Kauppila, N. Talaty, P. K. Salo, T. Kotiaho, R. Kostiainen and R. G. Cooks, *Rapid Commun. Mass Spectrom.*, 2006, **20**, 2143–2150.
49 H. Chen, N. N. Talaty, Z. Takáts and R. G. Cooks, *Anal. Chem.*, 2005, **77**, 6915–6927.
50 J. M. Wiseman, D. R. Ifa, Y. Zhu, C. B. Kissinger, N. E. Manicke, P. T. Kissinger and R. G. Cooks, *Proc. Natl. Acad. Sci. U. S. A.*, 2008, **105**, 18120–18125.
51 L. S. Eberlin, C. R. Ferreira, A. L. Dill, D. R. Ifa and R. G. Cooks, *Biochim. Biophys. Acta, Mol. Cell Biol. Lipids*, 2011, **1811**, 946–960.
52 N. Talaty, Z. Takáts and R. G. Cooks, *Analyst*, 2005, **130**, 1624–1633.
53 A. L. Lane, L. Nyadong, A. S. Galhena, T. L. Shearer, E. P. Stout, R. M. Parry, M. Kwasnik, M. D. Wang, M. E. Hay and F. M. Fernandez, *Proc. Natl. Acad. Sci. U. S. A.*, 2009, **106**, 7314–7319.
54 J. H. Kennedy and J. M. Wiseman, *Rapid Commun. Mass Spectrom.*, 2010, **24**, 1305–1311.
55 B. Li, N. Bjarnholt, S. H. Hansen and C. Janfelt, *J. Mass Spectrom.*, 2011, **46**, 1241–1246.
56 T. Müller, S. Oradu, D. R. Ifa, R. G. Cooks and B. Kräutler, *Anal. Chem.*, 2011, **83**, 5754–5761.
57 G. J. Van Berkel and V. Kertesz, *Anal. Chem.*, 2006, **78**, 4938–4944.
58 S. P. Pasilis, V. Kertesz and G. J. Van Berkel, *Anal. Chem.*, 2007, **79**, 5956–5962.
59 Y. Zhang, Z. Yuan, H. D. Dewald and H. Chen, *Chem. Commun.*, 2011, **47**, 4171–4173.
60 J. E. Chipuk and J. S. Brodbelt, *J. Am. Soc. Mass Spectrom.*, 2008, **19**, 1612–1620.
61 R. Haddad, R. Sparrapan and M. N. Eberlin, *Rapid Commun. Mass Spectrom.*, 2006, **20**, 2901–2905.
62 L. Nyadong, A. S. Galhena and F. M. Fernández, *Anal. Chem.*, 2009, **81**, 7788–7794.
63 C.-C. Chan, M. S. Bolgar, S. A. Miller and A. B. Attygalle, *J. Am. Soc. Mass Spectrom.*, 2010, **21**, 1554–1560.
64 C. N. Ferguson, S. A. Benchaar, Z. Miao, J. A. Loo and H. Chen, *Anal. Chem.*, 2011, **83**, 6468.

65 A. R. Venter, A. Kamali, S. Jain and S. Bairu, *Anal. Chem.*, 2010, **82**, 1674–1679.
66 A. Venter and R. G. Cooks, *Anal. Chem.*, 2007, **79**, 6398–6403.
67 B. Thomson and J. Iribarne, *J. Chem. Phys.*, 1979, **71**, 4451–4463.
68 L. L. Mack, P. Kralik, A. Rheude and M. Dole, *J. Chem. Phys.*, 1970, **52**, 4977–4986.
69 E. E. Dodd, *J. Appl. Phys.*, 1953, **24**, 73–80.
70 O. S. Ovchinnikova, V. Kertesz and G. J. Van Berkel, *Anal. Chem.*, 2011, **83**, 1874–1878.
71 V. Kertesz and G. J. Van Berkel, *J. Mass Spectrom.*, 2010, **45**, 252–260.
72 A. D. Modestov, S. Srebnik, O. Lev and J. Gun, *Anal. Chem.*, 2001, **73**, 4229–4240.
73 G. J. Van Berkel, V. Kertesz and R. C. King, *Anal. Chem.*, 2009, **81**, 7096–7101.
74 R. D. Espy, A. R. Muliadi, Z. Ouyang and R. G. Cooks, *Int. J. Mass Spectrom.*, 2012, **325**, 167–171.
75 J. Liu, H. Wang, N. E. Manicke, J.-M. Lin, R. G. Cooks and Z. Ouyang, *Anal. Chem.*, 2010, **82**, 2463–2471.
76 N. E. Manicke, P. Abu-Rabie, N. Spooner, Z. Ouyang and R. G. Cooks, *J. Am. Soc. Mass Spectrom.*, 2011, **22**, 1501–1507.
77 Y. Su, H. Wang, J. Liu, P. Wei, R. G. Cooks and Z. Ouyang, *Analyst*, 2013, **138**, 4443–4447.
78 B. Hu, P.-K. So, H. Chen and Z.-P. Yao, *Anal. Chem.*, 2011, **83**, 8201–8207.
79 C.-P. Kuo and J. Shiea, *Anal. Chem.*, 1999, **71**, 4413–4417.
80 K. Hiraoka, K. Nishidate, K. Mori, D. Asakawa and S. Suzuki, *Rapid Commun. Mass Spectrom.*, 2007, **21**, 3139–3144.
81 L. C. Chen, K. Nishidate, Y. Saito, K. Mori, D. Asakawa, S. Takeda, T. Kubota, H. Hori and K. Hiraoka, *J. Phys. Chem. B*, 2008, **112**, 11164–11170.
82 J. Liu, H. Wang, R. G. Cooks and Z. Ouyang, *Anal. Chem.*, 2011, **83**, 7608–7613.
83 R. GrahamáCooks, *Analyst*, 2012, **137**, 1082–1084.
84 J. I. Zhang, X. Li, Z. Ouyang and R. G. Cooks, *Analyst*, 2012, **137**, 3091–3098.
85 B. Hu, L. Wang, W.-C. Ye and Z.-P. Yao, *Sci. Rep.*, 2013, **3**, 2104.
86 Q. Yang, H. Wang, J. D. Maas, W. J. Chappell, N. E. Manicke, R. G. Cooks and Z. Ouyang, *Int. J. Mass Spectrom.*, 2012, **312**, 201–207.
87 S. Saha, M. K. Mandal and K. Hiraoka, *Anal. Methods*, 2013, **5**, 4731–4738.
88 Y. Ren, H. Wang, J. Liu, Z. Zhang, M. N. McLuckey and Z. Ouyang, *Chromatographia*, 2013, **76**, 1339–1346.
89 J. Liu, R. G. Cooks and Z. Ouyang, *Anal. Chem.*, 2011, **83**, 9221.
90 A. Li, H. Wang, Z. Ouyang and R. G. Cooks, *Chem. Commun.*, 2011, **47**, 2811–2813.
91 X. Yan, R. Augusti, X. Li and R. G. Cooks, *ChemPlusChem*, 2013, **78**, 1142–1148.
92 J. S. Wiley, J. T. Shelley and R. G. Cooks, *Anal. Chem.*, 2013, **85**, 6545–6552.
93 F. J. Andrade, J. T. Shelley, W. C. Wetzel, M. R. Webb, G. Gamez, S. J. Ray and G. M. Hieftje, *Anal. Chem.*, 2008, **80**, 2646–2653.
94 J. D. Harper, N. A. Charipar, C. C. Mulligan, X. Zhang, R. G. Cooks and Z. Ouyang, *Anal. Chem.*, 2008, **80**, 9097–9104.
95 N. Na, M. Zhao, S. Zhang, C. Yang and X. Zhang, *J. Am. Soc. Mass Spectrom.*, 2007, **18**, 1859–1862.
96 Z. Takáts, I. Cotte-Rodriguez, N. Talaty, H. Chen and R. G. Cooks, *Chem. Commun.*, 2005, 1950–1952.
97 G. A. Harris and F. M. Fernández, *Anal. Chem.*, 2008, **81**, 322–329.
98 J. M. Nilles, T. R. Connell and H. D. Durst, *Analyst*, 2010, **135**, 883–886.
99 K. P. Pfeuffer, J. T. Shelley, S. J. Ray and G. M. Hieftje, *J. Anal. At. Spectrom.*, 2013, **28**, 379–387.
100 G. T. Winter, J. A. Wilhide and W. R. LaCourse, *J. Visualized Exp.*, 2016, **7**, e54195.
101 J. Balog, T. Szaniszlo, K.-C. Schaefer, J. Denes, A. Lopata, L. Godorhazy, D. Szalay, L. Balogh, L. Sasi-Szabo and M. Toth, *Anal. Chem.*, 2010, **82**, 7343–7350.
102 O. Golf, N. Strittmatter, T. Karancsi, S. D. Pringle, A. V. Speller, A. Mroz, J. M. Kinross, N. Abbassi-Ghadi, E. A. Jones and Z. Takats, *Anal. Chem.*, 2015, **87**, 2527–2534.
103 H. Wang, W. Sun, J. Zhang, X. Yang, T. Lin and L. Ding, *Analyst*, 2010, **135**, 688–695.
104 J. S. Wiley, J. Cyriac, J. T. Shelley and R. G. Cooks, in *19th International Mass Spectrometry Conference*, Kyoto, Japan, 2012.
105 J. T. Shelley, J. S. Wiley, J. K. Dalgleish, G. C. Y. Chan, G. M. Hieftje and R. G. Cooks, in *60th Annual American Society for Mass Spectrometry Conference*, Vancouver, BC, Canada, 2012.
106 J. T. Shelley, J. S. Wiley, G. C. Chan, G. D. Schilling, S. J. Ray and G. M. Hieftje, *J. Am. Soc. Mass Spectrom.*, 2009, **20**, 837–844.
107 L. V. Ratcliffe, F. J. Rutten, D. A. Barrett, T. Whitmore, D. Seymour, C. Greenwood, Y. Aranda-Gonzalvo, S. Robinson and M. McCoustra, *Anal. Chem.*, 2007, **79**, 6094–6101.
108 J. Kratzer, Z. Mester and R. E. Sturgeon, *Spectrochim. Acta, Part B*, 2011, **66**, 594–603.
109 J. T. Shelley and G. M. Hieftje, *J. Anal. At. Spectrom.*, 2010, **25**, 345–350.
110 L. Song, S. C. Gibson, D. Bhandari, K. D. Cook and J. E. Bartmess, *Anal. Chem.*, 2009, **81**, 10080–10088.
111 C. N. McEwen and B. S. Larsen, *J. Am. Soc. Mass Spectrom.*, 2009, **20**, 1518–1521.
112 L. Song, A. B. Dykstra, H. Yao and J. E. Bartmess, *J. Am. Soc. Mass Spectrom.*, 2009, **20**, 42–50.
113 T. M. Brewer and J. R. Verkouteren, *Rapid Commun. Mass Spectrom.*, 2011, **25**, 2407–2417.
114 E. Horning, M. Horning, D. Carroll, I. Dzidic and R. Stillwell, *Anal. Chem.*, 1973, **45**, 936–943.
115 I. Dzidic, D. Carroll, R. Stillwell and E. Horning, *Anal. Chem.*, 1976, **48**, 1763–1768.

116 M. S. Heywood, N. Taylor and P. B. Farnsworth, *Anal. Chem.*, 2011, **83**, 6493–6499.
117 J. P. Wright, M. S. Heywood, G. K. Thurston and P. B. Farnsworth, *J. Am. Soc. Mass Spectrom.*, 2013, **24**, 335–340.
118 G. C.-Y. Chan, J. T. Shelley, J. S. Wiley, C. Engelhard, A. U. Jackson, R. G. Cooks and G. M. Hieftje, *Anal. Chem.*, 2011, **83**, 3675–3686.
119 J. T. Shelley, G. C.-Y. Chan and G. M. Hieftje, *J. Am. Soc. Mass Spectrom.*, 2012, **23**, 407–417.
120 J. Shiea, M. Z. Huang, H. J. HSu, C. Y. Lee, C. H. Yuan, I. Beech and J. Sunner, *Rapid Commun. Mass Spectrom.*, 2005, **19**, 3701–3704.
121 A. S. Galhena, G. A. Harris, L. Nyadong, K. K. Murray and F. M. Fernández, *Anal. Chem.*, 2010, **82**, 2178–2181.
122 J. J. Coon, K. J. McHale and W. Harrison, *Rapid Commun. Mass Spectrom.*, 2002, **16**, 681–685.
123 I. X. Peng, J. Shiea, R. R. O. Loo and J. A. Loo, *Rapid Commun. Mass Spectrom.*, 2007, **21**, 2541–2546.
124 P. Nemes, A. A. Barton, Y. Li and A. Vertes, *Anal. Chem.*, 2008, **80**, 4575–4582.
125 K. Dreisewerd, *Chem. Rev.*, 2003, **103**, 395–426.
126 R. B. Van Breemen, M. Snow and R. J. Cotter, *Int. J. Mass Spectrom. Ion Phys.*, 1983, **49**, 35–50.
127 T. Schmitz, J. Koch, D. Günther and R. Zenobi, *Appl. Phys. B: Lasers Opt.*, 2010, **100**, 521–533.
128 T. A. Schmitz, J. Koch, D. Günther and R. Zenobi, *J. Appl. Phys.*, 2011, **109**, 123106.
129 C. Leela, S. Bagchi, V. R. Kumar, S. P. Tewari and P. P. Kiran, *Laser Part. Beams*, 2013, **31**, 263–272.
130 J. S. Sampson, A. M. Hawkridge and D. C. Muddiman, *Rapid Commun. Mass Spectrom.*, 2007, **21**, 1150–1154.
131 R. A. Jockusch, P. D. Schnier, W. D. Price, E. F. Strittmatter, P. A. Demirev and E. R. Williams, *Anal. Chem.*, 1997, **69**, 1119.
132 M. Dole, L. Mack, R. Hines, R. Mobley, L. Ferguson and M. D. Alice, *J. Chem. Phys.*, 1968, **49**, 2240–2249.
133 E. D. Inutan and S. Trimpin, *J. Proteome Res.*, 2010, **9**, 6077–6081.
134 C. B. Lietz, A. L. Richards, Y. Ren and S. Trimpin, *Rapid Commun. Mass Spectrom.*, 2011, **25**, 3453–3456.
135 E. Inutan and S. Trimpin, *J. Am. Soc. Mass Spectrom.*, 2010, **21**, 1260–1264.
136 E. D. Inutan and S. Trimpin, *Mol. Cell. Proteomics*, 2013, **12**, 792–796.
137 M. Yamashita and J. B. Fenn, *J. Phys. Chem.*, 1984, **88**, 4671–4675.
138 A. Hirabayashi, M. Sakairi and H. Koizumi, *Anal. Chem.*, 1994, **66**, 4557–4559.
139 C. N. McEwen, B. S. Larsen and S. Trimpin, *Anal. Chem.*, 2010, **82**, 4998–5001.
140 F. Zydel, S. Trimpin and C. N. McEwen, *J. Am. Soc. Mass Spectrom.*, 2010, **21**, 1889–1892.
141 J. Li, E. D. Inutan, B. Wang, C. B. Lietz, D. R. Green, C. D. Manly, A. L. Richards, D. D. Marshall, S. Lingenfelter and Y. Ren, *J. Am. Soc. Mass Spectrom.*, 2012, **23**, 1625–1643.
142 B. Lindner and U. Seydel, *Anal. Chem.*, 1985, **57**, 895–899.
143 A. R. Dow, A. M. Wittrig and H. I. Kenttämaa, *Eur. J. Mass Spectrom.*, 2012, **18**, 77–92.
144 S.-C. Cheng, M.-Z. Huang and J. Shiea, *Anal. Chem.*, 2009, **81**, 9274–9281.
145 B. Lindner, *Int. J. Mass Spectrom. Ion Processes*, 1991, **103**, 203–218.
146 R. C. Shea, C. J. Petzold, J. L. Campbell, S. Li, D. J. Aaserud and H. I. Kenttämaa, *Anal. Chem.*, 2006, **78**, 6133–6139.
147 S. R. Heron, R. Wilson, S. A. Shaffer, D. R. Goodlett and J. M. Cooper, *Anal. Chem.*, 2010, **82**, 3985.

B. *Theobroma cacao* methyltransferase TcCS2

(UniProt accession number A0A061E330)

```
10         20         30         40         50         60
MGSSHHHHHH SSGLVPRGSH MSKTGALDLA SGLGGKIEKT DVLSAVEKYE KYHFFYGGEE

         70         80         90        100        110        120
EERKANYTDM VNKYYDLVTS FYEFGWGESF HFAPRWNGES LRESIKRHEH FLALQLGLKP

        130        140        150        160        170        180
GHKVLDVGCG IGGPLREIAR FSSTSVTGLN NNEYQIERGK ELNRIAGVDK TCNFVKADFM

        190        200        210        220        230        240
KMPFPDSSFD AVYAIEATCH APDAYGCYKE IYRVLKPGQY FAAYEWCMTD SFDPNNQEHQ

        250        260        270        280        290        300
KIKAEIEIGD GLPDIRLTRQ CLEALKQAGF EVIWDKDLAV DSSIPWYLPL DKNHFSLSSF

        310        320        330        340        350        360
RLTAIGRFVT KNMVKALEFV GFAPRGSQRV QEFLEKAAEG LVEGGRKEIF TPMYFFLARK

QLAKSQ
```

Figure B1. Sequence of His-tagged IPCS3, the basic amino acids have been highlighted for predicting HOCS and HICS

Table B1. Calculated charge states of TcCS2

TcCS2 (MW 41498)	
z	m/z
21	1977.1
22	1887.3
23	1805.3
24	1730.1
25	1660.9
26	1597.1
27	1538.0
28	1483.1
29	1432.0
30	1384.3
31	1339.6
32	1297.8
33	1258.5
34	1221.5
35	1186.7
36	1153.7
37	1122.6
38	1093.1
39	1065.1
40	1038.5
41	1013.1
42	989.0
43	966.1
44	944.1
45	923.2
46	903.1
47	883.9
48	865.5
49	847.9
50	831.0
51	814.7
52	799.0
53	784.0
54	769.5
55	755.5
56	742.0
57	729.0
58	716.5

C. **Biosafety Project Approval**

WESTERN MICHIGAN UNIVERSITY

Institutional Biosafety Committee

Institutional Biosafety Committee

2021
Project Approval Certification

For Institutional Biosafety Committee Use Only

Project Title: Ghost of Evolution Past: Resurrecting Ancestral Enzymes to Understand the Evolution of Modern-Day Enzyme Activities

Principal Investigator: Todd Barkman

Project Number: 21TBa

Date Received by the Institutional Biosafety Committee: November 20, 2020

☒ Reviewed by the Institutional Biosafety Committee

☒ Approved
☐ Approval not required

/ Silvia Rybbach
Chair of Institutional Biosafety Committee Signature

12/11/2020
Date

251 W. Walwood Hall, Kalamazoo, MI 49008-5456
PHONE: (269) 387-8293, FAX: (269) 387-8276